LPA-dependent Regulation of VCAM-1 in the Ovarian Cancer Metastatic Microenvironment and its Impact on Mesothelial Invasion

Timothy André Raines
Fort Wayne, Indiana

M.S., University of Virginia, 2012
M.S., North Carolina Agricultural and Technical State University, 2010
B.S., North Carolina Agricultural and Technical State University, 2006

A Dissertation presented to the Graduate Faculty
of the University of Virginia in Candidacy for the Degree of
Doctor of Philosophy

Department of Microbiology, Immunology and Cancer Biology

University of Virginia
May, 2017

Abstract

Ovarian cancer is the second most common gynecological cancer and is the leading cause of all reproductive cancer deaths in the United States. The poor prognosis is attributed to 75% of patients being diagnosed with advanced stage disease which is accompanied by an overall five-year survival rate of approximately 20-25%. Advanced staged disease is characterized by peritoneal and distant metastasis. Peritoneal metastasis involves the ovarian cancer cells disseminating within the peritoneal cavity where they will implant on surfaces of organs including the omentum, diaphragm, and large and small bowel serosa. The surfaces of these organs are covered by mesothelium, a monolayer of mesothelial cells. Mesothelial cells actively participate in promoting invasion by expressing adhesion molecules including vascular cell adhesion molecule 1 (VCAM-1). Previously, VCAM-1 was demonstrated as an important regulator of mesothelial invasion within the ovarian cancer tumor microenvironment; however, it is not known what regulates mesothelial VCAM-1 expression in ovarian cancer. Lysophosphatidic acid (LPA), a bioactive lipid found at elevated levels in the malignant ascites, regulates several cellular functions critical for tumorigenesis and metastasis such as proliferation, angiogenesis, migration and invasion. Therefore, this we investigated whether LPA targets the ovarian cancer microenvironment, specifically the mesothelium, to promote ovarian cancer metastasis. Using mice that lack expression of the LPA phosphatase, LPP1 (LPP1 KO), and have elevated circulating concentrations of LPA, this thesis reports LPP1 KO mice showed increased peritoneal ovarian cancer growth and a significantly higher incidence of invasive tumors as compared to wild type. Additionally, LPP1 KO had increased mesothelial VCAM-1 expression. From these data, we further studied LPA regulation of mesothelial VCAM-1 to promote mesothelial invasion. Utilizing

a co-culture assay system, we observed a significantly reduced ovarian cancer cell invasion of the mesothelium after inhibition of LPA1. Moreover, blocking or inhibiting LPA1 in human mesothelial cells derived from ovarian cancer patients' ascitic fluid decreased VCAM-1 expression and accumulation both at the transcript and protein level. Furthermore, pulse labeling with S^{35}-Met/Cys indicated a significant decrease in VCAM-1 protein synthesis in cells lacking LPA1 expression compared to control. Importantly, re-expression of exogenous VCAM-1 after LPA1 knockdown in mesothelial cells restores trans-mesothelial invasion of ovarian cancer cells. Taken together, these data demonstrate LPA promotes mesothelial invasion through the regulation of mesothelial VCAM-1 expression. Furthermore, the work in this thesis provides a further understanding of the role LPA plays in ovarian cancer metastatic progression, and these findings provide a potential model for other conditions associated with elevated LPA and chronic VCAM-1 expression.

Acknowledgements

I would like to give all the honor and glory to God, thanking him for his many blessings and all that he has done for me. I would next like to thank my family and friends for giving me the encouragement to continue my education after all the trials and tribulations that I have gone through during my life's journey. Particularly, I would like to acknowledge my cousin, Rhonda Kinchen, who passed from ovarian cancer. My interest and reason for obtaining a Ph.D. in the area of cancer biology is because of her and my mother who passed from lung cancer. I also would like to thank my parents for their love and support during the time I had with them. Although they have both passed away, their memory shall live on through me forever.

This experience would not have been so remarkable without the support of my advisor, Dr. Jill Slack-Davis. Thank you for support and guidance. I am very grateful and appreciative to have worked with a wonderful scientist who has helped me to think critically through my project. You have truly helped me grow as a scientist. I would like to further acknowledge and thank my committee members, Dr. Amy Bouton, Dr. Ulrike Lorenz, Dr. Sally Parsons, Dr. Kevin Lynch, and Dr. Kevin Janes for your feedback and advice throughout the years. I would also like to thank the members of the Slack-Davis lab, past and present, especially Eli Casarez and Michelle Edwards (soon to be Dr. Michelle Edwards) for providing support.

Lastly, I would like to thank the faculty and staff of the Microbiology, Immunology, and Cancer Biology department and Cell Biology department for their support. I would be remiss if I did not thank Mary Hall and Sandy Weirich for their assistance and support throughout this experience. Thank you!

Dedication

I dedicate this thesis in the memory of my parents, Donna Kaye and Willie Clark Raines. If tears could build a stairway and memories a lane, I would walk right up to heaven to bring the both of you home again. You both have instilled in me the passion to succeed and the drive to conquer anything I put my mind to. You may be gone, but never shall you be forgotten.

Table of Contents

List of Figures

FIGURES **PAGE**

FIGURES **PAGE**

FIGURES **PAGE**

List of Tables

TABLES **PAGE**

List of Abbreviations

AGK	Acylglycerol Kinase
ANOVA	Analysis of variance
ATX	Autotaxin
ECM	Extracellular Matrix
FACS	Fluorescence-Activated Cell Sorting
FIGO	Federation of Gynecology and Obstetrics
GFP	Green Fluorescent Protein
GUSB	β glucuronidase
HA	Hyaluronic Acid
HGF	Hepatocyte Growth Factor
HIF-1 α	Hypoxia-Induced Factor 1α
HPG	L-homoproparglyglycine
ICAM-1	Intracellular Adhesion Molecule 1
IF	Immunofluorescence
IFN-γ	Interferon-γ
IHC	Immunohistochemistry
IL	Interleukin
IP	Intraperitoneal
LFA	Lymphocyte Function-Associated Antigen

LPA	Lysophosphatidic Acid
LPA1	Lysphophatdic Acid Receptor 1
LPC	Lysophosphatidylcholine
LPP	Lipid Phosphate Phosphohydrolase
LPPAT	LPA Acyltransferase
MAG	Monoacylglcerol
MAPK	Mitogen-Activated Protein Kinase
MFI	Mean Fluorescence Intensity
MLC	Myosin Light Chain
MMP	Matrix Metalloproteinases
MYPT-1	Myosin Phosphatase Subunit
NF-κB	Nuclear Factor-κB
P13K	Phosphoinositide 3-Kinase
PA	Phosphatidic Acid
PECAM-1	Platelet-Endothelial Cell Adhesion Molecule 1
qRT-PCR	Quantitative Real Time PCR
SEM	Standard Error of the Mean
SP	Smart Pool
TNF- α	Tumor Necrosis Factor α
TNFR	Tumor Necrosis Factor Receptor
uPA	Urokinase Plasminogen Activator

VCAM-1	Vascular Cell Adhesion Molecule 1
VEGF	Vascular Endothelial Growth Factor
VEGFR	Vascular Endothelial Growth Factor Recepotor
WT	Wild Type

Chapter 1: Introduction

1.1. Ovarian Cancer

Ovarian cancer is the fifth cause of cancer-related death in women but is the leading cause of all reproductive cancer deaths in the United States (Sankaranarayanan and Ferlay, 2006). Approximately 21,290 women will be diagnosed with ovarian cancer, and 14,180 deaths will occur each year (Siegel et al., 2015). Fifty percent of the new cases will be diagnosed in women over the age of 60. The overall 5-year survival rate is approximately 46.2%; however, the rate is stage dependent with localized ovarian cancer having a 92% 5-year survival rate and distant/metastatic disease having a 27% 5-year survival rate (Siegel et al., 2015). Unfortunately, 75% of new cases are diagnosed with metastatic disease (Hennessy et al., 2009).

Ovarian cancer arises from three cell types: epithelial cells, germ cells, and specialized stromal cells (Jelovac and Armstrong, 2011). The vast majority, approximately 90%, of ovarian cancers are epithelial in nature (Jelovac and Armstrong, 2011). Epithelial ovarian cancer is a heterogeneous disease that is histologically subtyped into two groups, Type I tumors and Type II tumors (Landen et al., 2008). Type I tumors have been linked to precursor lesions in the ovary and include low-grade endometrioid carcinoma, clear cell carcinoma, mucinous carcinoma, and low-grade serous carcinoma (Kurman and Shih, 2008; Landen et al., 2008). Type I tumors are defined by their slow growth, diagnosis at early stages, and genetic mutations including *KRAS*, *BRAF*, and *PTEN* (Koshiyama et al., 2014; Levanon et al., 2008). In contrast, Type II tumors are highly aggressive, confer a poorer prognosis, and are linked to precursors arising from the fallopian tube epithelium (Kurman and Shih, 2008; Lee et al., 2007; Shaw et al., 2009). The vast majority of

type II tumors harbor *TP53* mutations (Ahmed et al., 2010; Koshiyama et al., 2014; Levanon et al., 2008), and *BRCA1/BRACA2* mutations are strongly associated with hereditary cases of ovarian cancer in these tumor types (Koshiyama et al., 2014). Type II tumors include high-grade endometrioid and high-grade serous ovarian carcinoma. High-grade serous ovarian carcinoma accounts for almost 75% of all epithelial ovarian cancer.

Ovarian cancer is staged using a classification system established by the International Federation of Gynecology and Obstetrics (FIGO) (Jayson et al., 2014; Prat, 2015) (Figure 1.1). Stage I ovarian cancer is confined to one or both ovaries. Stage II involves one or both ovaries and includes progression of the tumor outside the ovaries but within the pelvic region (Prat, 2015). Stage III disease spreads within the peritoneal cavity including both pelvic and abdominal peritoneum and results in the accumulation of ascites (Prat, 2015). In addition to peritoneal metastasis, Stage IV ovarian cancer involves hematogenous dissemination to distant sites including the lungs or liver (Jelovac and Armstrong, 2011; Prat, 2015). Women diagnosed in stages I or II have a favorable prognosis, a ten-year survival rate of 80-95%, and tend to respond well to standard therapies (Hennessy et al., 2009; Ozols, 2005). However, approximately 20-25% of woman are diagnosed with early-stage ovarian cancer (Ozols, 2005). The overall poor prognosis of ovarian cancer is attributed to the diagnosis of over 75% of cases at an advanced stage (III or IV), which is accompanied with a ten-year survival rate of 10-30% (Hennessy et al., 2009; Ozols, 2005).

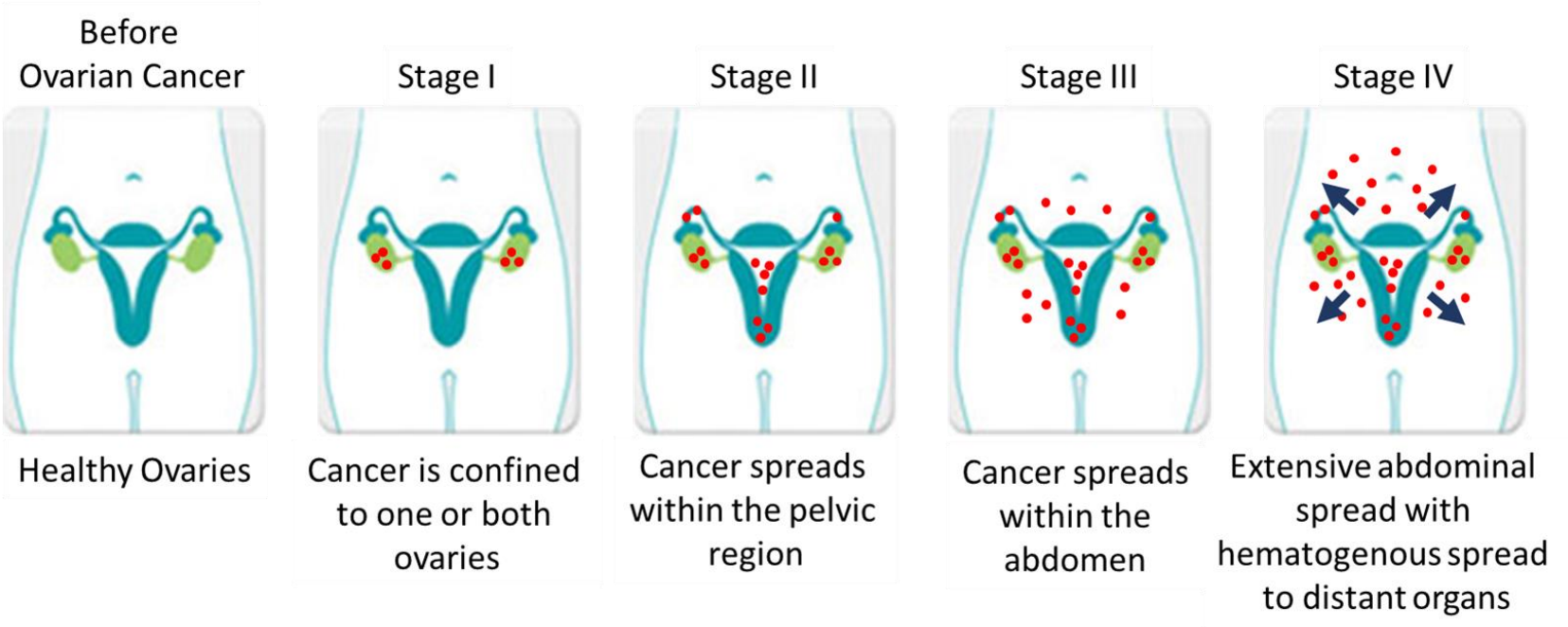
Before Ovarian Cancer
Stage I
Stage II
Stage III
Stage IV
Healthy Ovaries
Cancer is confined to one or both ovaries
Cancer spreads within the pelvic region
Cancer spreads within the abdomen
Extensive abdominal spread with hematogenous spread to distant organs

Figure 1.1. Staging of ovarian cancer. Early stages, I and II, show tumors confined to the ovary or spread within the pelvis. The majority of women are diagnosed with stage III disease where the cancer has metastasized within the peritoneal cavity most commonly to the omentum. Stage IV is hematogenous spread to distant organs such as liver and lung. Adapted from (http://www.deepammeditours.com/treatments/ovarian-cancer-cancer-of-the-ovaries/).

1.2 Ovarian Cancer Metastatic Microenvironment

Advanced-stage disease is characterized by rapid growth, widespread seeding within the peritoneal cavity, and ascites formation (Fagotti et al., 2010; Schorge et al., 2010). Unlike most solid tumors that metastasize by extravasation through blood vessels, ovarian cancer primarily undergoes transcoelomic spread throughout the peritoneal cavity. Within the peritoneal cavity, there is no anatomical barrier to prevent ovarian cancer cells from spreading by direct extension to adjacent organs. Specifically, ovarian cancer cells detach from the primary tumor site as single cells or clusters of cells, disseminate throughout the peritoneal cavity in peritoneal fluid, and finally settle on any peritoneal cavity organ surface such as the peritoneum, omentum, diaphragm, and large and small bowel serosa (Lengyel, 2010; Sehouli et al., 2009) (Figure 1.2). Once implanted, tumor nodule development and growth lead to significant clinical complications such as bowel obstructions; patients often succumb from malnutrition and dehydration.

With ovarian cancer spreading by direct extension from the primary site to neighboring organs, ascites is a major component that supports this passive process. Ascites is the accumulation of fluid within the peritoneal cavity. Ascites accumulates when tumors spread throughout the peritoneal cavity resulting in increased leakiness of the tumor microvasculature, lymphatic obstruction, and increased production of peritoneal fluid by cells lining the peritoneal cavity (Adam and Adam; Feldman et al., 1972; Kipps et al., 2013). The term malignant ascites is given to the peritoneal fluid once cancer cells have been detected in the fluid (Adam and Adam; Kipps et al., 2013). The presence of malignant ascites correlates with peritoneal metastasis, a grave prognosis, and a reduced five-year survival rate, thus contributing to the morbidity

Model of Ovarian Cancer Metastasis

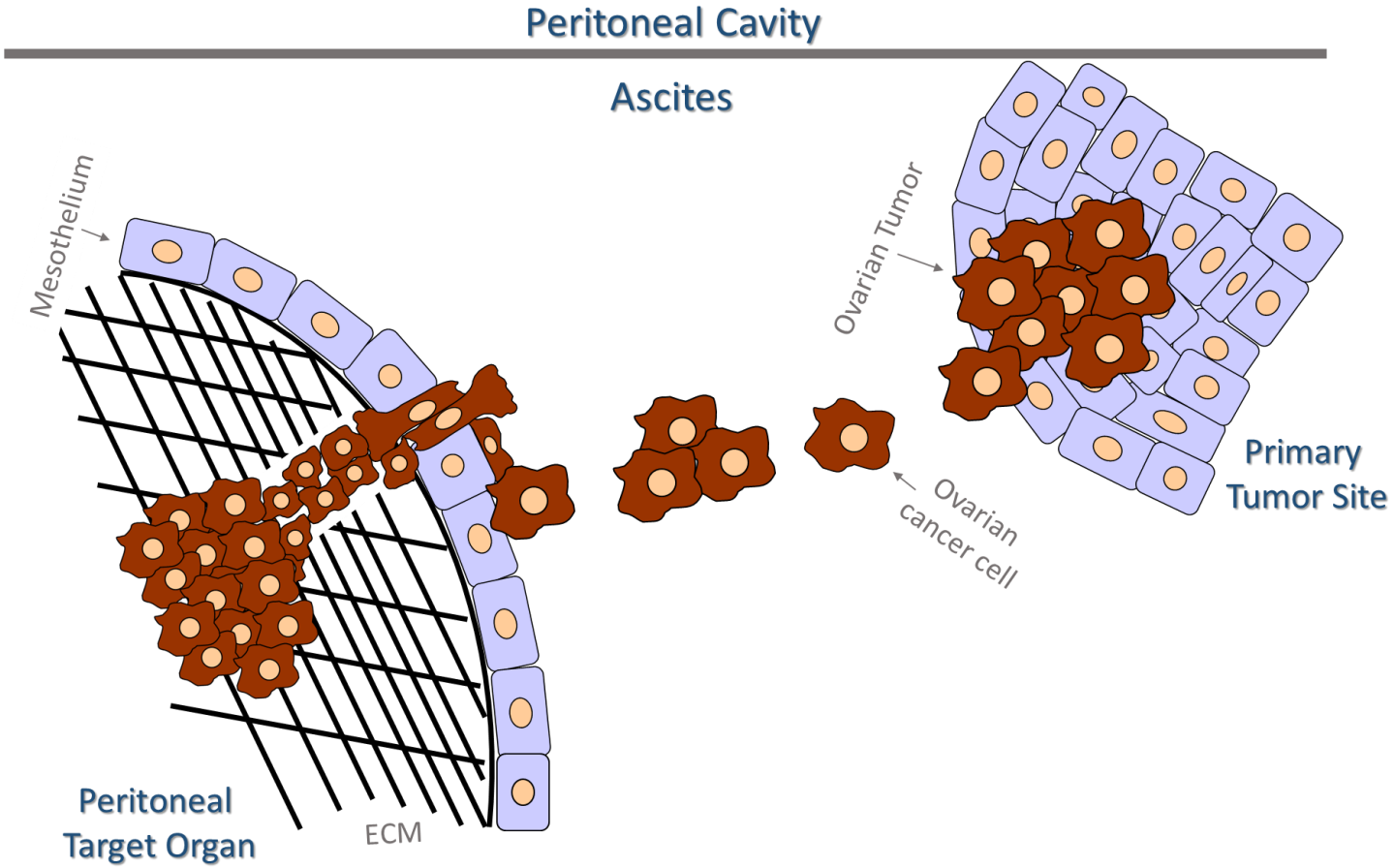

Figure 1.2. Ovarian cancer metastatic progression. Malignant ovarian cancer will exfoliate from the primary tumor site and shed into the peritoneal cavity as single cells or multi-cellular aggregates. The ovarian cancer cells are passively taken to the secondary site by ascites. The ovarian cancer cells will attach and invade the targeted organ within the peritoneal cavity.

associated with advanced stage disease (Ahmed and Stenvers, 2013; Ezzati et al., 2014; Kipps et al., 2013; Puls et al.). Additionally, malignant ascites can cause many of the symptoms linked to ovarian cancer including abdominal pain and satiety (Kipps et al., 2013). Thus, gaining a better understanding of the role malignant ascites plays to support and promote ovarian cancer progression and metastasis is likely to provide more effective therapeutic intervention for ovarian cancer.

1.3 The Role of Malignant Ascites in the Ovarian Cancer Metastasis

The accumulation of ascitic fluid is a hallmark of advanced-stage ovarian cancer and plays a vital role in ovarian cancer metastatic progression because it creates a tumor-friendly microenvironment that stimulates tumor progression (Kipps et al., 2013; Matte et al., 2012). Functionally, the role of ascites is to facilitate ovarian cancer metastasis by providing a milieu of soluble factors secreted by both cancer and stromal cells (Kipps et al., 2013). The soluble factors within the ascites include growth factors, cytokines, and bioactive lipids influence ovarian cancer metastasis by promoting adhesion, invasion, and migration of the cancer cells (Meunier et al., 2010; Puiffe et al., 2007). One prominent soluble factor that is abundant in the ovarian cancer metastatic microenvironment is lysophosphatidic acid (LPA). LPA was initially identified as ovarian cancer activating factor because it was a primary functional component of the malignant ascites (Xu et al., 1995). LPA has pleiotropic effects on both the cancer cells and stromal cells within the ovarian cancer metastatic microenvironment (Mills and Moolenaar, 2003; Ren et al., 2006).

1.3.1 Lysophosphatidic Acid (LPA)

Lysophosphatidic acid is a family of naturally occurring phospholipids that consist of a single fatty acid chain attached to a glycerol backbone with a phosphate group (Figure 1.3). LPA mediates multiple biological responses in almost every cell type, both normal and transformed, via G-protein coupled receptors (Mills and Moolenaar, 2003; van Corven et al., 1989). The cellular responses LPA evokes include proliferation (van Corven et al., 1989), survival (Li et al., 2003; Weiner and Chun, 1999; Ye et al., 2002), migration and invasion (Bian et al., 2006; Bian et al., 2004; Imamura et al., 1993; Xu et al., 1995), wound healing (Lee et al., 2000), aggregation of platelets (Gerrard et al., 1979), smooth muscle cell contraction (Gerrard et al., 1979), cytoskeleton reorganization (Chrzanowska-Wodnicka and Burridge, 1994), and increased endothelial permeability (Amerongen et al., 2000). Although LPA primarily plays a role in cell viability, it also causes necrosis and apoptosis in some cases (Holtsberg et al., 1998; Steiner et al., 2000).

Several enzymatic pathways lead to the generation and degradation of LPA. Autotaxin (ATX), an extracellular lysophospholipase D, cleaves choline from lysophosphatidylcholine (LPC) to produce LPA (Mills and Moolenaar, 2003) (Figure 1.4). LPA is also produced through the action of phospholipases A1 (PLA1) and A2 (PLA2), which hydrolyze the *sn-1* or *sn-2* ester bond, respectively, from surface-exposed phosphatidic acid (Ren et al., 2006) (Figure 1.4). Moreover, LPA is degraded by the action of two exophosphatases, lipid phosphate phosphohydrolase (LPP) types 1 and 3. LPP1 and 3 are integral membrane proteins localized to the plasma membrane that dephosphorylate LPA to generate MAG (Kai et al., 2006; Sciorra and Morris, 2002) (Figure 1.4).

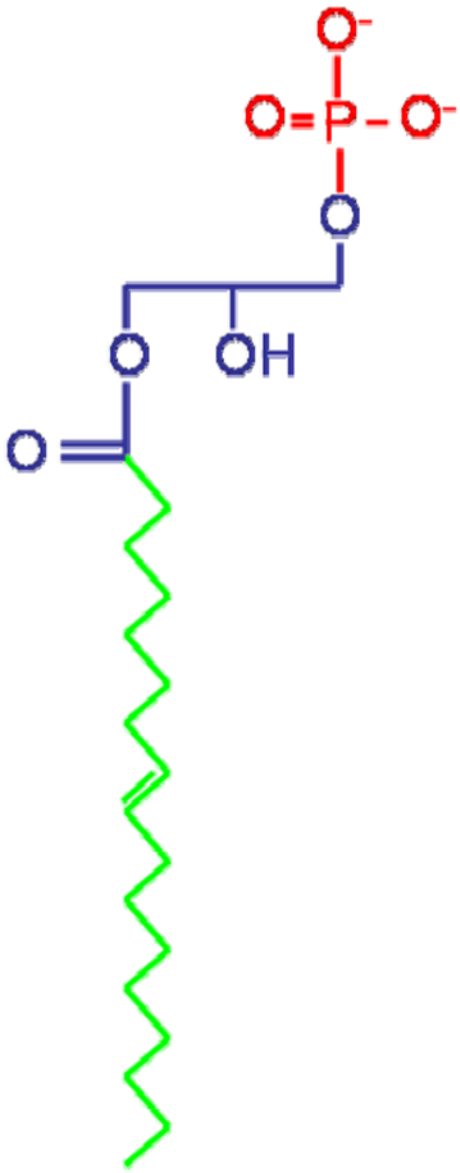
O⁻
O=P–O⁻
O
O
OH
O

Figure 1.3. Structure of Lysophosphatidic acid (LPA). LPA has a single fatty acyl chain attached to the glycerol backbone at either the sn-1 or sn-2 positions. A phosphate group is attached at the sn-3 position.

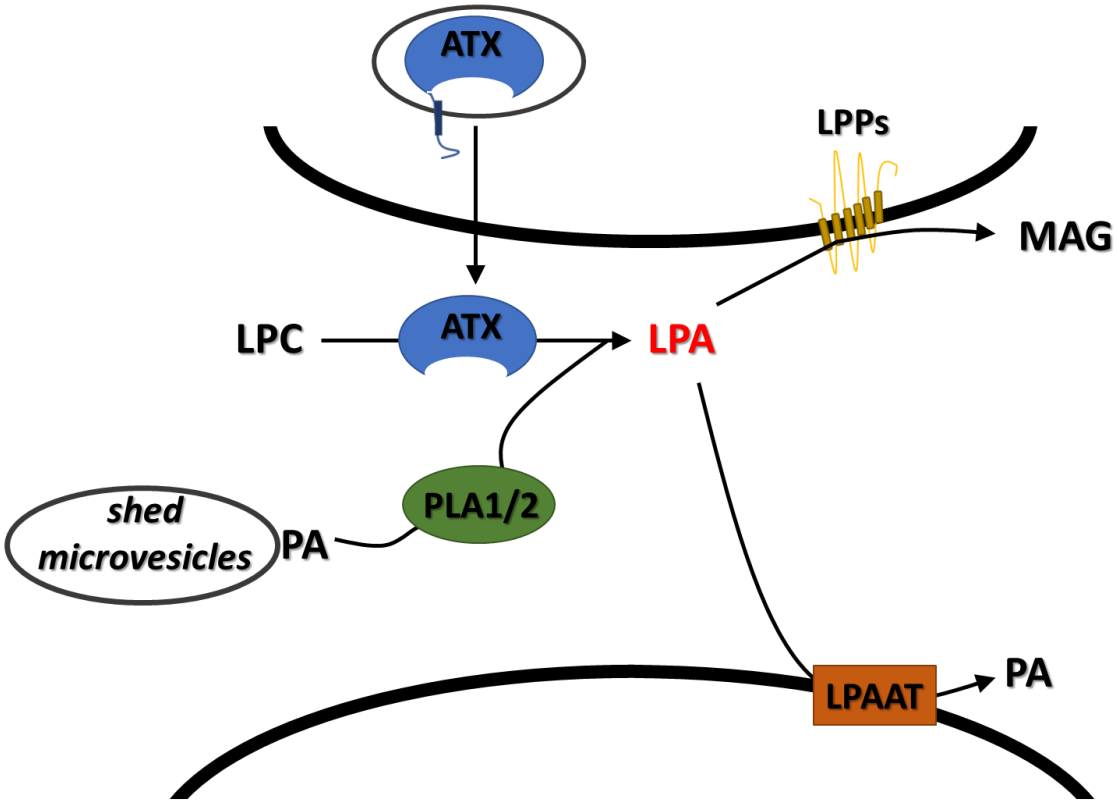
ATX
LPPs
MAG
LPC
ATX
LPA
PLA1/2
shed microvesicles
PA
LPAAT
PA

Figure 1.4. Pathways of LPA synthesis and degradation. A major source of extracellular LPA is generated by autotaxin (ATX) cleaving lysophosphatidylcholine (LPC) to LPA. LPA is generated from surface-exposed phosphatidic acid (PA) through the action of phospholipase A1 (PLA1) or phospholipase A2 (PLA2). LPA is degraded by the action of exophosphatases, lipid phosphate phosphohydrolases (LPPs) to MAG, or by LPA acyltransferase (LPPAT) acylation of LPA to PA. Adapted from (Meyer zu Heringdorf and Jakobs, 2007).

LPA is converted to PA by LPA acyltransferases, which catalyze the transfer of an acyl chain to either the *sn-1* or *sn-2* position of LPA (Leung, 2001) (Figure 1.4).

The cellular and biological actions of LPA occur through the activation of a family of six distinct G-protein coupled receptors, named LPA1-6 (Choi et al., 2010). These receptors have varying expression patterns in different tissues. LPA1 was the first identified and is expressed in the adult human brain, heart, uterus, stomach, colon, small intestine, kidney, placenta, ovary, spleen, and skeletal muscles; however, LPA1 is not expressed in the liver (An et al., 1998; Contos et al., 2000; Ye, 2008). The expression patterns of LPA2-6 are more restricted as compared to LPA1; however, LPA2 and 3 are often expressed in cancer, including ovarian cancer (Fang et al., 2000a; Mills and Moolenaar, 2003).

Once activated, the LPA receptors couple to and activate different G-proteins, such as Gαi, Gαq, Gα12/13, and Gαs (Anliker and Chun, 2004; Mills and Moolenaar, 2003). Upon activation of the G-proteins, they will stimulate a variety of signaling pathways including mitogen-activated protein kinase (MAPK), phosphoinositide 3-kinase (PI3K), Rho/Rho-kinase, and phospholipase C (Figure 1.5). Many of these signaling pathways support cell growth, survival, and migration (Choi et al., 2010).

1.3.2 The Role of Lysophosphatidic Acid in Ovarian Cancer Progression

Lysophosphatidic acid plays a major role in the initiation and progression of ovarian cancer and promotes ovarian cancer cell proliferation, growth, and survival as well as activities relevant to metastasis including migration and invasion. Increased concentrations of LPA are found in both

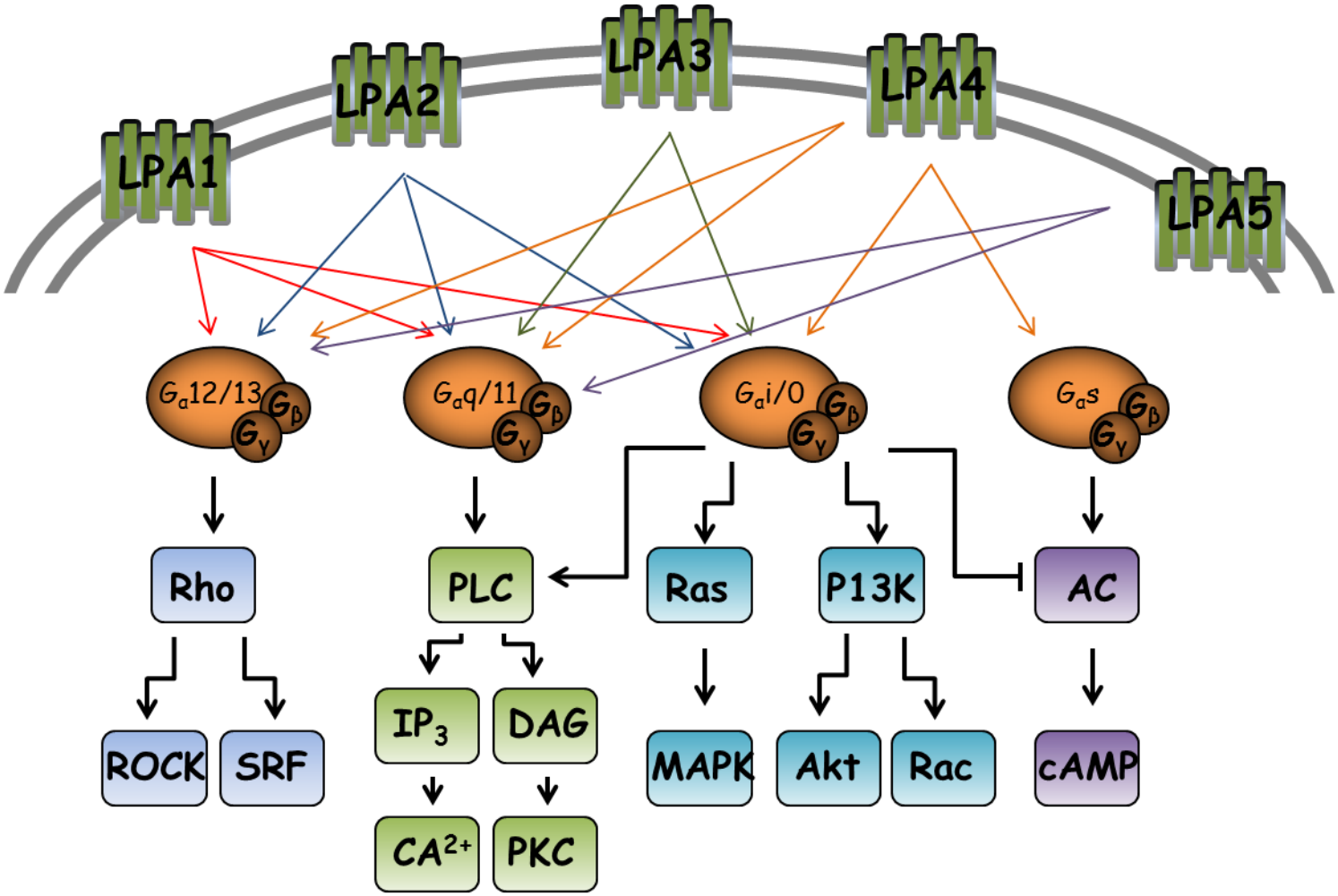
LPA1
LPA2
LPA3
LPA4
LPA5
Gα12/13
Gβ
Gγ
Gαq/11
Gβ
Gγ
Gαi/0
Gβ
Gγ
Gαs
Gβ
Gγ
Rho
PLC
Ras
P13K
AC
ROCK
SRF
IP3
DAG
MAPK
Akt
Rac
cAMP
CA2+
PKC

Figure 1.5. Signaling pathways activated by the LPA receptors. With the LPA receptors being G-coupled protein receptors, they will couple to and activate different G-proteins, such as Gαi, Gαq, Gα12/13, and Gαs [54, 83]. LPA1, LPA2, and LPA5 couple to Gαq and Gα12/13 with LPA1 and LPA2 also coupling with Gαi [54, 69]. LPA3 will activate Gαi and Gαq. LPA4 will interact with Gα12/13 and Gαs [69, 83]. Upon activation of these G-proteins, they will regulate a variety of signaling pathways. Specifically, Gαi induces MAPK/ERK, PI3K/AKT, and phospholipase C pathways while inhibiting adenylyl cyclase activity [84, 85]. Gαq signals through downstream effectors of phospholipase C pathway [69]. Gα12/13 mediates Rho/Rho-kinase pathway activation [69]. Lastly, Gαs activates the adenylyl cyclase pathway [86]. Adapted from (Choi et al., 2010).

malignant ascites and in plasma samples of ovarian cancer patients, suggesting a role for LPA as a potential biomarker of ovarian cancer (Sutphen et al., 2004; Xiao et al., 2001; Xiao et al., 2000; Xu et al., 1995). Within the ovarian cancer metastatic microenvironment, many cell types are capable of producing LPA including activated platelets, adipocytes, ovarian cancer cells, and mesothelial cells (Eichholtz et al., 1993; Mills and Moolenaar, 2003; Ren et al., 2006; Said et al., 2007; Valet et al., 1998). Specifically, ovarian cancer cells secrete autotaxin (ATX) (Mills and Moolenaar, 2003). ATX activity is increased in malignant ascites (Tokumura et al., 2007). Consequently, LPA concentrations are elevated in malignant ascites and exceed concentrations needed to optimally activate LPA receptors (Westermann et al., 1998; Xu et al., 1995). As previously mentioned, LPA is metabolized by the action of exophosphatases, LPPs. LPP1 and LPP3 activity and expression are reduced in human ovarian cancers relative to normal ovarian tissue, and over-expression of either LPP1 or LPP3 decreases ovarian cancer cell proliferation and increases apoptosis *in vitro* and *in vivo* (Tanyi et al., 2003a; Tanyi et al., 2003b).

In ovarian cancer, LPA activates three of the six G protein-coupled receptors, LPA1, LPA2, and LPA3. LPA1 is expressed in normal ovarian surface epithelium, while the expression of LPA2 and LPA3 is induced in the cancer cells (Fang et al., 2000a; Mills and Moolenaar, 2003). All three receptors regulate ovarian cancer cell migration and invasion directly following LPA-induced activation of pro-migratory signaling pathways (Bian et al., 2006; Bian et al., 2004). Additionally, LPA stimulates ovarian cancer growth and metastasis indirectly by inducing the production of proteases such as matrix metalloproteinases (MMPs) and urokinase plasminogen activator (uPA), which results in an enhanced metastatic phenotype (Fishman et al., 2001; Li et

al., 2005). LPA was shown to disrupt ovarian cancer cell-cell adhesions and to facilitate the invasion of ovarian cells (Jourquin et al., 2006; Smicun et al., 2007). Following engagement of LPA2 or LPA3, LPA also induces the production of cytokines, IL-6 and IL-8, which play a role in ovarian cancer invasion and metastasis (So et al., 2004). Furthermore, knockdown of LPA2 or LPA3 decreases IL-6 production, and their over-expression leads to increased serum levels of IL-6 resulting in increased tumor burden and decreased survival in an *in vivo* model of ovarian cancer peritoneal metastasis (Yu et al., 2008). LPA stimulates ovarian cancer metastasis in orthotopic and syngeneic mouse models. Daily injection or implantation of a pump producing LPA significantly increases tumor burden and stimulates tumor metastasis *in vivo* (Kim et al., 2006; Li et al., 2009). Taken together these observations indicate that LPA promotes ovarian cancer cell migration, invasion, and metastasis (Bian et al., 2006; Fang et al., 2000a; Kim et al., 2006; Li et al., 2009; Mills and Moolenaar, 2003); however, the effect of LPA on components within the ovarian cancer metastatic microenvironment to promote metastasis is poorly understood.

In recent years, the ovarian cancer metastatic microenvironment has become more appreciated because it supports tumor progression towards metastatic disease (Luo et al., 2016). The role LPA plays in influencing this microenvironment, specifically in mesothelial cells, should be considered because it may provide new therapeutic approaches to targeting ovarian cancer metastasis (Ren et al., 2006).

1.4 The Role of Mesothelial Cells in Ovarian Cancer Metastasis

The malignant ascites is not only comprised of soluble factors; ovarian cancer cells and stromal cells can be found in the ascitic fluid (Kim et al., 2016). Among the various stromal cells present in the malignant ascites, mesothelial cells are the most abundant population (Davidson, 2004). Mesothelial cells are epithelial-like cells, that surround all the organs and line surfaces within the peritoneal cavity as a continuous monolayer forming the mesothelium (Mutsaers, 2004; Mutsaers and Wilkosz, 2007). A normal function for the mesothelium is to provide a frictionless interface and protective surface to allow intracoelomic movement of the organs within the peritoneal cavity (Mutsaers, 2004). During ovarian cancer metastasis, the mesothelium produces and/or secretes extracellular matrix (ECM) proteins and growth factors into the ascites to enhance adhesion, migration, and invasion of ovarian cancer cells (Jones et al., 1995; Kenny et al., 2014; Lee et al., 1993; Offner et al., 1996; Ren et al., 2006; Rieppi et al., 1999; Stadlmann et al., 2005). In particular, mesothelial cells produce and secrete LPA through the action of PLA2, and conditioned media from mesothelial cells containing LPA stimulate ovarian cancer cell adhesion and migration (Ren et al., 2006). Additionally, the malignant ascites stimulates mesothelial cell proliferation and migration (Kim et al., 2016; Matte et al., 2014a; Matte et al., 2014b).

As the ovarian cancer cells disseminate within the peritoneal cavity, mesothelial invasion plays a predominant role in ovarian cancer pathobiology. Mesothelial invasion involves an active participation of the mesothelial cells to stimulate the cancer cell adhesion, migration, and invasion of the mesothelium (Eder et al., 2000; Heyman et al., 2010; Lessan et al., 1999; Li et al., 2009; Slack-Davis et al., 2009) (Figure 1.6). Mesothelial invasion is associated with an unfavorable

prognosis in ovarian cancer (Bell et al., 2004). Therefore, understanding the mechanisms that govern ovarian cancer mesothelial invasion are necessary to help identify additional therapeutic targets that regulate metastasis so that more effective therapeutic intervention for ovarian cancer can be developed.

1.5 Mechanisms Governing Ovarian Cancer Peritoneal Metastasis

Mesothelial invasion involves a disruption of the mesothelium to allow ovarian cancer cells access to the underlying stroma (Niedbala et al., 1985) (Figure 1.6). Many studies focus on adhesion molecules that promote ovarian cancer cell attachment to the ECM components on the mesothelium; however, the mechanisms regulating how ovarian cancer cells intercalate between the mesothelial monolayer are not as well understood (Cannistra et al., 1993; Cannistra et al., 1994; Kenny et al., 2008; Lessan et al., 1999). Therefore, it is important to understand the mechanisms that promote ovarian cancer mesothelial invasion.

1.5.1 Ovarian Cancer Cell Interactions with Mesothelium Extracellular Matrix Proteins

Mesothelial invasion involves interactions with ECM proteins that play a role in tumor cell attachment to the mesothelium. The mesothelium basement membrane is composed of collagen I, collagen IV, laminin, vitronectin, hyaluronic acid (HA), and fibronectin (Heyman et al., 2008; Lessan et al., 1999; Strobel and Cannistra, 1999; Witz et al., 2001). Ovarian cancer cells bind to hyaluronic acid, vitronectin, and fibronectin (Cannistra et al., 1993; Cannistra et al., 1995; Lessan et al., 1999). These three cell-matrix interactions will be defined further.

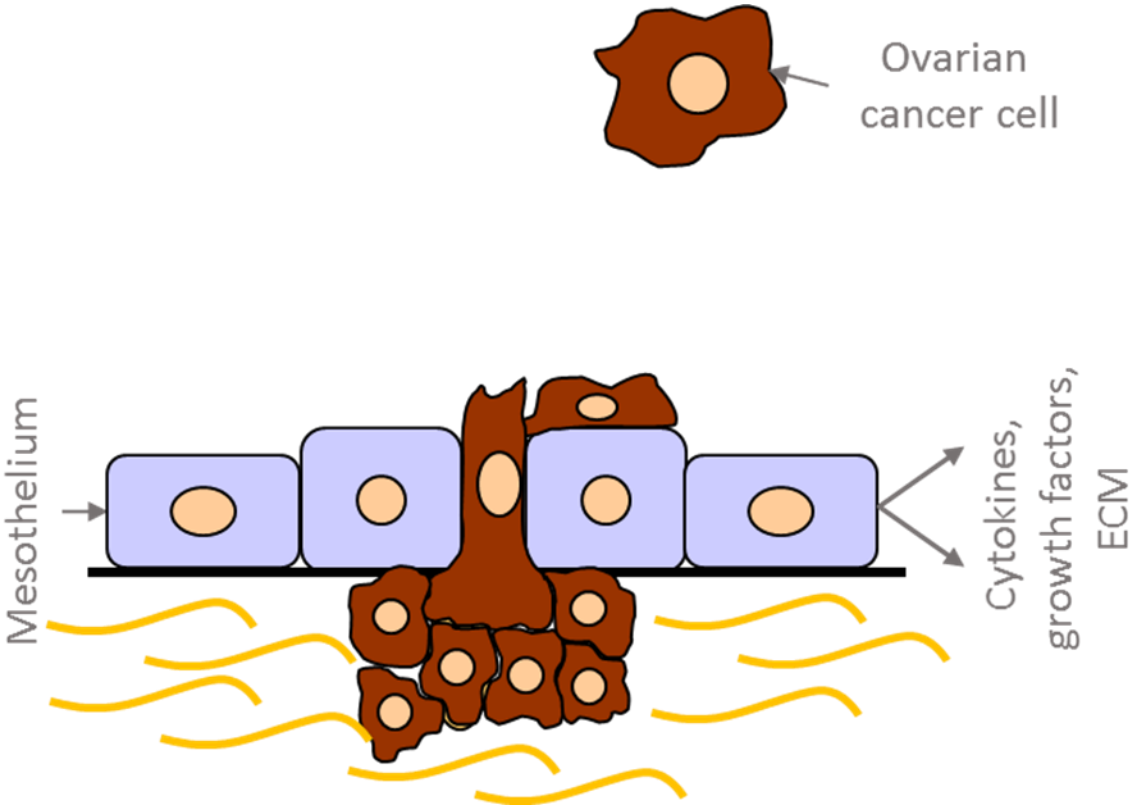
Ovarian
cancer cell
Mesothelium
Cytokines,
growth factors,
ECM

Figure 1.6. Model of mesothelial invasion. Ovarian cancer cells will adhere to, interact with, and invade through the mesothelium, a single cell layer of mesothelial cells that lines the peritoneal cavity, to access underlying stroma.

1.5.1.1 CD44 and Hyaluronic Acid

CD44 interaction with hyaluronic acid promotes ovarian cancer cell adhesion to mesothelial cells. CD44 is a transmembrane glycoprotein that is expressed on ovarian cancer cells and the principal receptor for hyaluronic acid (Bourguignon et al., 2005; Cannistra et al., 1993; Garlanda and Mantovani, 1999). Hyaluronic acid is a glycosaminoglycan produced by mesothelial cells and expressed around the cell membrane of mesothelial cells (Gardner et al., 1995; Jones et al., 1995; Lessan et al., 1999). The use of an anti-CD44 antibody partially prevented the adhesion of CD44 expressing ovarian cancer cells to hyaluronic acid on the mesothelial cells *in vitro* and *in vivo* (Cannistra et al., 1993; Gardner et al., 1996). Furthermore, hyaluronic acid found in conditioned medium from cultured mesothelial cells inhibits ovarian cancer cell adhesion, conceivably by engaging CD44 on tumor cells and preventing their binding to hyaluronic acid on the mesothelial cell surface (Jones et al., 1995).

1.5.1.2 αVβ3 integrin-Vitronectin

Recent evidence demonstrates a role for vitronectin, a multifunctional adhesive ECM glycoprotein, and its receptor, αVβ3 integrin, in promoting the cross talk between the mesothelium and ovarian cancer cells (Heyman et al., 2008; Heyman et al., 2010; Kenny et al., 2008). A few groups demonstrated vitronectin staining in human peritoneal mesothelium tissue samples and omentum samples (Heyman et al., 2008; Kenny et al., 2008). Vitronectin- αVβ3 integrin interactions facilitate cancer adhesion, motility, and mesothelial invasion (Heyman et al., 2008; Heyman et al., 2010). Specifically, ovarian cancer adhesion to the mesothelium is mediated by

αVβ3/vitronectin interactions and is blocked by using anti-vitronectin and anti-αV blocking antibodies (Heyman et al., 2008). This group further demonstrated that mesothelial cells secrete vitronectin, and conditioned media from mesothelial cells promoted ovarian cancer cell migration (Heyman et al., 2010). Moreover, a vitronectin blocking antibody was utilized and inhibited ovarian cancer cell migration *in vitro* (Heyman et al., 2010).

1.5.1.3 α5β1 integrin-Fibronectin

Fibronectin interaction with α5β1 integrins is posited as a major mechanism for mesothelial invasion due to the mesothelial basement membrane expressing fibronectin at higher levels than any other ECM component (Kenny et al., 2008; Lessan et al., 1999). Fibronectin is expressed by mesothelial cells (Kenny et al., 2014; Lessan et al., 1999). Additionally, fibronectin is highly expressed in ascites from ovarian cancer patients (Kenny et al., 2014). Moreover, conditioned media from mesothelial cells was shown to contain fibronectin that stimulated ovarian cancer migration (Rieppi et al., 1999). A recent study revealed that ovarian cancer cells stimulate mesothelial cell production of fibronectin thereby helping ovarian cancer cells metastasis (Kenny et al., 2014). In this same study, blocking antibodies to α5 or β1 were utilized and reduced metastasis in a mouse model of ovarian cancer (Kenny et al., 2014). Additionally, the interactions of α5β1-integrin with fibronectin mediate ovarian cancer cell attachment, and this attachment can be blocked utilizing neutralizing antibodies to α5β1 (Casey et al., 2001). Dr. Joan Brugge's research group showed that ovarian cancer spheroids clear the mesothelial monolayer by a force-dependent mechanism utilizing α5β1 integrin, talin I, and myosin expressed in the cancer cells

(Iwanicki et al., 2011). Specifically, ovarian cancer spheroids cluster α5β1 integrin and strongly adhere to mesothelial fibronectin. Talin I is recruited in the cancer cells to stabilize and reinforce the α5β1 adhesions, and the ovarian cancer cell α5β1 integrin and mesothelial fibronectin interaction activates myosin contractility in the tumor cells to exert force on the mesothelial cells for clearance (Iwanicki et al., 2011). The clearance of the mesothelial cells will allow the ovarian cancer spheroids to gain access to the underlying matrix. This mechanism has been termed mesothelial clearance (Iwanicki et al., 2011).

The interaction of α5β1 integrins and fibronectin is an important mediator in this invasive process by providing the point of attachment (Iwanicki et al., 2011; Niedbala et al., 1985). However, while the proposed mechanism of mesothelial clearance supports cell-matrix association, it does not demonstrate how traction force exerted on the mesothelial cells disrupts cell-cell junctions to allow the ovarian cancer cells to pass between them. Therefore, mesothelial invasion will also need to involve cell-cell adhesions between cancer and mesothelial cells.

1.5.2 Ovarian Cancer Cell Interaction with Mesothelial Cell Adhesion Molecule

Mesothelial cells express adhesion molecules such as intercellular adhesion molecule 1 (ICAM-1), platelet-endothelial cell adhesion molecule-1 (PECAM-1), and/or vascular cell adhesion molecule 1 (VCAM-1) (Bittinger et al., 1996; Gardner et al., 1995). ICAM-1 expression was induced in cultured mesothelial cells after tumor necrosis factor α (TNF-α) and interferon-γ (IFN-γ) stimulation (Garlanda and Mantovani, 1999; Jonjić et al., 1992). However, expression of the receptor for ICAM-1, lymphocyte function-associated antigen (LFA)-1, has not been reported

in ovarian cancer cells, lending to the idea that this adhesion molecule does not support ovarian cancer mesothelial invasion. Otherwise, PECAM-1 is an essential molecule for leukocyte transmigration for activated endothelial cells (Garlanda and Mantovani, 1999). PECAM-1 is expressed at intercellular junctions and endothelial barriers and increasing its expression would impede extravasation (Lertkiatmongkol et al., 2016). Additionally, blocking PECAM-1 inhibited trans-endothelial migration of leukocytes without affecting leukocyte adhesion (Muller et al., 1993). Moreover, mesothelial cells show a low constitutive expression of PECAM-1 which cannot be induced further by inflammatory cytokines suggesting this molecule could participate in an alternative mechanism to promote mesothelial invasion (Bittinger et al., 1996). Interestingly, VCAM-1 is expressed on mesothelial cells isolated from ascites of patients with ovarian cancer (Cannistra et al., 1994). Additionally, VCAM-1 binds α4β1 integrins, which are expressed on ovarian cancer cells (Cannistra et al., 1995). Furthermore, VCAM-1 promotes ovarian cancer mesothelial invasion and metastatic progression (Slack-Davis et al., 2009). Thus, this dissertation will highlight the importance of VCAM-1 as an important factor in governing ovarian cancer mesothelial invasion and metastasis.

1.5.2.1 The Structural and Functional Role of VCAM-1

VCAM-1 is a type I transmembrane glycoprotein characterized by seven extracellular C2-type immunoglobulin (Ig) domains (Cybulsky et al., 1991; Hession et al., 1992; Hession et al., 1991; Osborn et al., 1989; Pigott et al., 1992). While the seven-domain form of VCAM-1 is the most common form of VCAM-1, an alternatively spliced form has been identified that lacks the

4th Ig domain through alternate posttranscriptional splicing resulting in a six-domain form of VCAM-1 (Cybulsky et al., 1991; Hession et al., 1992; Osborn et al., 1989) (Figure 1.7). VCAM-1 sequences are quite similar across species, such that the rat, mouse, and human molecules are approximately 75% identical (Hession et al., 1992). The alignments of VCAM-1 cytoplasmic domain amino acid sequences among different species shows significant homology with conservation at 17 of 19 amino acid residues (Chuang et al., 1997).

VCAM-1 is most commonly studied on endothelial cells during inflammation. Its expression is induced by pro-inflammatory cytokines such as interleukin-1β (IL-1β), interleukin-4 (IL-4), IFN-γ, and TNF-α (Carlos and Harlan, 1994; Croft et al., 1999; Swerlick et al., 1992). Activated mesothelium, smooth muscle cells, and macrophages in atherosclerotic plaques express VCAM-1 (Cannistra et al., 1994; Carlos and Harlan, 1994; O'Brien et al., 1993; Osborn et al., 1989). Normally, VCAM-1 is not expressed on unstimulated endothelium and mesothelium (Carlos and Harlan, 1994). Upon stimulation, VCAM-1 is expressed transiently and then rapidly internalized and turned over (Meerschaert and Furie, 1994; Meerschaert and Furie, 1995; Swerlick et al., 1992). The VCAM-1 co-receptor or ligand is α4β1 integrin, and this integrin is expressed on lymphocytes, basophils, eosinophils, NK cells, and monocytes (Bhasin et al., 2004; Larbi et al., 2000; Meerschaert and Furie, 1994; Meerschaert and Furie, 1995). The engagement of VCAM-1 and α4β1 integrin mediates the binding of these leukocytes to the mesothelium (Cannistra et al., 1994) and stimulates the formation of actin-rich membrane extensions that form docking structures or transmigratory cups on the endothelium that facilitate firm adhesion and extravasation of leukocytes (Barreiro et al., 2002; Carman and Springer, 2004). This process ultimately leads to

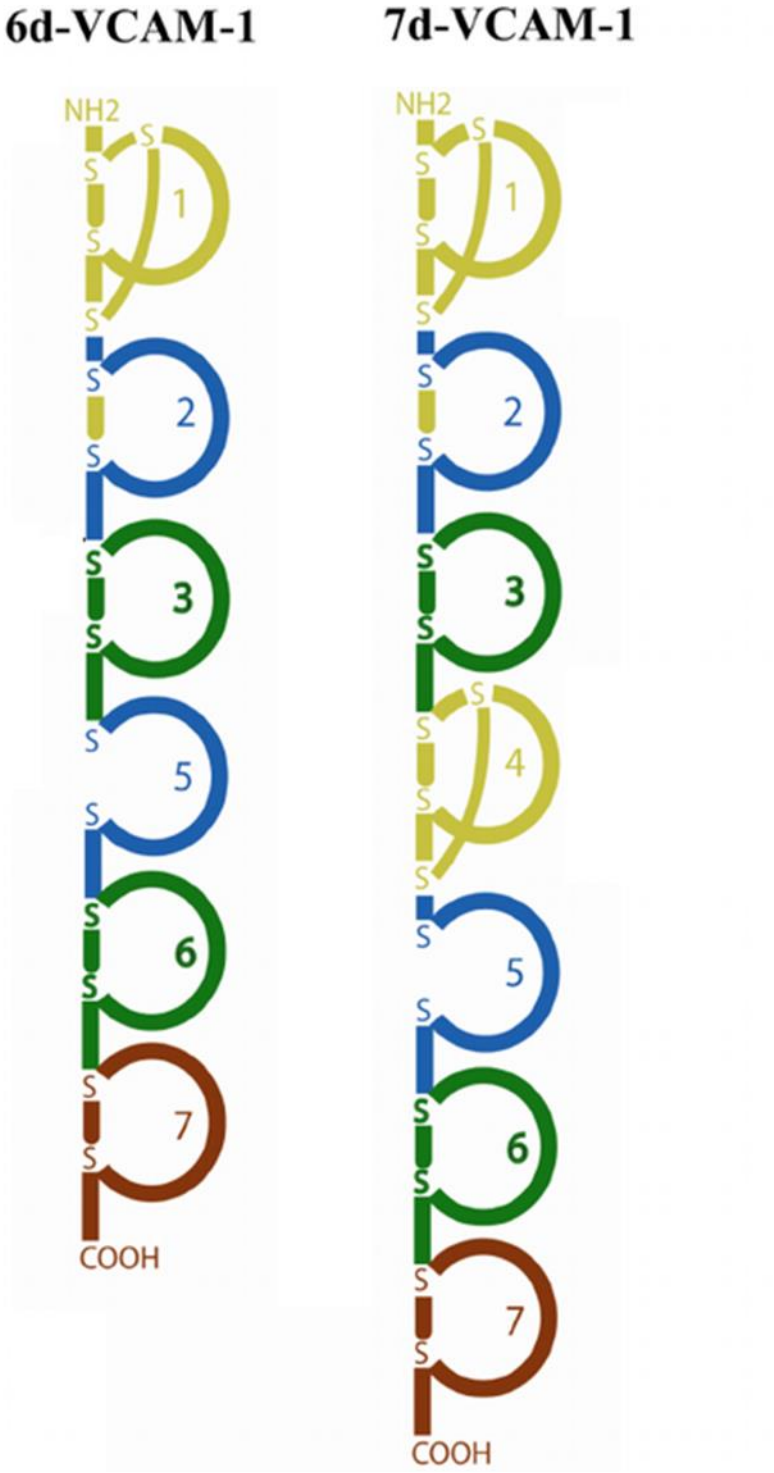
6d-VCAM-1
7d-VCAM-1
NH2
1
2
3
5
6
7
COOH
NH2
1
2
3
4
5
6
7
COOH

Figure 1.7. Structure of VCAM-1 splice forms. The seven domain (7d) form is considered the predominant form of VCAM-1. A six domain (6d) form (the 4th domain missing) can also occur. Adapted from (Barthel et al., 2008).

gap formation between endothelial cells to allow passage of the leukocytes (Barreiro et al., 2002). In these docking structures, adaptor and linker molecules such as ezrin, radixin, and moesin are recruited after ligation of VCAM-1 resulting in the subsequent activation of the Rho-p160ROCK pathway (Barreiro et al., 2002). The interaction of VCAM-1 and α4β1 integrin results in endothelial cell actin-based cytoskeleton to polymerize, cross-link, and reorganize into actin stress fibers (Barreiro et al., 2002).

1.5.2.2 The Functional Role of VCAM-1 in Metastatic Progression of Ovarian Cancer

VCAM-1 interaction with α4β1 integrin is implicated in ovarian cancer metastatic progression. Ovarian cancer mesothelial invasion is mediated, in part, by the interaction of α4β1 integrin, found on the cancer cells, and its ligand, VCAM-1, found on the mesothelial cells (Scalici et al., 2013; Slack-Davis et al., 2009) (Figure 1.8). Previously, a role for VCAM-1 was demonstrated in peritoneal metastasis (Slack-Davis et al., 2009). Utilizing a co-culture assay system to measure the ability of cancer cells to invade the mesothelium, Slack-Davis et. al showed that functional blocking antibodies to VCAM-1 or α4β1integrin inhibited mesothelial invasion of the cancer cells by 40% (Slack-Davis et al., 2009). Furthermore, treatment of mesothelial cells with VCAM-1 siRNA or cancer cells with α4 siRNA decreased mesothelial invasion (Slack-Davis et al., 2009). Moreover, inhibition of VCAM-1 function reduced tumor burden and mesothelial invasion and increased survival in a mouse model implicating VCAM-1 as an important regulator of ovarian cancer metastasis (Slack-Davis et al., 2009).

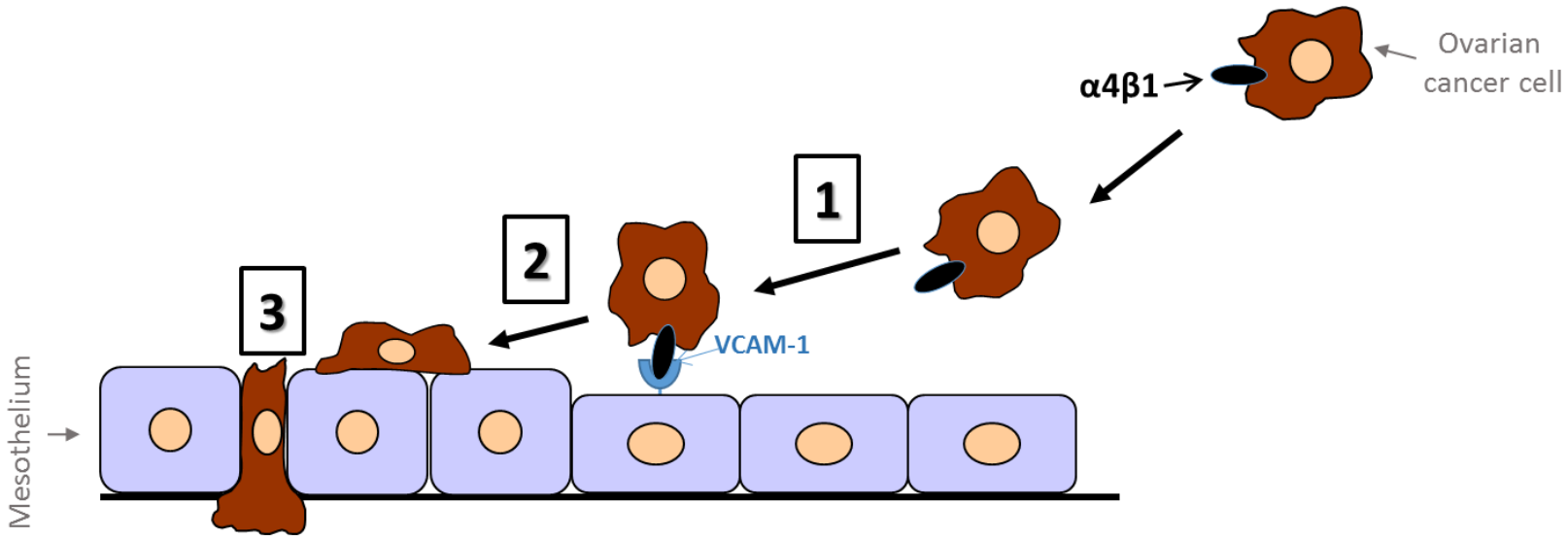
α4β1
Ovarian cancer cell
1
2
3
VCAM-1
Mesothelium

Figure 1.8. Trans-invasion of ovarian cancer through the mesothelium. This process is believed to be like leukocyte extravasation where the cancer cells will roll over the mesothelium (1), adhere by α4β1 integrin interaction with VCAM-1 and spread onto the mesothelium (2), and trans-invade the mesothelium (3).

Patient data also support a role for VCAM-1 in metastatic progression. Particularly, increased VCAM-1 mRNA and protein expression was observed on the mesothelium of ovarian cancer patients compared with the peritoneum of patients with benign gynecologic conditions (Slack-Davis et al., 2009; Wang et al., 2005) (Figure 1.9). Moreover, through a retrospective analysis of omental or peritoneal biopsies, the incidence of VCAM-1 expression increased with tumor stage and is associated with peritoneal metastasis (Scalici et al., 2013). Recently, mesothelial VCAM-1 expression was reported to be associated with an unfavorable prognosis for ovarian cancer patients (Scalici et al., 2016). Specifically, the data showed a significantly poorer progression-free and overall survival in patients expressing mesothelial VCAM-1 (Scalici et al., 2016). These observations implicate a potential role for VCAM-1 to function as a marker of ovarian cancer progression.

1.6 Significance and overview

The factors and conditions that promote VCAM-1 expression on the mesothelium in the ovarian cancer metastatic microenvironment are poorly understood. Intriguingly, components within the ovarian cancer metastatic microenvironment, such as growth factors found at elevated levels in the malignant ascites, may fulfill this regulatory role. With the elevated concentrations of LPA in ovarian cancer patients (Xiao et al., 2001; Xiao et al., 2000; Xu et al., 1995) and its ability to induce VCAM-1 expression in endothelial cells (Shimada and Rajagopalan, 2010; Sun and Yang, 2010), this bioactive lipid is an attractive candidate for regulating VCAM-1 expression

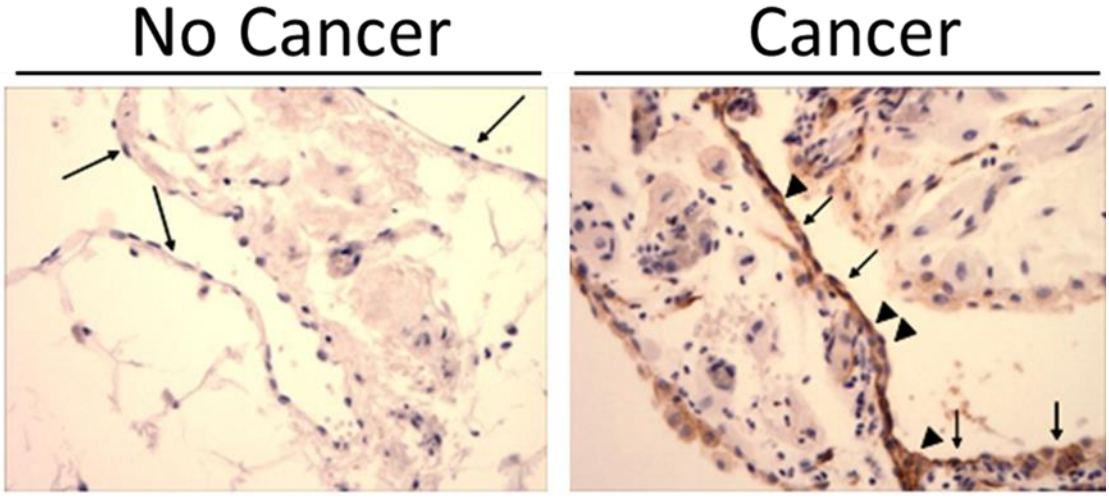
No Cancer
Cancer

Figure 1.9. Mesothelial VCAM-1 expression. Immunohistochemistry was used to detect VCAM-1 expression (arrowhead) on the mesothelium (arrow) of peritoneal biopsies from women with no cancer or with ovarian cancer. Adapted from (Slack-Davis et al., 2009).

observed on the mesothelium. Therefore, the overall objective is to evaluate the contributions of LPA in promoting mesothelial invasion and tumor progression through the regulation of mesothelial VCAM-1 within the ovarian cancer metastatic microenvironment.

Previous studies demonstrated that LPA stimulates ovarian cancer metastasis in orthotopic and syngeneic ovarian cancer mouse models (Kim et al., 2006; Li et al., 2009). Daily injection or implantation of a pump producing LPA significantly increases tumor burden and enhances tumor metastasis *in vivo* (Kim et al., 2006; Li et al., 2009). While the effects of LPA on ovarian cancer progression are clear, the effects of LPA metabolism within the tumor microenvironment on peritoneal metastasis have not been reported. **Chapter 2** reports the effects of LPA metabolism within the tumor microenvironment to promote peritoneal metastasis. We hypothesized that increased LPA within the tumor microenvironment would promote ovarian cancer tumor progression and metastasis. We tested this hypothesis by utilizing a syngeneic mouse model of ovarian cancer and mice deficient in LPP1 expression (LPP1 KO). We evaluated mesothelial invasion and tumor progression, as well as mesothelial VCAM-1 expression. **Chapter 3**, documents a role for LPA in regulating mesothelial VCAM-1 expression. We hypothesize that LPA promotes mesothelial invasion through the regulation of mesothelial VCAM-1 expression within the ovarian cancer tumor microenvironment (Figure 1.10). We tested this hypothesis by inhibiting or blocking the activity of the LPA receptor, LPA1, in mesothelial cells to determine how LPA influences mesothelial invasion and regulates mesothelial VCAM-1 expression. Finally, in **Chapter 4**, we discuss the importance of the *in vivo* and *in vitro* studies described in **Chapters 2** and **3** in context to what is known in the field. Future experiments are proposed to elucidate the

LPA-mediated signaling pathways leading to VCAM-1 expression. Moreover, experiments have been proposed to determine a role for the tumor cells in initiating VCAM-1 expression. These studies are necessary to provide insights regarding the role LPA plays in promoting and regulating VCAM-1 expression within the ovarian cancer metastatic microenvironment because identifying the mechanism that regulate ovarian cancer metastasis will provide much needed additional opportunities for the treatment of ovarian cancer.

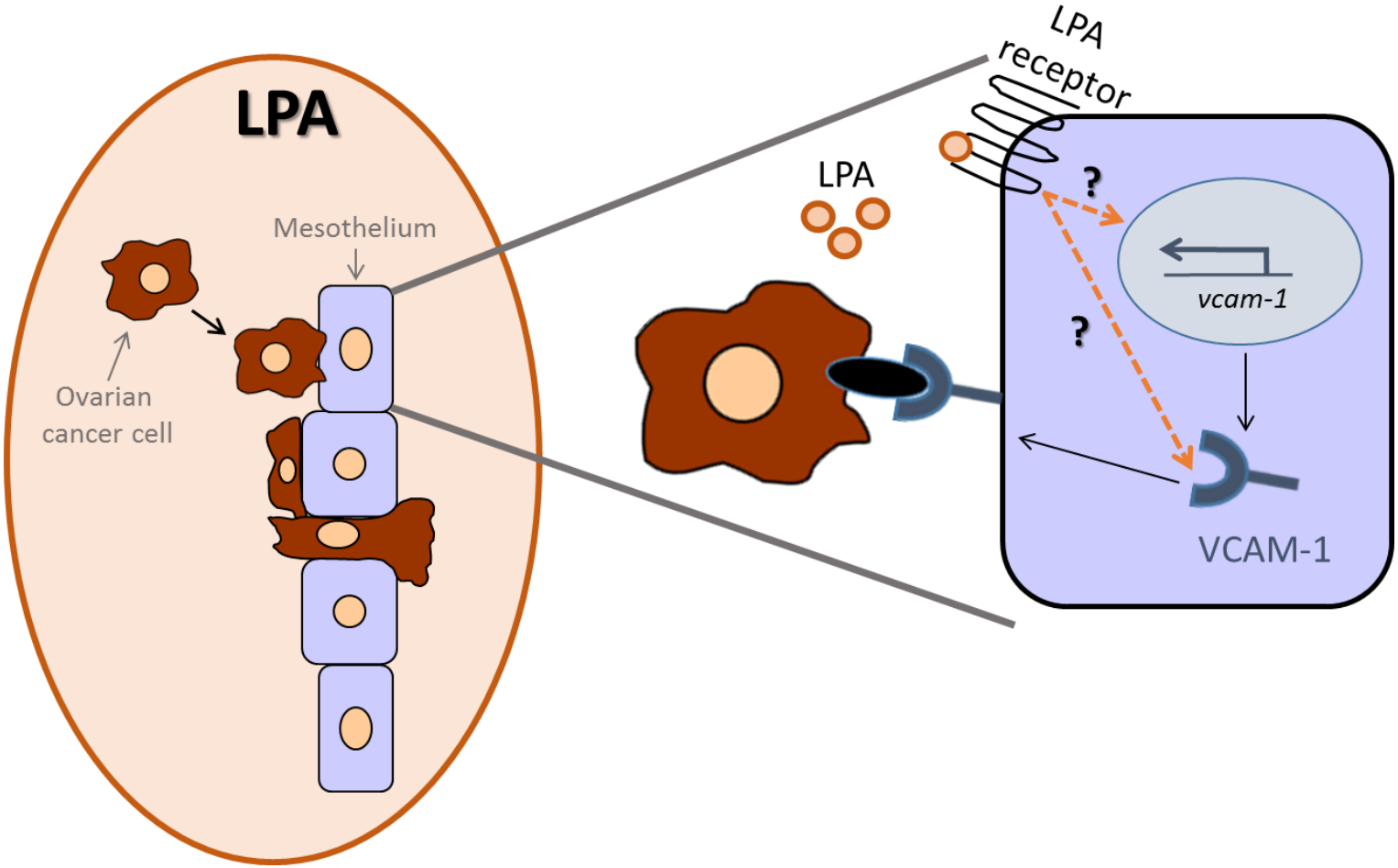
LPA
Mesothelium
Ovarian
cancer cell
LPA
receptor
LPA
?
?
vcam-1
VCAM-1

Figure 1.10 Model of hypothesis. LPA targets the ovarian cancer metastatic microenvironment to promote mesothelial invasion through the upregulation of mesothelial VCAM-1 expression.

Chapter 2. Increased Early Tumorigenesis and Metastasis in LPP1 KO Mice.

*Adapted from Nakayama, J., **Raines, T.A.**, Lynch, K.R., Slack-Davis, J.K. (2015). Decreased peritoneal ovarian cancer growth in mice lacking expression of lipid phosphate phosphohydrolase 1. PLoS One, 10 (13), e0120071.

**All figures, except for Figure 2.1A, were completed by TAR. Figure 2.1A was completed by JN.

2.1 Abstract

Lysophosphatidic acid (LPA) is a bioactive lipid that enhances ovarian cancer cell proliferation, migration and invasion *in vitro* and stimulates peritoneal metastasis *in vivo*. LPA is generated through the action of autotaxin or phospholipases, and degradation begins with lipid phosphate phosphohydrolase (LPP)-dependent removal of the phosphate. While the effects of LPA on ovarian cancer progression are clear, the effects of LPA within the tumor microenvironment on peritoneal metastasis have not been reported. We examined the contribution of lipid phosphatase activity to ovarian cancer peritoneal metastasis using mice deficient in LPP1 expression. Homozygous deletion of LPP1 (LPP1 KO) results in elevated levels and decreased turnover of LPA *in vivo*. Within two weeks of intraperitoneal injection of syngeneic mouse ovarian cancer cells, we observed enhanced tumor seeding in the LPP1 KO mice compared to wild type. Additionally, in LPP1 KO mice we observed a higher incidence of microscopic tumor nodules and mesothelial invasion as compared to wild type mice, which was coincident with increased expression of vascular cell adhesion molecule-1 (VCAM-1); VCAM-1 is elevated on the mesothelium of OC patients where it functions to promote mesothelial invasion and tumor progression. Together, these observations demonstrate that the elevated levels of LPA in LPP1 KO mice affect the tumor microenvironment to promote mesothelial invasion *in vivo*.

2.2 Introduction

Lysophosphatidic acid (LPA) is a bioactive lipid that regulates several cellular functions critical for tumorigenesis and metastasis including proliferation, survival, cytoskeletal reorganization, migration, invasion and cytokine production (Bian et al., 2006; Fang et al., 2000a; Fang et al., 2000b; Goldsmith et al., 2011; Mills and Moolenaar, 2003). The importance of LPA to ovarian cancer progression was established when it was identified as a growth factor in malignant ascites (Xu et al., 1995). LPA stimulates cellular activities via at least three (LPA1, LPA2, and LPA3) and perhaps as many as 6 (LPA4-6) G-protein coupled receptors. LPA1 is expressed on normal ovarian surface epithelium; the expression of LPA2 and LPA3 is induced in the cancer cells (Fang et al., 2000a). Upon binding its receptor, LPA stimulates ovarian cancer cell proliferation through activation of Gα12 (Goldsmith et al., 2011). All three receptors regulate ovarian cancer cell migration and invasion directly by activating pro-migratory Rac and Rho-dependent signaling pathways (Bian et al., 2006; Bian et al., 2004). In addition, LPA promotes ovarian cancer growth and metastasis indirectly by stimulating the production of proteases (MMP and urokinase plasminogen activator (uPA) (Fishman et al., 2001; Li et al., 2005), and cytokines (IL-6 and IL-8), which play a role in ovarian cancer invasion and metastasis (So et al., 2004). LPA binding to LPA2 or LPA3 increases production of IL-6, IL-8, and VEGF. Indeed, knockdown of LPA2 or LPA3 decreases IL-6 production, and their over-expression leads to increased serum levels of IL-6 and VEGF, increased tumor burden and shortened survival times in a mouse model of ovarian cancer peritoneal metastasis; modulation of LPA1 had no significant effect in this study (Yu et al., 2008).

LPA is produced by a variety of cells within the tumor microenvironment including platelets, mesothelial cells, adipocytes, endothelial cells and ovarian cancer cells (Pagès et al., 2001; Ren et al., 2006), and in the absence of cancer, concentrations are tightly maintained below one μM. Levels of LPA are significantly elevated in plasma and ascites (up to 50 μM) of women with ovarian cancer (Xiao et al., 2001), and increased plasma LPA has been suggested as a biomarker for ovarian cancer (Sutphen et al., 2004). Members of the phospholipase A_1 (PLA_1) and PLA_2 families remove a fatty acid chain from phosphatidic acid to form LPA. Autotaxin (ATX), an extracellular lysophospholipase D also generates LPA following the removal of choline from lysophosphatidylcholine. PLA_2 and autotaxin are elevated in ovarian cancer patients (Cai et al., 2012; Tokumura et al., 2007), and a positive feedback loop exists between vascular endothelial growth factor (VEGF) and ATX production by ovarian cancer cells (Ptaszynska et al., 2008).

LPA catabolism is initiated by lipid phosphate phosphohydrolases (LPPs), types 1, 2 and 3, which remove the phosphate to generate monoacylglycerol (MAG). MAG is further cleaved by monoacylglycerol lipase to release the fatty acid chain from glycerol. LPP1 and LPP3 expression are reduced in human ovarian cancers relative to normal ovarian tissue (Tanyi et al., 2003b), while forced over-expression of either LPP1 or LPP3 decreases tumorigenesis of ovarian cancer cells in mouse models presumably from decreased levels of LPA (Tanyi et al., 2003a; Tanyi et al., 2003b).

In addition to regulating ovarian cancer cell proliferation, survival, migration, and invasion in vitro, the ability of LPA to promote ovarian cancer invasion and growth has been demonstrated in mouse models of peritoneal metastasis; daily injection or implantation of pumps producing high concentrations of LPA increased tumor burden in immune compromised and syngeneic mouse

models (Kim et al., 2006; Li et al., 2009). However, the effects of LPA metabolism within the tumor microenvironment on peritoneal metastasis have not been reported. We sought to determine whether impaired LPA phosphatase (specifically LPP1) activity affected ovarian cancer peritoneal metastasis. Rather than target LPP1 activity in the tumor cells, we examined the effect of LPP1 loss in the tumor microenvironment using mice lacking LPP1 expression following the insertion of an exon-trap (LPP1 KO) (Tomsig et al., 2009) and syngeneic mouse ovarian cancer cells (Roby et al., 2000). Lipid phosphatase activity in LPP1 KO mice is markedly decreased (35-95%) in multiple tissues, including those found within the peritoneal cavity (Tomsig et al., 2009). Additionally, plasma LPA is metabolized four times more slowly than wild type mice, and plasma concentrations of LPA are significantly elevated in the LPP1 KO mice (Tomsig et al., 2009). Here, we report that peritoneal ovarian cancer growth in LPP1 KO mice was elevated as early as two weeks after initiation relative to wild type controls; LPP1 KO mice harbored increased invasive microscopic nodules; and mesothelial vascular cell adhesion molecule 1 (VCAM-1) expression was increased in LPP1 KO mice. Together, these observations support the notion that LPA influences the tumor microenvironment to promote mesothelial invasion *in vivo*, potentially through the regulation of mesothelial VCAM-1 protein expression.

2.3 Results

2.3.1 Increased Tumor Seeding of the Peritoneum in LPP1 KO Mice

LPA stimulates many aspects of ovarian cancer cell biology including ovarian cancer growth and progression (Bian et al., 2006; Bian et al., 2004; Fang et al., 2000a; Fishman et al.,

2001; Goldsmith et al., 2011; Li et al., 2005; So et al., 2004; Yu et al., 2008); however a role for LPA in the tumor microevinronmnt is underexplored. We investigated the effect of reduced LPA turnover on metastatic peritoneal ovarian cancer growth and progression using mice lacking the lipid phosphatase, LPP1 (LPP1 KO) and a syngeneic mouse ovarian cancer cell line, ID8ip2Luc. *In vivo* imaging of mice following intraperitoneal (IP) injection of ID8ip2Luc cells revealed increased luminescence in LPP1 KO mice compared to wild type within two weeks (Figure 2.1A). The weights of the omentums were not different (Figure 2.1B). Importantly, significantly more microscopic nodules were detected in omentum from LPP1 KO mice compared to wild type (Figure 2.1C). Together, these observations indicate that loss of LPP1 in the tumor microenvironment facilitates tumor seeding and mesothelial invasion of the peritoneal cavity.

2.3.2 LPP1 KO Mice Exhibit Increased Invasive Microscopic Tumor Nodules

Since LPP1 KO mice demonstrated increased tumor seeding, H&E stained sections of omentums from wild type and LPP1 KO were evaluated for invasion. Tissues were scored for the presence of tumors and whether they were invasive (Figure 2.2A). Noninvasive tumors show a smooth interface between tumor, and underlying tissue and invasive tumors spider into the fat of the omentums (Figure 2.2A). Evaluation of H&E stained sections of the omentum revealed the presence of microscopic tumor nodules (Figure 2.2A), consistent with previous observations (Slack-Davis et al., 2009). LPP1 KO mice were more likely to harbor invasive lesions as compared to wild type mice (Figure 2.2B). Together, these observations indicate that loss of LPP1 in the tumor microenvironment facilitates mesothelial invasion.

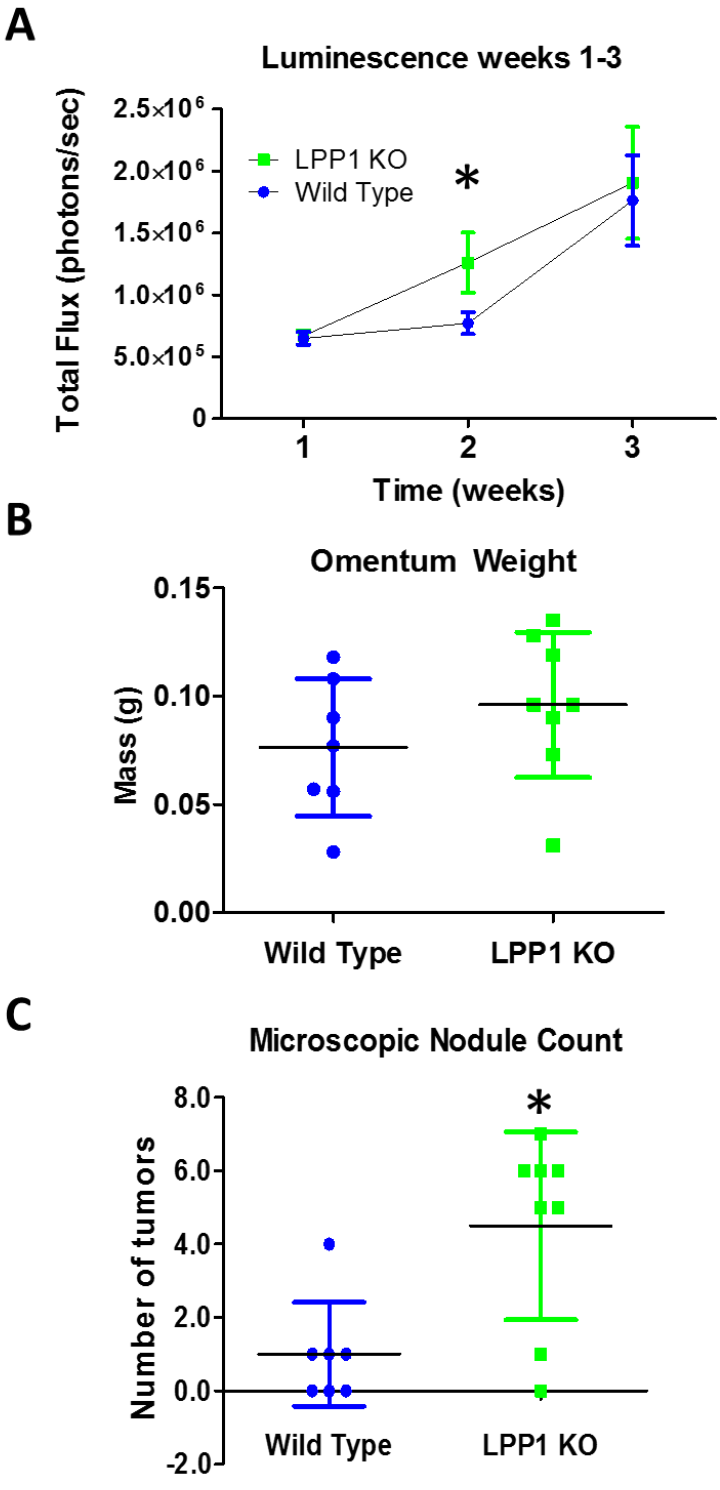
A
Luminescence weeks 1-3
Total Flux (photons/sec)
2.5×10⁶
2.0×10⁶
1.5×10⁶
1.0×10⁶
5.0×10⁵
0
LPP1 KO
Wild Type
*
1
2
3
Time (weeks)
B
Omentum Weight
Mass (g)
0.15
0.10
0.05
0.00
Wild Type
LPP1 KO
C
Microscopic Nodule Count
Number of tumors
8.0
6.0
4.0
2.0
0.0
-2.0
*
Wild Type
LPP1 KO

Figure 2.1. Increased peritoneal tumor seeding in LPP1 KO mice**. A.** Mice (wild type n=10; LPP1 KO n=12) were imaged weekly following tumor initiation to monitor tumor growth. Data represent mean total flux (photons/second) ± std err and were analyzed by 2-way ANOVA followed by Tukey's multiple comparisons test. **B.** Omentums were removed and weighed two weeks after tumor initiation from wild type and LPP1 KO mice. Data represent mean +/- std dev for all animals, each of which is indicated by a single point. **C.** The total number of microscopic tumor nodules was counted in an individual, randomly selected, H&E stained section of omentum per mouse obtained two weeks after tumor initiation (WT n=7; LPP1 KO n=8). Data represent the mean ± std dev of all animals (indicated by individual points) and were analyzed with a Student t-test; *, $p < 0.05$.

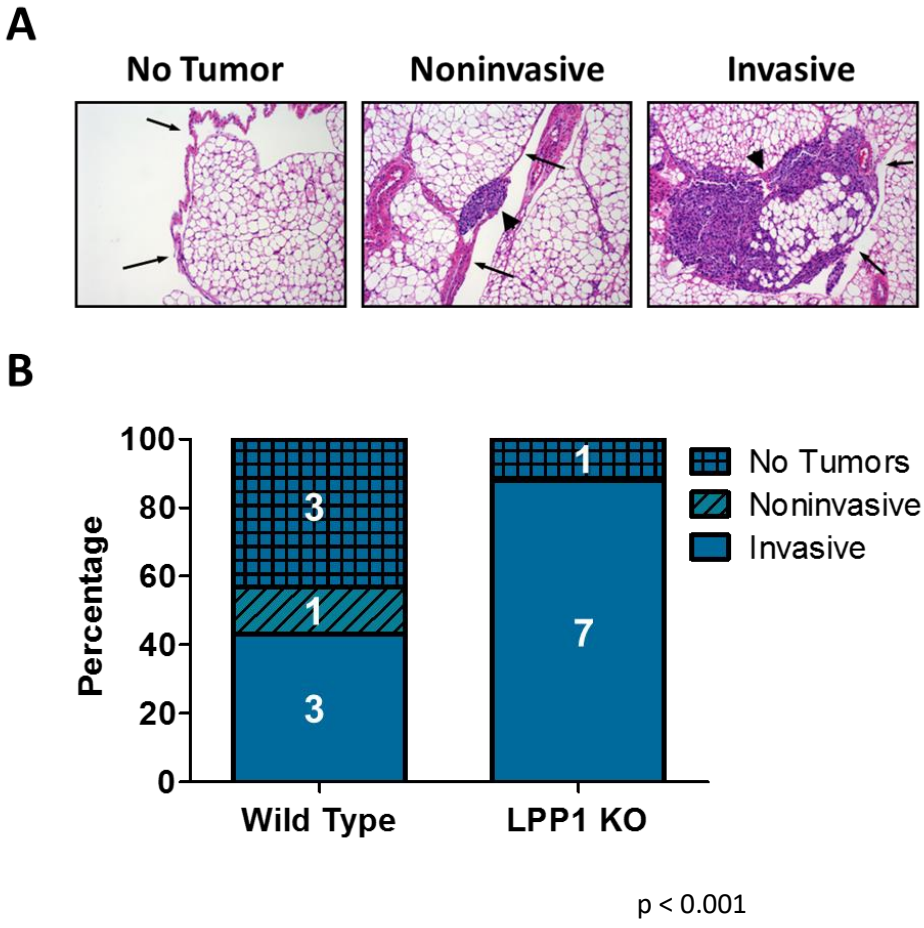
A
No Tumor
Noninvasive
Invasive
B
Percentage
100
80
60
40
20
0
3
1
3
1
7
No Tumors
Noninvasive
Invasive
Wild Type
LPP1 KO
p < 0.001

Figure 2.2. LPP1 KO mice have increased mesothelial invasion. ID8ip2Luc ovarian cancer cells were injected IP into C57/Bl6 (WT, n = 7) or LPP1 KO (n = 8) mice. **A.** H&E stained sections of omentum were evaluated for microscopic tumors and the extent of invasion. Arrows indicate the mesothelium; arrowheads indicate tumor. Non-invasive tumors were characterized as having a smooth interface between the tumor and underlying tissue. Invasive tumors were scored as those spidering through and taking over the underlying tissue, in this case, omental fat. **B.** The percentage of wild type or LPP1 KO mice with invasive tumors (solid bars), non-invasive tumors (striped bar), and no tumors (checkered bars) 2 weeks after tumor initiation. Number of mice per outcome is indicated. Significance determined by Fisher's Exact Test; *, $p < 0.001$.

2.3.3 Mesothelial VCAM-1 Expression Increased in LPP1 KO Mice

Previously, a role for VCAM-1 expressed on the mesothelium was demonstrated as an important regulator of ovarian cancer invasion *in vitro* and *in vivo* (Slack-Davis et al., 2009). Particularly, VCAM-1 was expressed on the mesothelium of patients with ovarian cancer where it functions to promote mesothelial invasion. Additionally, mice treated with a VCAM-1 blocking antibody had more non-invasive tumors as compared to the control treatment group demonstrating that VCAM-1 is also an important regulator of mesothelial invasion. Next, we sought to determine VCAM-1 expression on the mesothelium. Interestingly, LPP1 KO mice had a higher incidence of mesothelial VCAM-1 expression (Figure 2.3A and B) offering the possibility that LPA regulates VCAM-1 expression to promote mesothelial invasion.

2.4 Discussion

LPA is an important regulator of ovarian cancer growth and metastasis. In addition to the increased levels found in ascites, ATX activity is elevated, and the tumors themselves have a de novo expression of LPA receptors (LPA2 and LPA3) (Fang et al., 2000a) and decreased expression of LPP1 and LPP3 (Tanyi et al., 2003a; Tanyi et al., 2003b). Here, we show that loss of LPP1 expression within the tumor microenvironment has an effect on the establishment and growth of ovarian cancer within the peritoneal cavity. Loss of LPP1 expression within the tumor microenvironment led to increased tumor seeding following IP injection of ovarian cancer cells, increased invasive microscopic tumor nodules, and increased mesothelial VCAM-1 expression.

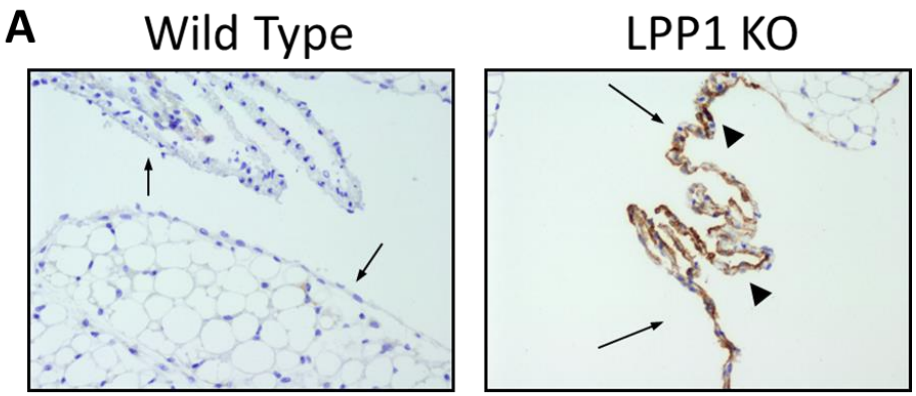
A
Wild Type
LPP1 KO

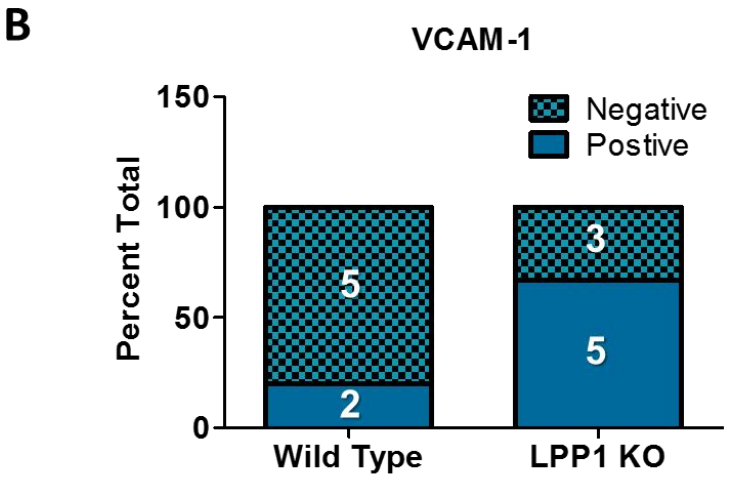
B
VCAM-1
Negative
Postive
Percent Total
150
100
50
0
5
2
3
5
Wild Type
LPP1 KO

$p < 0.001$

Figure 2.3. LPP1 KO mice have increased VCAM-1 expression. **A.** Omentums from wild type (left panel) and LPP1 KO (right panel) mice were obtained 2 weeks after tumor initiation and stained for VCAM-1 expression using IHC (see Materials and Methods). Representative images depict the mesothelium (arrows) and positive VCAM-1 staining (arrowheads) in the LPP1 KO mice with the lack of VCAM-1 reactivity on the mesothelium of wild type mice. **B.** The percentage wild type or LPP1 KO mice with (positive, solid bars) or without (negative, checkered bars) mesothelial VCAM-1 staining by IHC. Number of mice per outcome is indicated. Significance determined by Fisher's Exact Test; *, $p < 0.001$.

LPP1 KO mice have increased plasma LPA levels due to reduced LPA turnover (Tomsig et al., 2009). We observed an increase in tumor seeding early after tumor initiation in LPP1 KO mice. These data are consistent with previous findings which revealed that LPA promoted tumorigenesis *in vivo* (Li et al., 2009). Specifically, utilizing a syngeneic mouse model of ovarian cancer, daily injection of LPA showed increased tumor development as compared to mice injected with control PBS (Li et al., 2009). Moreover, immunocompromised mice orthotopically transplanted with human ovarian cancer cells onto their ovaries and also injected daily with LPA demonstrated early tumor initiation and development as compared to control (Kim et al., 2006; Sengupta et al., 2006). These findings, in conjunction with the literature, suggest that LPA in the ovarian cancer tumor microenvironment promotes tumorigenesis.

In this study, an increase in mesothelial invasion was observed in LPP1 KO mice. Furthermore, LPP1 KO mice had more invasive tumor nodules as compared to wild type. These results are consistent with the effects of LPA on cell migration and invasion of established and primary ovarian cancer cells (Bian et al., 2006; Fang et al., 2000a; Sengupta et al., 2006). LPA has also been reported to stimulate mesothelial invasion in cell culture models (Ren et al., 2006) and *in vivo*, although a mechanism has not been defined (Li et al., 2009). Interestingly, LPP1 KO mice had a higher incidence of mesothelial VCAM-1 expression. Previously, a role for mesothelial VCAM-1 was demonstrated in the regulation of ovarian cancer invasion *in vitro* and *in vivo* (Slack-Davis et al., 2009). Particularly, VCAM-1 was elevated on the mesothelium of ovarian cancer patients where it functions to promote mesothelial invasion and tumor progression (Slack-Davis et al., 2009). Taken together, these observations offer the possibility that LPA might regulate

VCAM-1 expression to promote mesothelial invasion. However, LPP1 hydrolyzes phosphates in other bioactive lipids, including sphingosine-1-phosphate (S1P), which stimulates ovarian cancer cell invasion and migration (Park et al., 2007a; Sciorra and Morris, 2002; Wang et al., 2008). Moreover, VCAM-1 expression can be induced by S1P (Sashio et al., 2012). Therefore, the loss of LPP1 might affect VCAM-1 expression by increasing levels of more than one bioactive lipid.

Chapter 3. LPA-dependent Regulation of VCAM-1 in the Ovarian Cancer Metastatic Microenvironment Promotes Mesothelial Invasion.

3.1 Abstract

The ovarian cancer microenvironment plays an important role in metastatic progression. Interactions between ovarian cancer cells and non-transformed mesothelial cells facilitate ovarian cancer cell attachment to and invasion through the mesothelium, which is a necessary step in metastatic dissemination. Lysophosphatidic acid (LPA) is a bioactive lipid that has pleotropic cellular effects and is abundant in a variety of pathological conditions including ovarian cancer where it promotes cancer cell growth and metastasis. In this study, we examined the effects of LPA on mesothelial cells to regulate mesothelial invasion. Utilizing a co-culture assay system and inhibiting the activity or expression of the LPA receptor, LPA1, in human mesothelial cells reduced ovarian cancer cell invasion of mesothelial monolayers. We previously demonstrated that vascular cell adhesion molecule-1 (VCAM-1), which is expressed on the mesothelium of ovarian cancer patients, regulates mesothelial invasion. Here, we report that LPA1 knockdown in mesothelial cells or treatment with an antagonist targeting LPA1 decreased VCAM-1 protein and mRNA expression. Metabolic labeling of human mesothelial cells indicated a significant decrease in VCAM-1 protein synthesis in cells lacking LPA1 expression compared to control. Importantly, exogenous expression of VCAM-1 in cells deficient in LPA1 expression restored mesothelial invasion. Taken together, these observations indicate that LPA regulates VCAM-1 expression on the mesothelium to promote ovarian cancer cell invasion.

3.2 Introduction

Ovarian cancer is the most lethal gynecologic malignancy due in large part to the high incidence of advanced-stage, metastatic disease at the time of diagnosis (Ozols, 2005). Ovarian cancer metastasizes by forming secondary implants throughout the peritoneal cavity. Following detachment from the primary tumor site, ovarian cancer cells attach to and invade through the mesothelium, a single cell layer of mesothelial cells that lines the peritoneal cavity, to access underlying stroma (Eder et al., 2000; Iwanicki et al., 2011; Slack-Davis et al., 2009; Strobel and Cannistra, 1999). Ovarian cancer invasion of the mesothelium is associated with an unfavorable prognosis (Bell et al., 2004). Mesothelial cells actively participate in promoting ovarian cancer cell invasion by 1) producing growth factors and extracellular matrix proteins that attract ovarian cancer cells to sites of invasion (Kenny et al., 2014; Lee et al., 1993; Offner et al., 1996; Ren et al., 2006; Said et al., 2007; Stadlmann et al., 2005) and 2) expressing adhesion molecules that allow ovarian cancer cell attachment and passage through the mesothelium (Cannistra et al., 1993; Lessan et al., 1999; Slack-Davis et al., 2009). We demonstrated that expression of vascular cell adhesion molecule-1 (VCAM-1), a cell surface receptor, is induced on the mesothelium of ovarian cancer patients (Slack-Davis et al., 2009). Functionally blocking mesothelial VCAM-1 inhibits ovarian cancer cell invasion of the mesothelium, decreases tumor burden, and increases survival in a mouse model of ovarian cancer peritoneal metastasis (Slack-Davis et al., 2009). Moreover, VCAM-1 expression increases with tumor stage (Scalici et al., 2013) and is associated with an unfavorable prognosis(Scalici et al., 2016). However, the mechanisms that regulate mesothelial VCAM-1 expression within the ovarian cancer microenvironment are unclear.

Increased concentrations of lysophosphatidic acid (LPA) are found in both malignant ascites and plasma samples of ovarian cancer patients (Sutphen et al., 2004; Xiao et al., 2001; Xiao et al., 2000; Xu et al., 1995). LPA stimulates proliferation, survival, adhesion, migration, and invasion of ovarian cancer cells (Bian et al., 2006; Fang et al., 2000a; Mills and Moolenaar, 2003). However, apart from stimulating angiogenesis (Jeon et al., 2010), little is known about the effects of LPA on the non-transformed cells within the tumor microenvironment. In **Chapter 2**, we showed that intraperitoneal injection of mouse ovarian cancer cells into mice that lack expression of the LPA phosphatase, LPP1 (LPP1 KO), which results in elevated circulating concentrations of LPA produces a higher incidence of tumors invading the mesothelium compared to wild type mice (Nakayama et al., 2015). Also, LPP1 KO mice display increased expression of VCAM-1 on the mesothelium shortly after tumor initiation (Nakayama et al., 2015). Based on these observations, we investigated whether LPA targets the mesothelium to promote *in vitro* ovarian cancer invasion through the regulation of mesothelial VCAM-1 expression.

3.3 Results

3.3.1 LPA Receptor Expression in Mesothelial Cells

LPA is abundant in the ovarian cancer metastatic microenvironment where it promotes ovarian cancer cell migration and invasion (Bian et al., 2006; Fang et al., 2000a; Kim et al., 2006; Li et al., 2009; Mills and Moolenaar, 2003; Nakayama et al., 2015); however, apart from stimulating angiogenesis (Jeon et al., 2010), a role for LPA in the tumor microenvironment is poorly understood. Previous studies in human peritoneal mesothelial cells isolated from gastric cancer patients demonstrated *LPA1* was the predominately expressed receptor with weak

expression or no expression of *LPA2* or *LPA3*, respectively (Sako et al., 2006). Using multiple primer sets (Figure 3.1A), we confirmed abundant expression of *LPA1* and low expression of *LPA2* by quantitative RT-PCR (qRT-PCR) in LP9 mesothelial cells isolated from a woman with ovarian cancer (Connell and Rheinwald, 1983) (Figures 3.1B and C). *LPA3* was not expressed (Figures 3.1B and C). The results are in accordance with the previous findings that *LPA1* and *LPA2* are expressed in mesothelial cells.

3.3.2 LPA1 Promotes Ovarian Cancer Cell Trans-Mesothelial Invasion

To determine whether LPA1 or LPA2 expression in mesothelial cells contributed to ovarian cancer cell invasion of the mesothelium, each receptor was knocked down in LP9 mesothelial cells with siRNA, and the ability of SKOV3ip1 ovarian cancer cells to invade LP9 monolayers was determined using a co-culture assay system (henceforth referred to as "trans-mesothelial invasion") (Slack-Davis et al., 2009). Following transfection of LP9 cells with siRNA directed against LPA1, qRT-PCR showed a 75% reduction in *LPA1* expression with no effect on *LPA2* expression (Figure 3.2A, left panel). Knockdown of *LPA2* showed no statistically significant effect on *LPA1* and *LPA2* expression (Figure 3.2A, right panel). *LPA1* knockdown in LP9 mesothelial cells reduced SKOV3ip1 cell invasion by 65% while siLPA2 treatment had a marginal effect (Figure 3.2B). Treatment of the co-culture with VPC51299, an antagonist against LPA1 and LPA3 (East et al., 2011), also inhibited trans-mesothelial invasion by 40% (Figure 3.2C). These observations indicate that LPA1 expression on mesothelial cells promotes ovarian cancer cell invasion of the mesothelium.

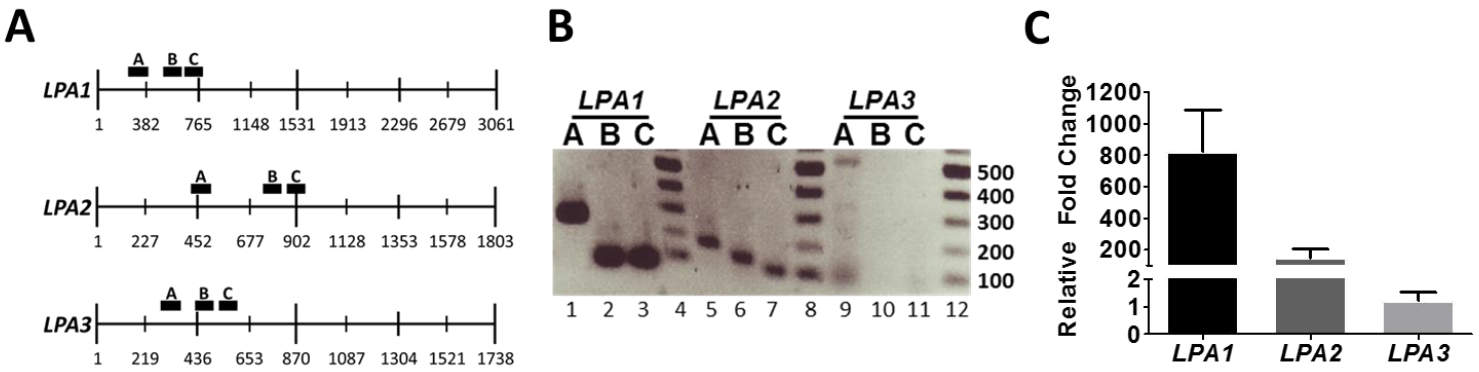
A
LPA1
A B C
1 382 765 1148 1531 1913 2296 2679 3061
LPA2
A B C
1 227 452 677 902 1128 1353 1578 1803
LPA3
A B C
1 219 436 653 870 1087 1304 1521 1738
B
LPA1 LPA2 LPA3
A B C A B C A B C
500
400
300
200
100
1 2 3 4 5 6 7 8 9 10 11 12
C
Relative Fold Change
1200
1000
800
600
400
200
2
1
0
LPA1
LPA2
LPA3

Figure 3.1. LPA receptor expression in LP9 mesothelial cells. **A.** Diagram of multiple primers (A, B, and C) for the indicated sequences of *LPA1*, *LPA2*, and *LPA3*. **B.** Expression of LPA receptors 1, 2, and 3 in LP9 mesothelial cells was determined by PCR using multiple primer sets (A, B, and C) listed in Table 5.1. **C.** Relative expression of *LPA1, LPA2, and LPA3* mRNA in LP9 mesothelial cells determined by quantitative RT-PCR compared to β glucuronidase (GUSB) using the delta-delta Ct method. Primer sets for *LPA1-A*, *LPA2-A*, *LPA3-A*, and *GUSB* are listed in Table 5.1.

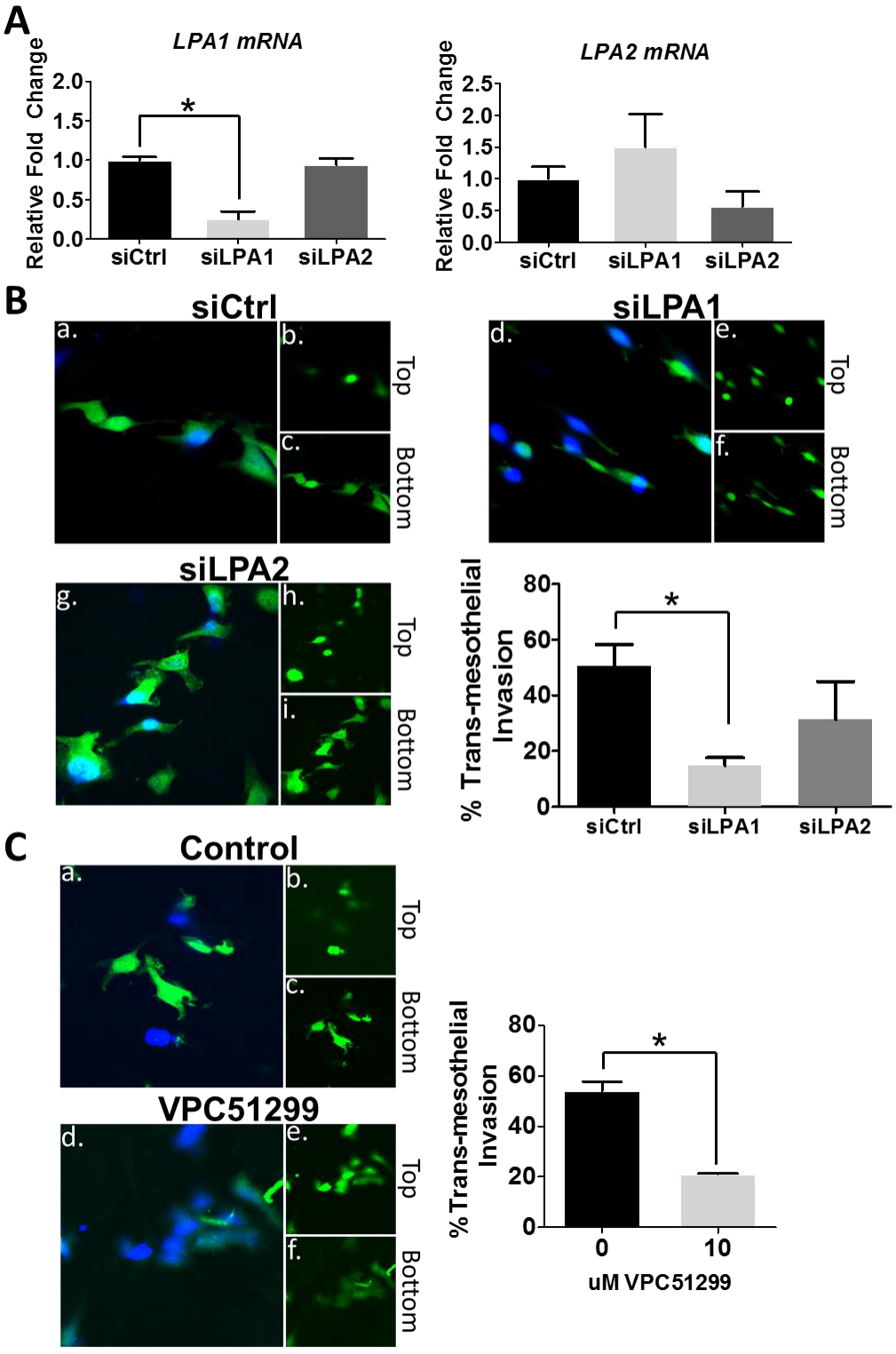
A
LPA1 mRNA
Relative Fold Change
2.0
1.5
1.0
0.5
0.0
*
siCtrl
siLPA1
siLPA2
LPA2 mRNA
Relative Fold Change
2.5
2.0
1.5
1.0
0.5
0.0
siCtrl
siLPA1
siLPA2
B
siCtrl
a.
b.
c.
Top
Bottom
siLPA1
d.
e.
f.
Top
Bottom
siLPA2
g.
h.
i.
Top
Bottom
% Trans-mesothelial Invasion
80
60
40
20
0
*
siCtrl
siLPA1
siLPA2
C
Control
a.
b.
c.
Top
Bottom
VPC51299
d.
e.
f.
Top
Bottom
% Trans-mesothelial Invasion
80
60
40
20
0
*
0
10
uM VPC51299

Figure 3.2. Mesothelial LPA1 promotes ovarian cancer cell invasion. **A.** *LPA1* (left panel) and *LPA2* (right panel) mRNA expression in LP9 mesothelial cells were determined by qRT-PCR following knockdown with specific siRNA oligos or scrambled control (siCtrl). Data are expressed relative to siCtrl. **B.** Representative images (a-i) of SKOV3ip1 ovarian cancer cell invasion through mesothelial monolayers (trans-mesothelial invasion) was performed as described previously (Slack-Davis et al., 2009). SKOV3ip1 cells (green) were plated on a monolayer of LP9 mesothelial cells (orange) previously subjected to siCtrl (***a.-c.***), siLPA1 (***d.-f.***), or siLPA2 (**g.-*i.***) knockdown. Confocal microscopy was used to obtain 1µm Z-stacks; SKOV3ip1 cells in an image from the top third of the Z-stack (top; b, e, and h) were pseudo-colored blue and merged with an image from the bottom third of the Z-stack (bottom; c, f, and i). Percent trans-mesothelial invasion of SKOV3ip1 was determined by the ratio of green to total cells in the merged images (a, d, and g). The graph depicts the mean ± SEM of three independent experiments. Significance determined by one-way ANOVA followed by Newman-Keuls multiple comparison test (**A** and **B**) **C.** Representative images of the trans-mesothelial invasion assay of untreated co-cultures (0 µM) (***a.-c.***) or those treated with 10 µM VPC51299 (***d.-f.***). Percent trans-mesothelial invasion was determined as described in **B.** Data represent the mean ± SEM of two independent experiments. Significance determined by an unpaired T-test; *, $p < 0.05$, relative to siCtrl or untreated control.

3.3.3 LPA1 Regulates Mesothelial VCAM-1 Expression

VCAM-1 regulates ovarian cancer cell invasion of the mesothelium *in vitro* and *in vivo*, and functional blockade of VCAM-1 in a mouse model of peritoneal ovarian cancer metastasis decreases mesothelial invasion, which is accompanied by reduced tumor burden, and increased survival (Slack-Davis et al., 2009). Additionally, VCAM-1 expression is elevated on the mesothelium of LPP1 KO mice compared to wild type mice with tumors (**Chapter 2**, Figure 2.3) (Nakayama et al., 2015). Therefore, we examined whether LPA regulated VCAM-1 expression in LP9 mesothelial cells to promote mesothelial invasion. Utilizing flow cytometry, VCAM-1 expression was detected on the cell surface (Figure 3.3A). Knockdown of *LPA1* resulted in a 50% reduction in cell surface expression of VCAM-1 (Figure 3.3B). Western analysis revealed an 80% reduction in total VCAM-1 protein following siRNA knockdown of *LPA1* (Figure 3.3C and D). To rule out non-specific effects of *LPA1* knockdown on VCAM-1 expression, *LPA1* was knocked down with the four individual oligomers of the SMART pool siRNA (Figure 3.4A). In each case, VCAM-1 expression paralleled the extent of *LPA1* knockdown (Figures 3.4B and C). Similar results were observed using a second human mesothelial cell line, LP3 (Figure 3.4D).

We next examined LPA effects on VCAM-1 mRNA expression. Knockdown of *LPA1* resulted in a 50% reduction in *VCAM1* mRNA expression in LP9 mesothelial cells (Figure 3.5A). To rule out the possibility that *LPA1* knockdown eliminated expression of alternatively spliced VCAM-1 transcripts rather than the entire gene, qRT-PCR was performed using primer sets that span the entire *VCAM1* mRNA sequence (Figure 3.5B, top panel). Knockdown of *LPA1* with each of the three individual oligomers that showed the greatest knockdown efficiency (oligomers

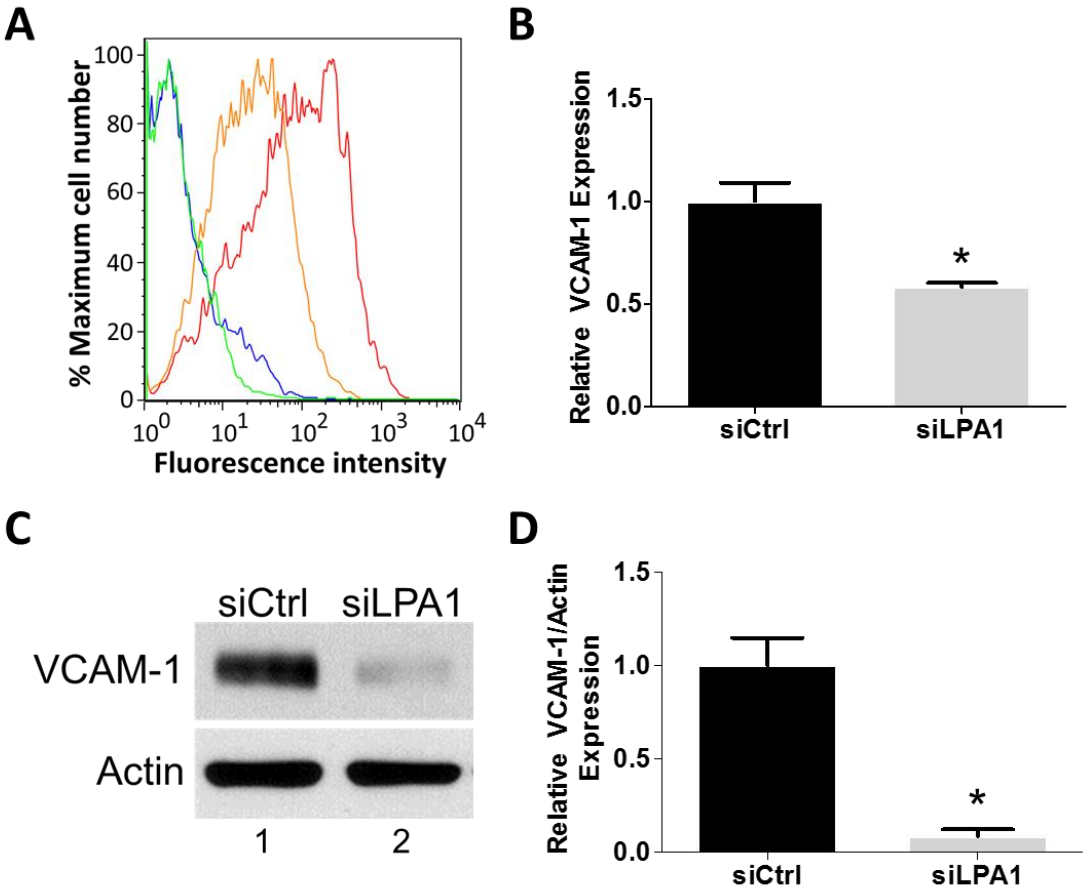
A
% Maximum cell number
100
80
60
40
20
0
10^0
10^1
10^2
10^3
10^4
Fluorescence intensity
B
Relative VCAM-1 Expression
1.5
1.0
0.5
0.0
*
siCtrl
siLPA1
C
siCtrl
siLPA1
VCAM-1
Actin
1
2
D
Relative VCAM-1/Actin Expression
1.5
1.0
0.5
0.0
*
siCtrl
siLPA1

Figure 3.3. LPA1 knockdown decreases VCAM-1 protein expression in mesothelial cells. **A.** Geometric mean fluorescence intensity (MFI) of VCAM-1 surface expression in LP9 cells transfected with control (red line) or LPA1,2 siRNA (orange line). Isotype control – blue and green lines. **B.** Quantification of flow cytometry analysis of VCAM-1 expression after control (siCtrl) or LPA1 (siLPA1) siRNA knockdown. In each case, the anti-VCAM-1 MFI was divided by the isotype control, and both are presented relative to siCtrl. Data represent the mean ± SEM of two independent experiments. **C.** Western analysis of LP9 cells transfected with siRNA against control or *LPA1* and blotted for VCAM-1 or actin (loading control). **D.** Quantification of signal intensities for VCAM-1 was normalized to actin and expressed relative to siCTrl. Data represent the mean ± SEM of three independent experiments Significance for **B** and **D** determined by an unpaired T-test; *, $p < 0.05$.

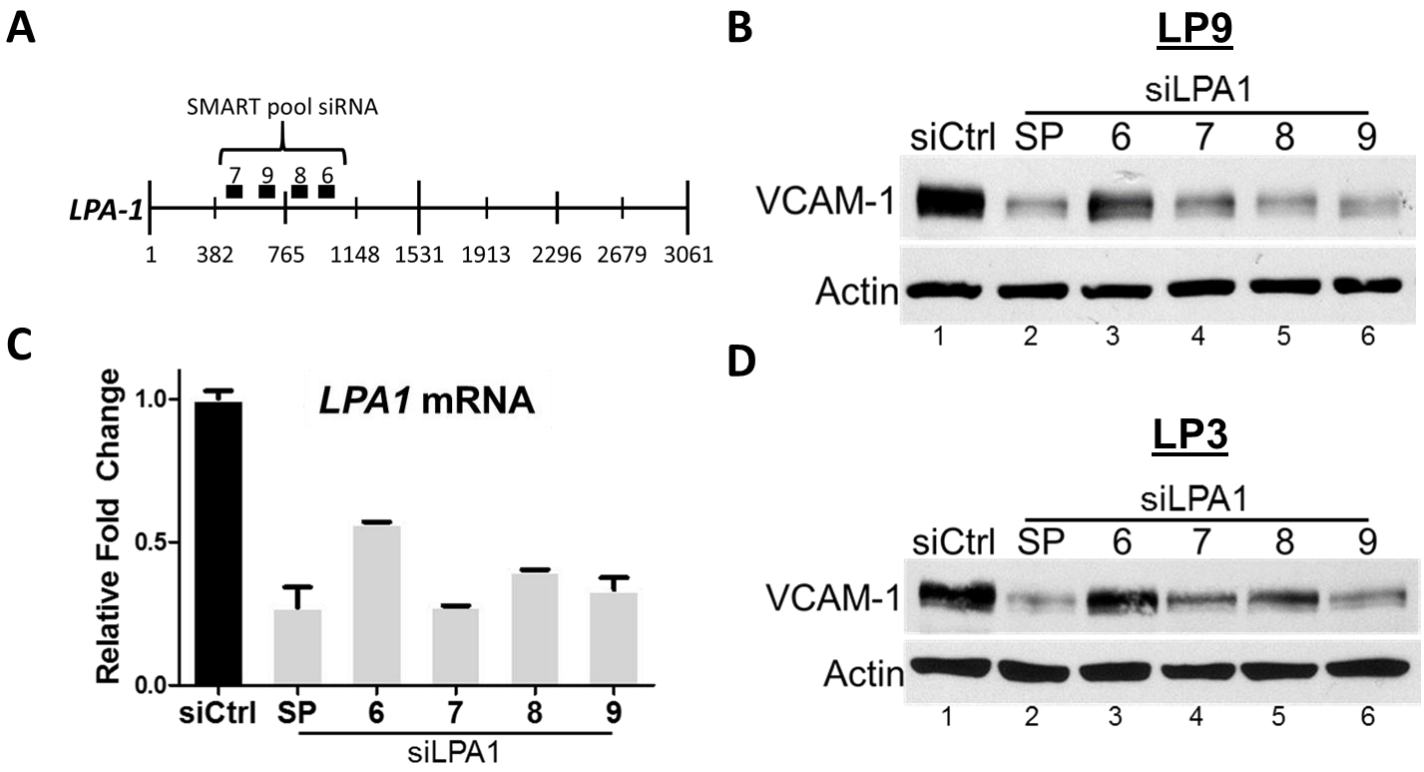
A
SMART pool siRNA
7 9 8 6
LPA-1
1 382 765 1148 1531 1913 2296 2679 3061
B
LP9
siLPA1
siCtrl SP 6 7 8 9
VCAM-1
Actin
1 2 3 4 5 6
C
LPA1 mRNA
Relative Fold Change
1.0
0.5
0.0
siCtrl SP 6 7 8 9
siLPA1
D
LP3
siLPA1
siCtrl SP 6 7 8 9
VCAM-1
Actin
1 2 3 4 5 6

Figure 3.4. LPA1 knockdown using Smart pool and siRNA oligos decreases VCAM-1 protein expression. **A.** Diagram of siRNA Smart pool and individual siRNA (6, 7, 8, 9) oligos targets on *LPA1* mRNA **B.** LP9 mesothelial cells were transfected with control (siCtrl), Smart Pool (SP), or individual oligos (6, 7, 8, and 9) targeting LPA1 for 48 hours. Lysates were analyzed by Western blot for VCAM-1 or actin (loading control). **C.** *LPA1* mRNA expression was determined by qRT-PCR in LP9 mesothelial cells following transfection with siRNA Smart Pool, individual siRNA (6, 7, 8, 9) or scrambled control (siCtrl) oligos. Data were analyzed using the delta-delta C_T method. The change in gene expression was normalized to *GUSB* and expressed relative to siCtrl. The graph depicts the mean ± SEM of two independent experiments. **D.** Western analysis of LP3 mesothelial cells 48 hours after LPA1 knockdown blotted for VCAM-1 or actin (loading control).

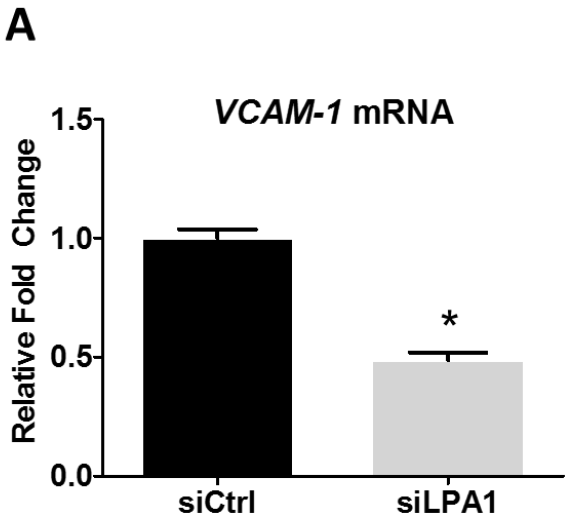
A
VCAM-1 mRNA
Relative Fold Change
1.5
1.0
0.5
0.0
*
siCtrl
siLPA1

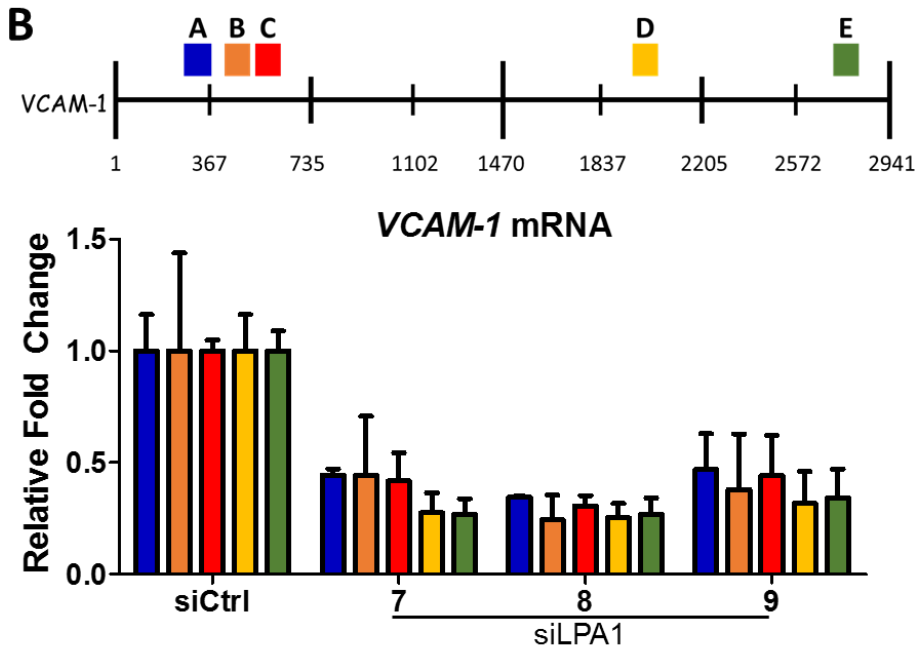
B
A B C
D
E
VCAM-1
1
367
735
1102
1470
1837
2205
2572
2941
VCAM-1 mRNA
Relative Fold Change
1.5
1.0
0.5
0.0
siCtrl
7
8
9
siLPA1

Figure 3.5. LPA1 knockdown decreases VCAM-1 mRNA expression in mesothelial cells. **A.** *VCAM1* mRNA expression in LP9 cells following knockdown with LPA1 siRNA or control (siCtrl). Primer sets for *VCAM-1-A* and *GUSB* in Table 5.1. The relative change in gene expression was normalized to GUSB and expressed relative to siCtrl. The graph depicts the mean ± SEM of three independent experiments. **B.** *VCAM1* mRNA expression in LP9 mesothelial cells following knockdown with LPA1 siRNA or control (siCtrl) using primers for the indicated sequences of *VCAM1* (top panel; VCAM-1-A, VCAM-1-B, VCAM-1-C, VCAM-1-D, VCAM-1-E) and GUSB (Table 5.1). Data were analyzed using the delta-delta C_T method. The relative change in gene expression was normalized to GUSB and expressed relative to siCtrl. The graph depicts the mean ± SEM of four independent experiments. *, $p < 0.05$.

7-9) decreased *VCAM1* mRNA expression across the entire transcript (Figure 3.5B). Taken together, the data indicate that LPA1 regulates VCAM-1 expression on the mesothelium.

3.3.4 Autocrine Production of LPA in Mesothelial Cells

LP9 mesothelial cells constitutively produce LPA and constitutively express VCAM-1 (Figure 3.5) (Cannistra et al., 1994; Ren et al., 2006; Slack-Davis et al., 2009). To confirm that LPA was produced by LP9 mesothelial cells (Ren et al., 2006), conditioned media from LP9 mesothelial cells was used to stimulate ERK phosphorylation in an independent cell line (SKOV3ip1) in the presence or absence of VPC51299. Conditioned media from LP9 mesothelial cells stimulated an 18-fold increase in ERK phosphorylation within 5 minutes of plating, which was similar to the increase observed following LPA stimulation (Figure 3.6A and B). VPC51299 treatment reduced LPA-stimulated ERK phosphorylation by 85% as expected. The effects of LP9 mesothelial cell-conditioned media on ERK phosphorylation were mitigated by 50% with VCP51299 treatment (Figure 3.6A and B), indicating that LPA was present in the conditioned media and that its action through LPA1 was at least partially responsible for ERK phosphorylation in SKOV3ip1 cells.

3.3.5 LPA Regulates VCAM-1 Expression in Mesothelial Cells

To evaluate whether the autocrine LPA production contributes to VCAM-1 expression, LP9 mesothelial cells were cultured for increasing periods of time in the presence or absence of VPC51299. Western analysis showed a 20-fold increase in VCAM-1 protein expression 48 hours after plating LP9 cells, and VPC51299 inhibited the accumulation by 50% over 24 hours of

treatment (Figure 3.7A and B). Similar results were observed with a second antagonist targeting LPA1, AM2996 (Swaney et al., 2010) (Figure 3.8C). Loss of *LPA1* in LP9 mesothelial cells following siRNA knockdown also reduced VCAM-1 protein accumulation by 50% (Figure 3.8A and B). Furthermore, in addition to reducing VCAM-1 protein expression, *VCAM-1* transcript levels were reduced by approximately 50%, 36 and 48 hours following *LPA1* knockdown (Figure 3.8C). Additionally, exogenous LPA stimulation increases VCAM-1 protein expression by 58%, 48 hours after plating LP9 cells (Figure 3.9A and B). Together, these observations are consistent with the notion that LPA promotes the accumulation of VCAM-1 expression by acting through LPA1.

3.3.6 LPA Promotes VCAM-1 Protein Synthesis

We next investigated whether LPA acting through LPA1 affected VCAM-1 accumulation on LP9 mesothelial cells by promoting protein synthesis or inhibiting degradation. Metabolic labeling with S^{35}-Met/Cys revealed a linear increase in VCAM-1 protein synthesis that did not differ between control and *LPA1* knockdown within the first 4 hours of labeling (Figure 3.10A); however, VCAM-1 synthesis continued to increase over the next 8 hours in the control, while expression plateaued following *LPA1* knockdown (Figure 3.10 A). To determine whether LPA1 contributes to VCAM-1 stability, cycloheximide, an inhibitor of protein synthesis was utilized. In control cells, VCAM-1 expression remained constant with 8 hours of cycloheximide treatment; however, VCAM-1 expression decreased within the first 4 hour by 50% following cycloheximide treatment (Figure 3.10B). To confirm this observation, pulse-chase labeling of VCAM-1 was completed. LP9 mesothelial cells were pulsed for 4 hours with S^{35}-Met/Cys and chased with cold

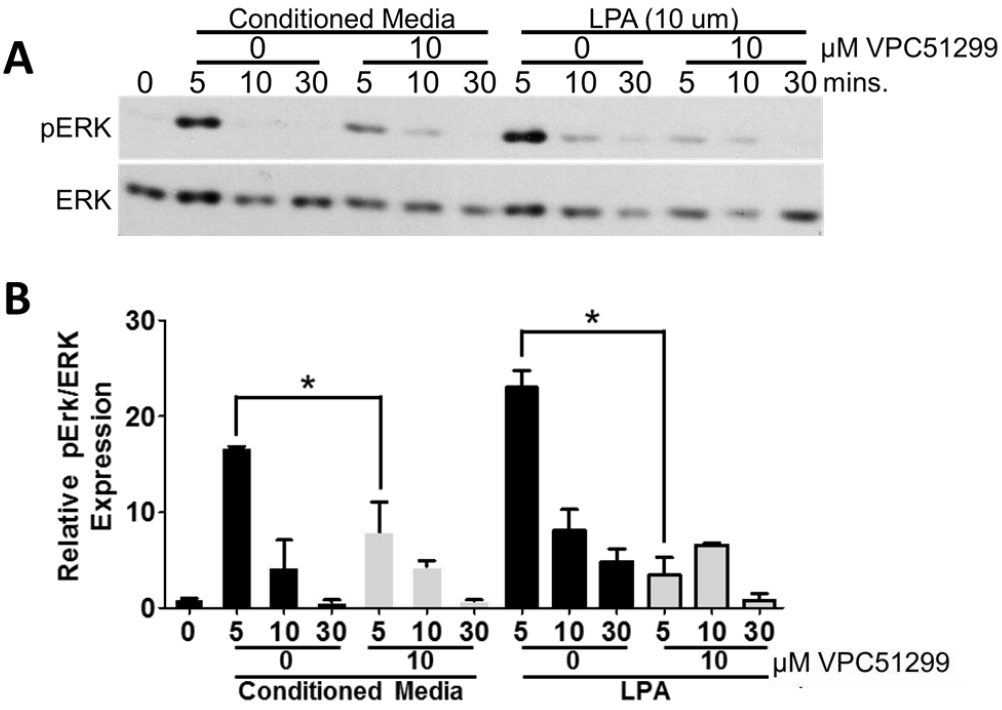
A
Conditioned Media
LPA (10 um)
0
10
0
10
μM VPC51299
0 5 10 30 5 10 30 5 10 30 5 10 30 mins.
pERK
ERK
B
Relative pErk/ERK Expression
30
20
10
0
*
*
0 5 10 30 5 10 30 5 10 30 5 10 30
0
10
0
10
μM VPC51299
Conditioned Media
LPA

Figure 3.6. LPA receptor antagonist blocks ERK phosphorylation induced by LP9 conditioned media in ovarian cancer cells. **A.** SKOV3ip1 cells were serum starved, treated with 10 μM VPC51299 or vehicle control for 30 minutes, and then stimulated for the indicated periods of time with conditioned media obtained from LP9 cells cultured for 24 hr or 10 μM LPA. Lysates were blotted for phosphorylated ERK (pERK) and total ERK. **B.** Signal intensities for pERK bands were normalized to total ERK and are expressed relative to time 0. Significance was determined by one-way ANOVA followed by Newman-Keuls multiple comparison test. Data represent the mean ± SEM of two independent experiments; *, $p < 0.05$.

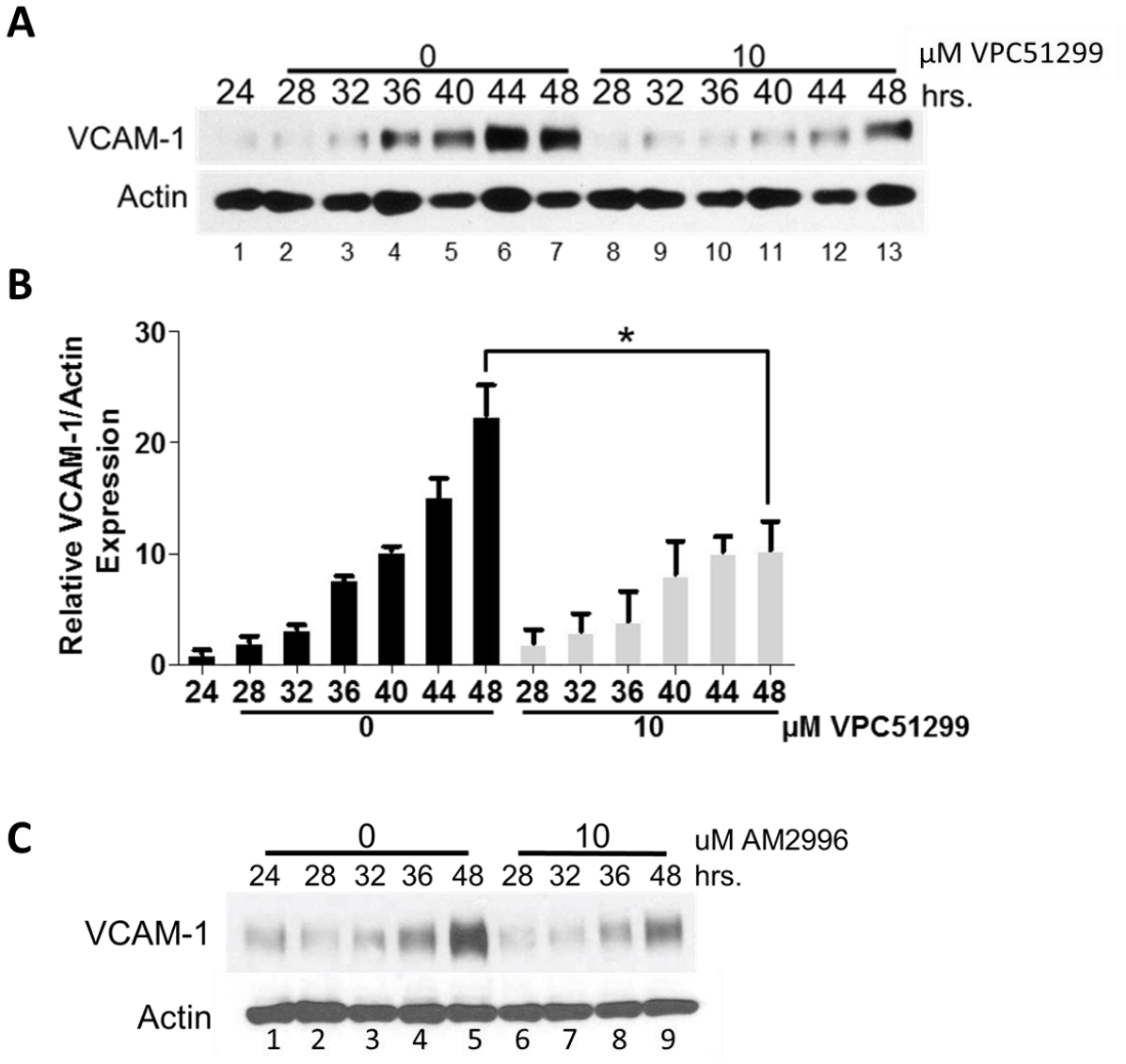
A
0
10
µM VPC51299
24 28 32 36 40 44 48 28 32 36 40 44 48 hrs.
VCAM-1
Actin
1 2 3 4 5 6 7 8 9 10 11 12 13
B
Relative VCAM-1/Actin Expression
30
20
10
0
*
24 28 32 36 40 44 48 28 32 36 40 44 48
0
10
µM VPC51299
C
0
10
uM AM2996
24 28 32 36 48 28 32 36 48 hrs.
VCAM-1
Actin
1 2 3 4 5 6 7 8 9

Figure 3.7. LPA1,3 receptor antagonist decreases VCAM-1 expression in mesothelial cells**. A.** LP9 mesothelial cells were treated with or without 10 μM VPC51299 24 hours after plating for the indicated times prior to lysis and immunoblotting for VCAM-1 or actin (loading control). **B.** Quantification of signal intensities for VCAM-1 was normalized to actin and expressed relative to the untreated 24 hr control. Significance determined by one-way ANOVA followed by Newman-Keuls multiple comparison test. The graph depicts the mean ± SEM of three independent experiments; *, $p < 0.05$. **C.** Western analysis of LP9 mesothelial cells treated with or without 10 μM AM2996 24 hours after plating for the indicated times.

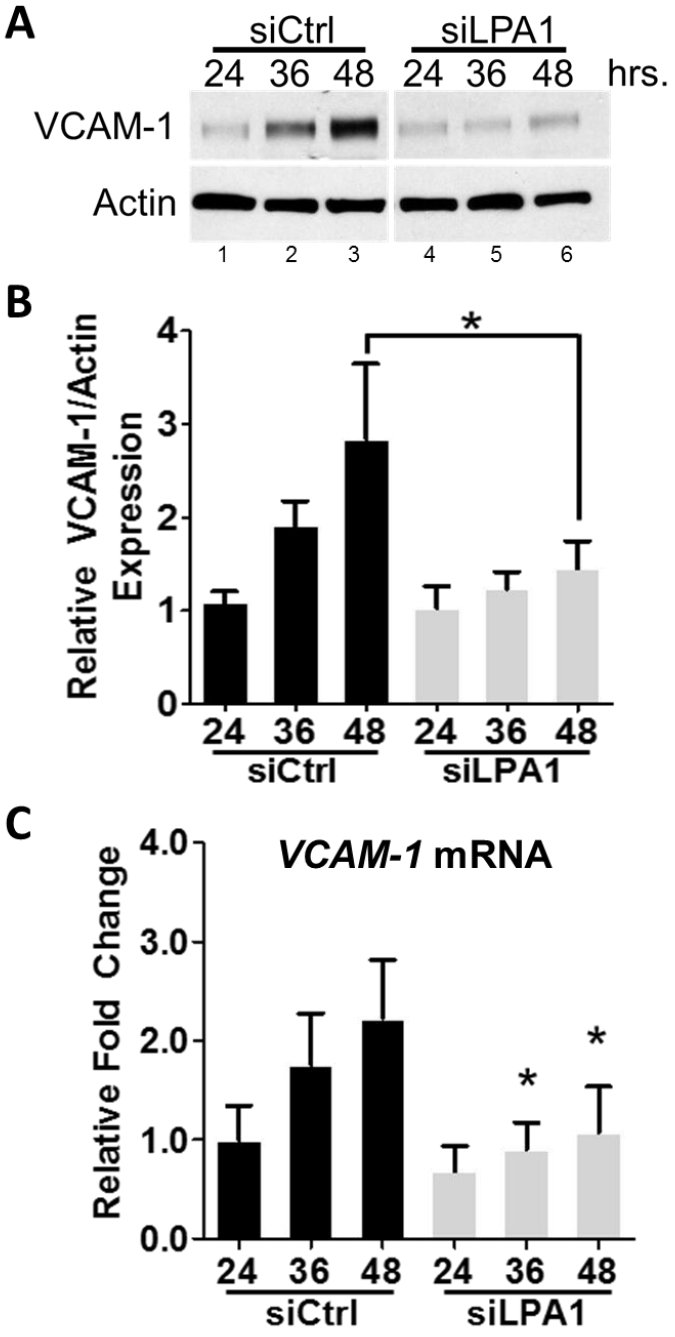
A
siCtrl
siLPA1
24 36 48 24 36 48 hrs.
VCAM-1
Actin
1 2 3 4 5 6
B
Relative VCAM-1/Actin Expression
*
0 1 2 3 4
24 36 48 24 36 48
siCtrl
siLPA1
C
VCAM-1 mRNA
Relative Fold Change
0.0 1.0 2.0 3.0 4.0
* *
24 36 48 24 36 48
siCtrl
siLPA1

Figure 3.8. LPA1 Knockdown Decreases VCAM-1 Accumulation in Mesothelial Cells. **A.** Lysates from LP9 cells transfected with either control siRNA or *LPA1* siRNA for indicated times were blotted for VCAM-1 or actin (loading control). **B.** Quantification of signal intensities for VCAM-1 was normalized to actin and expressed relative to 24hr siCtrl. Significance was determined by one-way ANOVA followed by Newman-Keuls multiple comparison test. Data are representative of 6 independent experiments. **C.** VCAM-1 mRNA levels were measured by qRT-PCR in LP9 mesothelial cells with or without LPA1 expression for the indicated times. Primer sets for *VCAM-1-A* and *GUSB* in Table 5.1. Significance determined by three-way ANOVA followed by F-tests based on contrasts to compare the effect of the knockdown at specific times. The graph depicts the mean ± SEM of four independent experiments; *, $p < 0.05$.

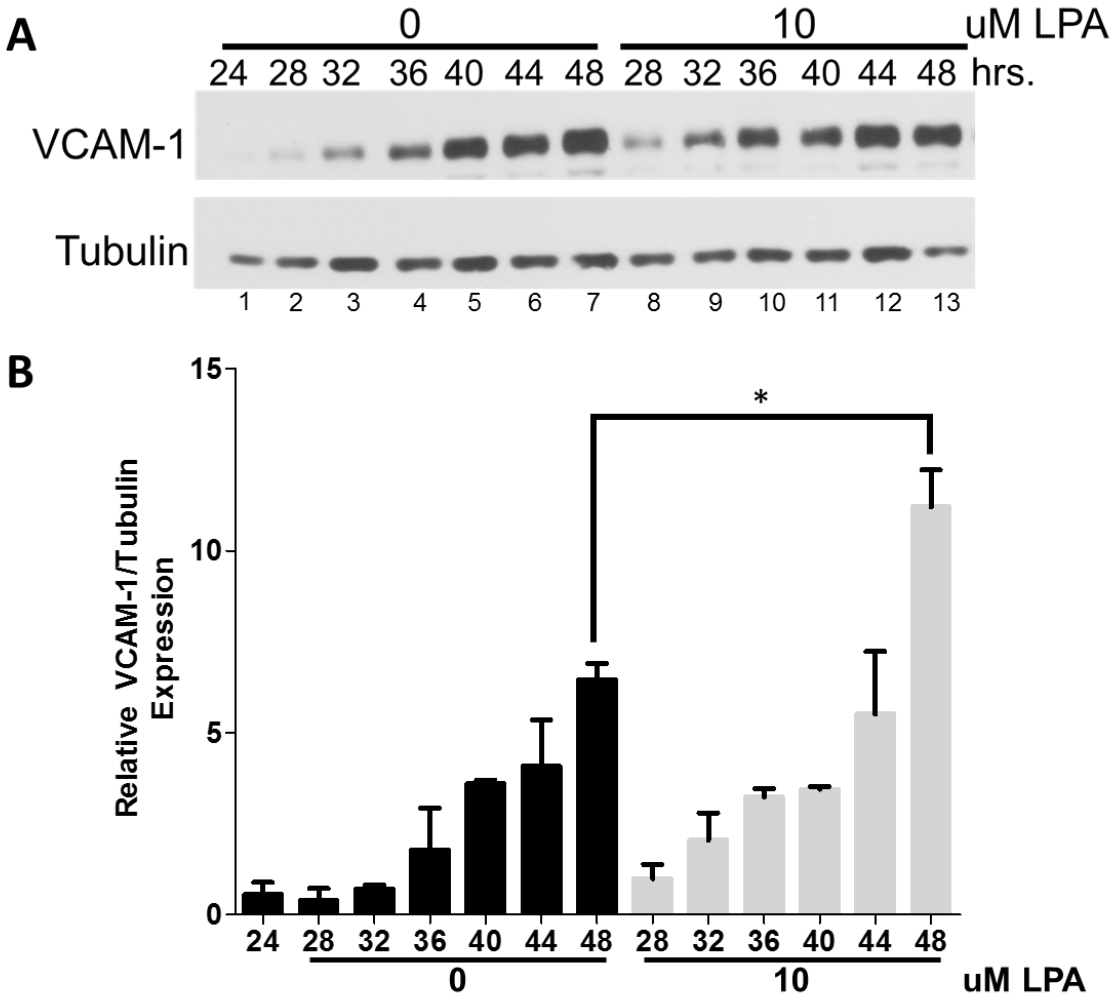
A
0
10
uM LPA
24 28 32 36 40 44 48 28 32 36 40 44 48 hrs.
VCAM-1
Tubulin
1 2 3 4 5 6 7 8 9 10 11 12 13
B
Relative VCAM-1/Tubulin Expression
15
10
5
0
*
24 28 32 36 40 44 48 28 32 36 40 44 48
0
10
uM LPA

Figure 3.9. Exogenous LPA stimulation increases VCAM-1 expression in mesothelial cells. **A.** LP9 mesothelial cells were treated with or without 10 μM LPA 24 hours after plating for the indicated times prior to lysis and immunoblotting for VCAM-1 or tubulin (loading control). **B.** Quantification of signal intensities for VCAM-1 was normalized to tubulin and expressed relative to the untreated 24 hr control. Significance determined by one-way ANOVA followed by Newman-Keuls multiple comparison test. The graph depicts the mean ± SEM of two independent experiments; *, $p < 0.05$.

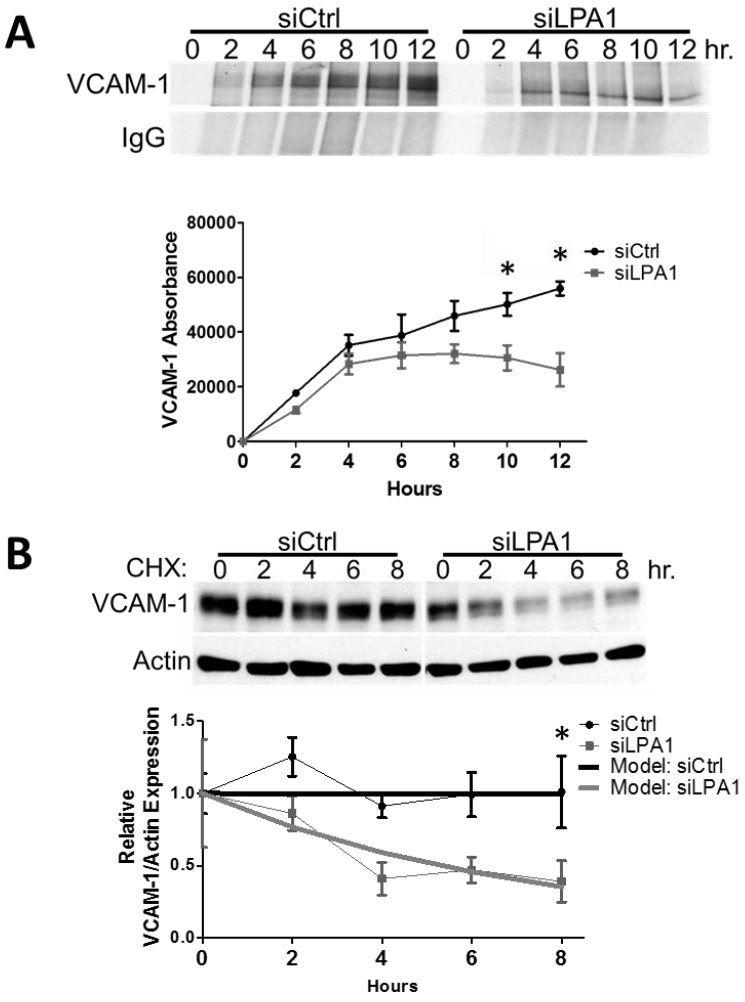
A
siCtrl
siLPA1
0 2 4 6 8 10 12 0 2 4 6 8 10 12 hr.
VCAM-1
IgG
VCAM-1 Absorbance
80000
60000
40000
20000
0
0 2 4 6 8 10 12
Hours
siCtrl
siLPA1
*
*
B
siCtrl
siLPA1
CHX: 0 2 4 6 8 0 2 4 6 8 hr.
VCAM-1
Actin
Relative VCAM-1/Actin Expression
1.5
1.0
0.5
0.0
0 2 4 6 8
Hours
siCtrl
siLPA1
Model: siCtrl
Model: siLPA1
*

Figure 3.10. LPA1 promotes VCAM-1 protein synthesis and degradation. **A.** LP9 mesothelial cells (± LPA1 expression) were labeled with [35-S]-Methionine/Cysteine for the indicated times. VCAM-1 was immunoprecipitated from cell lysates and subjected to SDS-PAGE followed by autoradiography. Quantification of VCAM-1 autoradiograph signal (lower panel); signal intensities for VCAM-1 were subtracted from time zero. Significance determined by one-way ANOVA followed by Newman-Keuls multiple comparison test. The graph depicts the mean ± SEM of three independent experiments. **B.** LP9 mesothelial cells ± LPA1 expression were treated with cycloheximide (CHX) (50 uM) for indicated time points and blotted for VCAM-1 or actin (loading control). Quantification of signal intensities (lower panel) for VCAM-1 was normalized to actin and expressed relative to time zero for siCtrl or siLPA1. Data represent the mean ± SEM of three independent experiments; *, $p < 0.05$.

media for the indicated time points. Pulse-chase labeling revealed no change in VCAM-1 protein levels within 8 hours for either the control or with *LPA1* siRNA (Figure 3.11A). Additionally, we also tested pulse-chase labeling with cycloheximide following LPA1 knockdown. While VCAM-1 protein levels appear to be lower in the control compared to siLPA1 at 8 hours, the differences are not statistically significant (Figure 3.11B). These observations indicate that LPA promotes VCAM-1 synthesis in mesothelial cells and that VCAM-1 is remarkably stable.

3.3.7 LPA Promotes Ovarian Cancer Trans-Mesothelial Invasion via VCAM-1

Since LPA acting through LPA1 promotes mesothelial invasion and regulates VCAM-1 expression, we investigated whether VCAM-1 was responsible for LPA1-dependent mesothelial invasion. As previously shown (Figure 3.2B), *LPA1* knockdown in LP9 mesothelial cells inhibited SKOV3ip1 cell invasion relative to control (Figures 3.12A a-c, g-i and 3.13B, solid gray bar vs. solid black bar). The ability of VCAM-1 expression to rescue mesothelial invasion following *LPA1* knockdown in LP9 mesothelial cells was determined by exogenously expressing GFP-tagged VCAM-1 at a concentration that approached endogenous levels (Figure 3.12C, lanes 1 vs. 11). GFP-VCAM-1 expression in LP9 mesothelial cells transfected with scrambled siRNA (Figures 3.12A d-f and 4B, checkered black bar) did not alter SKOV3ip1 ovarian cancer cell invasion of mesothelial monolayers relative to control (Figures 3.12A a-c and 3.12B, solid black bar). However, expression of GFP-VCAM-1 in LP9 mesothelial cells lacking *LPA1* expression restored SKOV3ip1 ovarian cancer cell invasion to control levels (Figures 3.12A j-l and 3.12B, checkered gray bar vs. solid black bar). Taken together, these observations indicate that LPA1

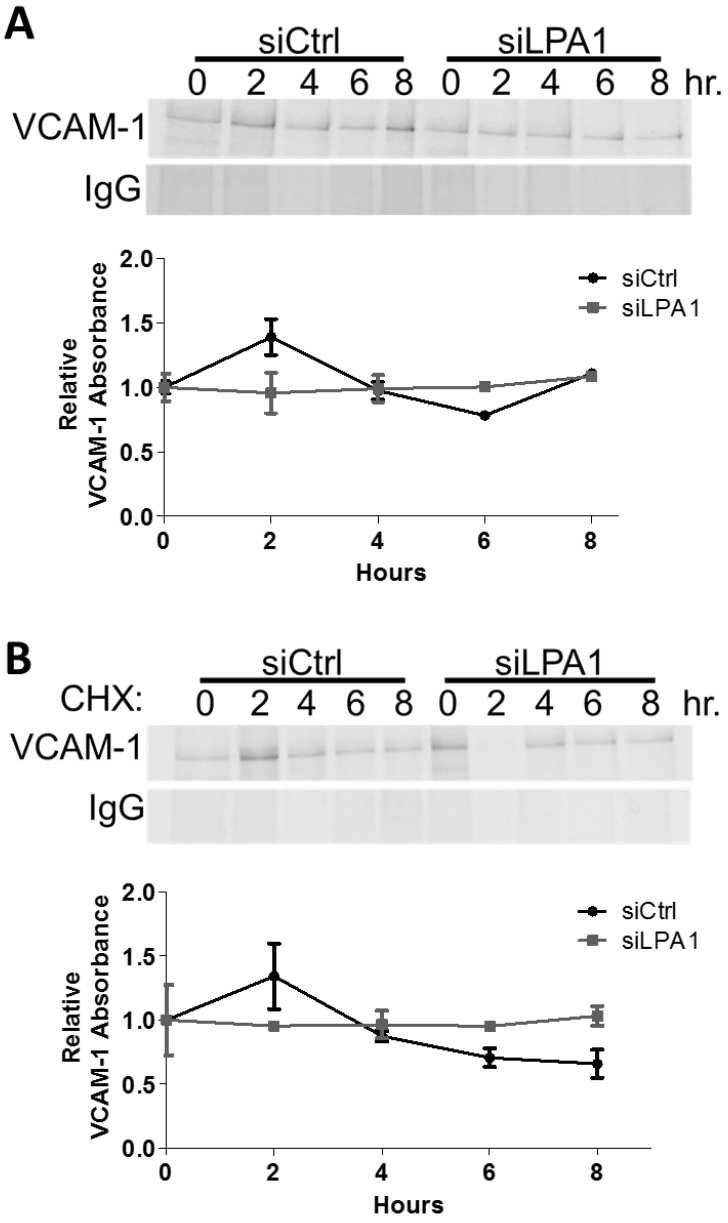
A
siCtrl
siLPA1
0 2 4 6 8 0 2 4 6 8 hr.
VCAM-1
IgG
Relative VCAM-1 Absorbance
2.0
1.5
1.0
0.5
0.0
0 2 4 6 8
Hours
siCtrl
siLPA1
B
CHX:
siCtrl
siLPA1
0 2 4 6 8 0 2 4 6 8 hr.
VCAM-1
IgG
Relative VCAM-1 Absorbance
2.0
1.5
1.0
0.5
0.0
0 2 4 6 8
Hours
siCtrl
siLPA1

Figure 3.11. LPA1 knockdown did not affect VCAM-1 degradation up to 8 hours. **A.** LP9 mesothelial cells ± LPA1 expression were pulsed with [35-S]-Methionine/Cysteine for 4 hours and chased for 2, 4, 6, and 8 hours with complete medium prior to VCAM-1 immunoprecipitation. Quantification of VCAM-1 autoradiograph data (lower panel) expressed relative to time zero for siCtrl or siLPA1. Data represent the mean ± SEM of four independent experiments. **B.** LP9 mesothelial cells ± LPA1 expression were pulsed with [35-S]-Methionine/Cysteine for 4 hours and chased with CHX in complete medium (50 uM) for 2, 4, 6, and 8 hours prior to VCAM-1 immunoprecipitation. Quantification of VCAM-1 autoradiograph data (lower panel) expressed relative to time zero for siCtrl or siLPA1. Data represent the mean ± SEM of two independent experiments.

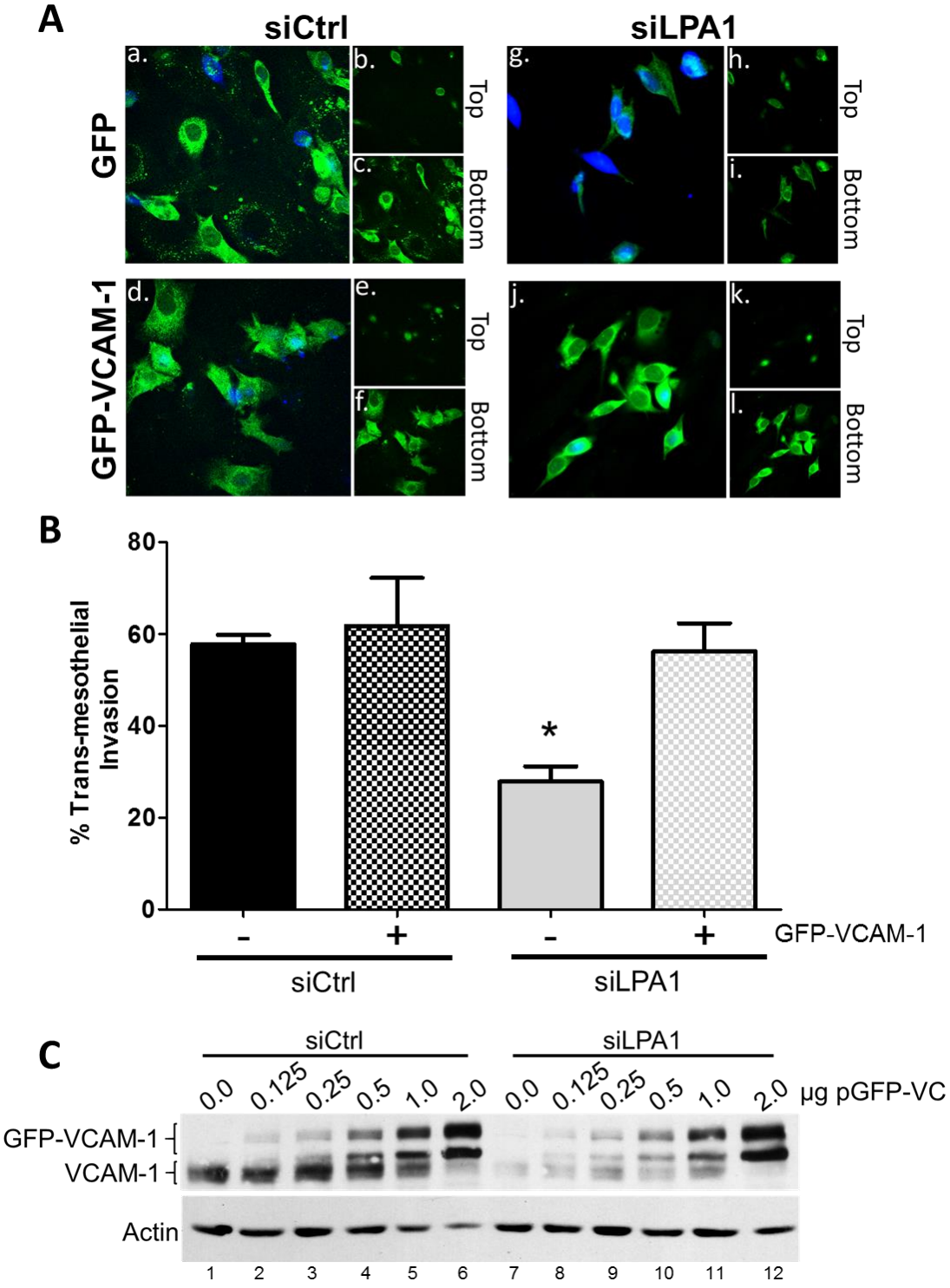
A
siCtrl
siLPA1
GFP
GFP-VCAM-1
a.
b.
c.
d.
e.
f.
g.
h.
i.
j.
k.
l.
Top
Bottom
B
% Trans-mesothelial Invasion
80
60
40
20
0
*
-
+
-
+
GFP-VCAM-1
siCtrl
siLPA1
C
siCtrl
siLPA1
0.0
0.125
0.25
0.5
1.0
2.0
µg pGFP-VC
GFP-VCAM-1
VCAM-1
Actin
1
2
3
4
5
6
7
8
9
10
11
12

Figure 3.12. Re-expression of VCAM-1 restores mesothelial invasion after LPA1 knockdown. **A**. LP9 mesothelial cells were transfected with GFP or GFP-VCAM-1 (1.0 µg) with control or siLPA1 siRNA oligos and used in the trans-mesothelial invasion assay as described in Figure 1D. Representative images of siCtrl + GFP (***a.-c.***), siCtrl + GFP-VCAM-1 (***d.-f.***), siLPA1 + GFP (***g.-i.***), and siLPA1 + GFP-VCAM-1 (***j.-l.***) that were used to quantify trans-mesothelial invasion. **B.** Percent trans-mesothelial invasion of SKOV3ip1 allowed to invade LP9 mesothelial monolayers expressing GFP or GFP-VCAM-1 with or without siCtrl or siLPA1 oligos. Significance determined by one-way ANOVA followed by Newman-Keuls multiple comparison test. Data represent the mean ± SEM of three independent experiments; *, $p < 0.05$ compared to all other samples. **C.** LP9 mesothelial cells were transfected with the indicated concentrations of GFP-VCAM-1 (pGFP-VC) prior to lysis and immunoblotting for VCAM-1 or actin (loading control).

promotes ovarian cancer invasion of the mesothelium through the regulation of mesothelial VCAM-1 protein expression.

3.4 Discussion

In summary, these studies provide further understanding into the role the ovarian cancer tumor microenvironment plays in regulating ovarian cancer mesothelial invasion. LPA, an essential ovarian cancer microenvironment factor, was found to promote ovarian cancer mesothelial invasion. Acting through its receptor, LPA1, LPA regulated VCAM-1 protein expression and accumulation on the mesothelium by increasing VCAM-1 protein synthesis. Most significantly, we showed that LPA1 regulates ovarian cancer mesothelial invasion by promoting mesothelial VCAM-1 expression. These in vitro trans-mesothelial invasion assays and experiments suggest that components within the ovarian cancer tumor microenvironment influence non-transformed cells to support ovarian cancer mesothelial invasion.

In this study we demonstrate that LPA not only influences the ovarian cancer cell to promote migration and invasion (Bian et al., 2004; Said et al., 2007), but also LPA impacts mesothelial cells to allow ovarian cancer cell invasion. Specifically, pharmacologic inhibition of LPA1/3 using VPC51299 decreased SKOV3ip1 ovarian cancer cells invasion of the mesothelium (Figure 3.2C). It is important to note that the parental SKOV3 cells express LPA1-3 receptors at varying levels (LPA2 >LPA3 >LPA1) (Yu et al., 2008). This indicates that VPC51299 targets both the cancer cell and the mesothelial cell; however, siRNA inhibition of LPA1 in mesothelial cells

alone significantly reduced mesothelial invasion by SKOV3ip1 ovarian cancer cells (Figure 3.2B). This observation parallels the impairment of hepatocarcinoma cells to invade mesothelial cells isolated from LPA1 KO mice (Lee et al., 2015). We are unable to rule out the contribution of LPA2 to mesothelial invasion (Figure 3.2B) due to the inability to knock it down sufficiently (Figure 3.2A). However, hepatocarcinoma cells were able to invade mesothelial monolayers obtained from LPA2 KO mice (Lee et al., 2015). Taken together, these observations demonstrate mesothelial LPA1 promotes ovarian cancer invasion of the mesothelium, and LPA2 may not contribute to this process, although further studies are necessary to confirm. Furthermore, the trans-mesothelial invasion data are consistent with a role for LPA in inducing ovarian cancer metastasis in orthotopic and syngeneic ovarian cancer mouse models (Kim et al., 2006; Li et al., 2009; Nakayama et al., 2015). Specifically, our current experiments are consistent with the data presented in **Chapter 2** where we demonstrated increased mesothelial invasion and tumor seeding in LPP1 KO mice (Nakayama et al., 2015).

LPA is abundant in the ovarian cancer metastatic microenvironment where it has pleiotropic effects on both the cancer cells and non-transformed cells (Eder et al., 2000; Mills and Moolenaar, 2003; Ren et al., 2006). Within the peritoneal cavity, many cell types are capable of producing LPA including activated platelets, adipocytes, ovarian cancer cells, and mesothelial cells (Eder et al., 2000; Eichholtz et al., 1993; Mills and Moolenaar, 2003; Ren et al., 2006; Said et al., 2007; Valet et al., 1998). Specifically, we confirmed mesothelial cells constitutively produce LPA (Figure 3.6) (Ren et al., 2006). Interestingly, paracrine communication via LPA between ovarian cancer cells and mesothelial cells has been reported (Eder et al., 2000; Ren et al., 2006);

however, autocrine stimulation of mesothelial cells by LPA has not been shown. We demonstrate that autocrine production of LPA promotes mesothelial VCAM-1 expression and accumulation (Figure 3.7). These observations are consistent with autocrine pathways in mesothelial cell-stimulated motility and proliferation (Warn et al., 2001). Moreover, the data also agree with the increased mesothelial VCAM-1 expression found in LPP1 KO mice (**Chapter 2**, Figure 2.3). Taken together, these observations suggest that autocrine production of LPA activates LPA1 to promote mesothelial VCAM-1 expression.

VCAM-1 expression on the endothelium or mesothelium is induced transcriptionally by tumor necrosis factor α (TNF- α) or interleukin-1β through the activation of the nuclear factor-κB (NF-κB) (Collins et al., 1995). In contrast, our data show that VCAM-1 expression accumulated in mesothelial cells in an LPA-LPA1-dependent manner. VCAM-1 protein synthesis was inhibited after LPA1 knockdown (Figures 3.10A). LPA1 knockdown reduced VCAM-1 protein synthesis, and VCAM-1 protein expression in LPA mesothelial cells (+/- LPA1) seems to be relatively stable up to 8 hours as demonstrated by pulse-chase labeling. (Figure 3.11). However, cycloheximide treatment following LPA1 knockdown displayed a decrease in VCAM-1 protein expression (Figure 3.10B). It is important to note that cycloheximide inhibits all protein synthesis, including additional proteins that may regulate LPA1-dependent VCAM-1 expression indirectly. These observations indicate that LPA-mediated VCAM-1 synthesis in conjunction with increased stability promotes VCAM-1 expression in mesothelial cells and could account for the chronic expression observed on the mesothelium of ovarian cancer patients where elevated levels of LPA have been reported (Slack-Davis et al., 2009; Xiao et al., 2001; Xu et al., 1995).

In conclusion, the data presented here show that LPA targets the mesothelium to promote ovarian cancer cell invasion by inducing VCAM-1 expression on mesothelial cells. Mesothelium VCAM-1 expression is associated with an unfavorable prognosis for ovarian cancer patients (Scalici et al., 2016), and blocking VCAM-1 function decreases tumor burden and increases survival in mouse models of peritoneal ovarian cancer metastasis (Slack-Davis et al., 2009). Thus, LPA and VCAM-1, key components within the ovarian cancer metastatic microenvironment, influence non-transformed cells to support ovarian cancer metastasis and progression. Additionally, this study offers insight into the chronic regulation of VCAM-1 expression by LPA, which could have implications for a variety of disease states in addition to ovarian cancer. Specifically, atherosclerosis and rheumatoid arthritis are associated with abundant LPA and chronic VCAM-1 expression (Bot et al., 2010; Davies et al., 1993; Li et al., 2000; Nikitopoulou et al., 2012). In atherosclerosis, LPA has been shown to accumulate at high concentrations inside atherosclerotic lesions (Bot et al., 2010; Rother et al., 2003). VCAM-1 is also highly expressed in atherosclerotic plaques (Ley and Huo, 2001). Additionally, this study offers insight into chronic regulation of VCAM-1 expression by LPA, which could have implications for a variety of disease states in addition to ovarian cancer. The mechanisms by which LPA promotes VCAM-1 expression are unclear. LPA stimulates VCAM-1 expression on vascular endothelial cells through the nuclear factor-κB (NF-κB) pathway (Collins et al., 1995; Palmetshofer, 1999; Rizza, 1999). However, this expression is transient unlike the chronic accumulation of VCAM-1 observed in mesothelial cells. Interestingly, synovial fibroblasts from rheumatoid arthritis maintain an elevated level of VCAM-1 expression following the transient increase observed with tumor

necrosis factor α stimulation (Li et al., 2000). Synovial fibroblasts also express autotaxin, an extracellular lysopholipase D that converts lysophosphatidylcholine to LPA (Nikitopoulou et al., 2012), thus affording the possibility that autocrine production of LPA could maintain the chronically elevated level of VCAM-1 expression, which would facilitate the recruitment of leukocytes to the joint and permit the chronic pro-inflammatory state. Overall, this study provides a further understanding for a role of non-transformed cells within the metastatic microenvironment in the regulation of ovarian cancer mesothelial invasion, and it potentially provides a model for other conditions associated with abundant LPA and chronic VCAM-1 expression.

Chapter 4. Perspectives

4.1 Summary of Thesis Background, Goals, and Findings

Since the majority of ovarian cancer cases are diagnosed with advanced-stage disease, characterized by metastasis and the accumulation of malignant ascites, it is imperative to understand the mechanisms that govern ovarian cancer metastasis. Before the studies presented in this dissertation, LPA was known to promote ovarian cancer cell proliferation, survival, migration and invasion directly (Bian et al., 2006; Bian et al., 2004; Said et al., 2007). Additionally, LPA stimulates ovarian cancer growth and metastasis indirectly by inducing the production of proteases such as matrix metalloproteinases (MMPs) and urokinase plasminogen activator (uPA) (Fishman et al., 2001; Li et al., 2005). Moreover, LPA also stimulates ovarian cancer metastasis in orthotopic and syngeneic ovarian cancer mouse models (Kim et al., 2006; Li et al., 2009). Despite the overwhelming evidence demonstrating the influence of LPA on regulating ovarian cancer cell biology, little was known about the effect of LPA on the tumor microenvironment, specifically on mesothelial cells, to promote ovarian cancer progression and metastasis.

This dissertation reports the discovery of a role for LPA in the ovarian cancer metastatic microenvironment in promoting mesothelial invasion. Ovarian cancer cells attach to and invade through the mesothelium; mesothelial invasion is associated with an unfavorable prognosis in ovarian cancer (Bell et al., 2004). The data in **Chapter 2** demonstrated that elevated levels of LPA in the microenvironment of a mouse model, LPP1 KO, correlated with increased tumor seeding and mesothelial invasion, which coincided with mesothelial VCAM-1 expression. VCAM-1 is elevated on the mesothelium of ovarian cancer patients where it functions to promote mesothelial

invasion and tumor progression (Slack-Davis et al., 2009). Mesothelium VCAM-1 expression is associated with an unfavorable prognosis for ovarian cancer patients (Scalici et al., 2016), and blocking VCAM-1 function decreases tumor burden and increases survival in mouse models of peritoneal ovarian cancer metastasis implicating VCAM-1 as an important target for the treatment of ovarian cancer (Slack-Davis et al., 2009). However, the mechanisms that regulate VCAM-1 expression on the mesothelium of metastatic ovarian cancer patients were unknown at the time these studies were initiated. The findings in **Chapter 2** developed the framework to evaluate whether LPA regulates mesothelial VCAM-1 expression (**Chapter 3**).

The contribution of LPA to VCAM-1 expression was evaluated in human mesothelial cells (LP9), which previously had been demonstrated to constitutively produce LPA (Ren et al., 2006). The data in **Chapter 3** demonstrated that LPA acting through LPA1 regulated mesothelial VCAM-1 expression to promote trans-mesothelial invasion. While much work remains to identify the molecular mechanisms by which LPA mediates VCAM-1 expression, these findings provide a novel role for LPA in influencing the tumor microenvironment to promote mesothelial invasion through the regulation of VCAM-1 expression.

4.2 Perspective on LPA Signaling Promoting VCAM-1 Expression

LPA stimulation leads to the activation of multiple downstream signaling pathways such as the Rho/Rho-Kinase, MAPK, and PI3K pathways through G-proteins (Figure 1.5). Many of these signaling cascades support ovarian cancer cell proliferation, migration, and invasion (Bian et al., 2005; Bian et al., 2004; Yu et al., 2008). Data from **Chapter 3** demonstrated that LPA stimulation

of the LPA1 receptor promotes VCAM-1 expression. Two potential pathways LPA-dependent pathways have been described to stimulate VCAM-1 expression, i.e., the Rho and PI3K pathways.

4.2.1 LPA Induction of Rho Pathway Promotes VCAM-1 Expression

LPA can induce VCAM-1 expression transcriptionally through the activation of the NF-κB pathway in endothelial cells (Shimada and Rajagopalan, 2010). LPA rapidly activated Rho kinase in human umbilical vein endothelial cells (HUVECs) leading to LPA promoted phosphorylation of NF-κB p65, a subunit of NF-kappa-B transcription complex, and induced expression of VCAM-1 (Shimada and Rajagopalan, 2010). Furthermore, siRNA inhibition of the Rho kinase isoform, Rho-Associated Protein Kinase 2 (ROCK2), inhibited NF-κB p65 phosphorylation and VCAM-1 mRNA and protein expression (Shimada and Rajagopalan, 2010). These data suggest that LPA activates ROCK2 followed by NF-κB p65 phosphorylation to induce VCAM-1 expression (Shimada and Rajagopalan, 2010). LPA1 activates the Rho-Rho kinase pathway through Gα12/13 (Choi et al., 2010; Inoue et al., 2004; Maruta et al., 2008). Therefore, our data demonstrating LPA acting through LPA1 promotes VAM-1 expression and the literature supports a pathway in which LPA stimulation of LPA1 induces VCAM-1 possibly through a ROCK2-mediated activation of NF-κB (Figure 4.1).

To determine whether the LPA-mediated LPA1-Rho-ROCK2-NF-κB pathway regulates VCAM-1 expression, we will analyze the pathway in a stepwise manner from the receptor to

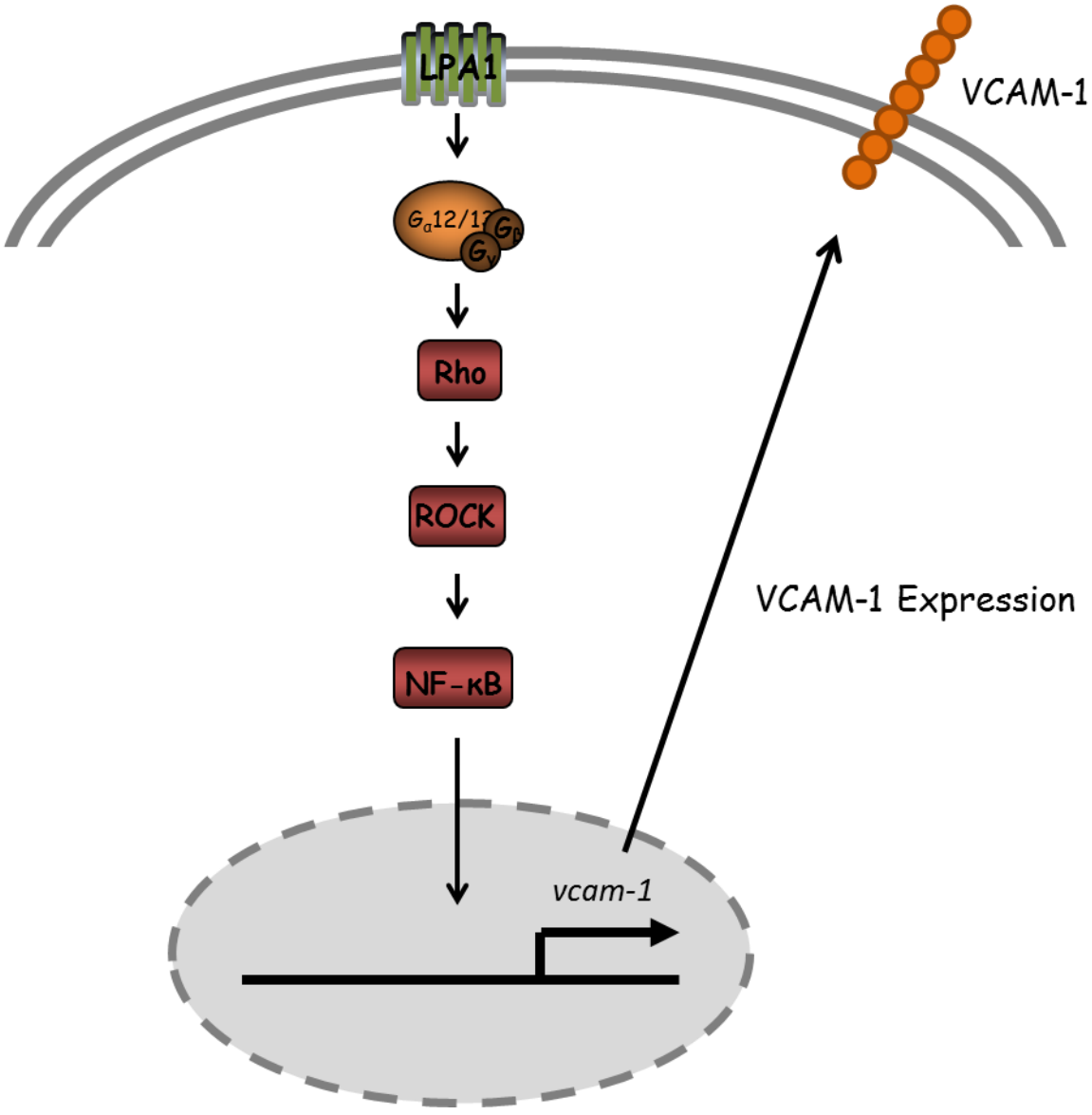
LPA1
VCAM-1
$G_\alpha 12/13$
G_β
G_γ
Rho
ROCK
NF-κB
VCAM-1 Expression
vcam-1

Figure 4.1. Proposed pathway of LPA inducing chronic VCAM-1 expression through the Rho pathway.

identify components that diminish VCAM-1 protein expression. LP9 mesothelial cells will be treated with an inhibitor of Rho (C3 toxin), and VCAM-1 protein and mRNA expression will be determined by western blot and qRT-PCR, respectively. To confirm the observations obtained from the inhibitor studies, siRNA directed against ROCK2 will be employed. To link the Rho pathway to the original observation that LPA1 influences VCAM-1 mRNA and protein levels, LP9 cells will be transfected with plasmids expressing constitutively activated ROCK2 in the context of LPA1 knockdown. We anticipate LPA1 signaling will lead to the activation the Rho pathway and VCAM-1 expression will be promoted. From the inhibitor screen, we expect to observe a decrease in VCAM-1 mRNA and protein expression. Knockdown of the ROCK2 will also show a similar trend as previously described. We predict VCAM-1 protein expression will be restored when mesothelial cells express an activated mutant of ROCK2 from following LPA1 knockdown.

4.2.2 LPA Activation of PI3K Potentially Leads to Chronic VCAM-1 Expression

LPA binding to its cognate receptor, LPA1 results in robust signaling of the phosphatidylinositol 3-kinase (PI3K) pathway (Choi et al., 2010). LPA1 couples with the G-protein, Gαi/βγ, to activate PI3K catalytic isoform p110β (Guillermet-Guibert et al., 2008). While most LPA-dependent signaling pathways progress through the Gα subunits, LPA-induced activation of PI3K/AKT pathway is mediated by the Gβγ complex (Kurosu et al., 1997; Maier et al., 1999; Murga et al., 2000). In atherosclerosis, chronic VCAM-1 expression in endothelial cells can be induced by the PI3K/AKT pathway (Tsoyi et al., 2010; Tsoyi et al., 2009). Tsoyi and group showed that upregulating or overexpressing PTEN, a negative regulator of the PI3K/AKT

pathway, inhibited VCAM-1 expression by blocking the PI3K/AKT/GSK-3β/GATA-6 pathway independently of inflammatory stimuli in activated endothelial cells (Tsoyi et al., 2010; Tsoyi et al., 2009). Specifically, overexpressing of PTEN blocked AKT phosphorylation, which promoted the binding of GSK to GATA-6 thus preventing GATA-6 from binding to the VCAM promoter. (Tsoyi et al., 2010; Umetani et al., 2001). From these observations, it is plausible that LPA signaling through LPA1 could induce the PI3K/AKT pathway leading to the chronic expression of VCAM-1 observed on mesothelial cells (Cannistra et al., 1994; Slack-Davis et al., 2009), thus promoting increased ovarian cancer invasion of the mesothelium (Figure 4.2).

To determine whether the P13K pathway links LPA to VCAM-1, we will knockdown LPA1 in LP9 mesothelial cells and evaluate AKT and GSK-3β phosphorylation as well as GATA-6 and VCAM-1 expression by immunoblot. LP9 mesothelial cells will also be treated with an inhibitor of P13K (LY294002) or PI3K-specific siRNA, and GATA-6 and VCAM-1 expression will be determined. To link the P13K pathway to the original observation that LPA1 promotes VCAM-1 mRNA and protein expression, LP9 cells will be transfected with plasmids expressing constitutively activated P13K in the context of LPA1 knockdown. For each experiment, VCAM-1 mRNA and protein expression will also be measured by western blot and qRT-PCR, respectively. We anticipate LPA1 signaling will lead to the activation of the P13K pathway. LPA1 knockdown will demonstrate a decrease in AKT phosphorylation, GATA-6, and VCAM-1 expression with an increase in GSK-3β phosphorylation. From the inhibitor studies, we expect to observe a decrease in VCAM-1 mRNA and protein expression as well as a decrease in GATA-6 protein expression. Knockdown of the P13K will also show a similar trend as previously described. We predict that

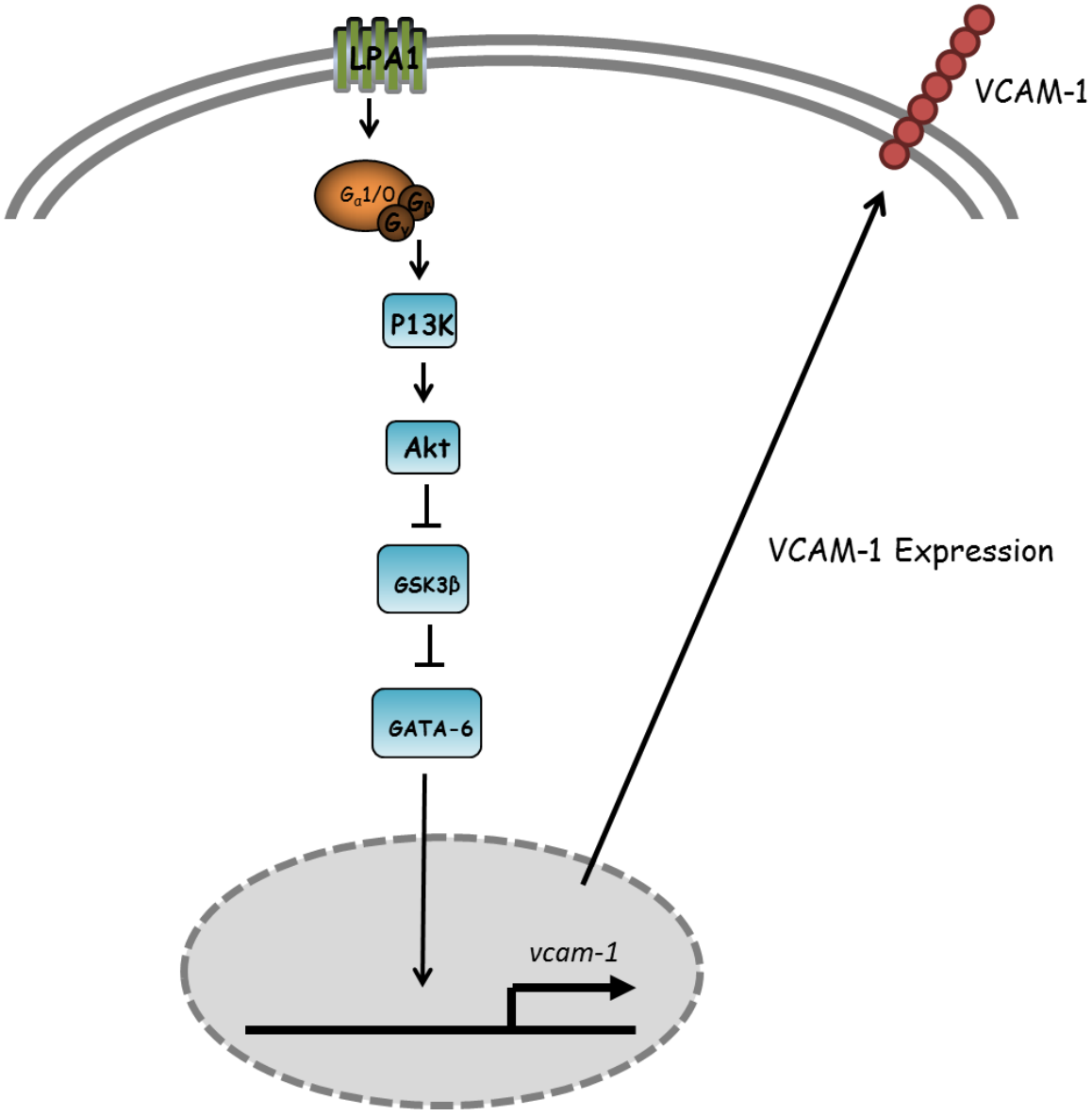
LPA1
VCAM-1
$G_{\alpha}1/0$
G_{β}
G_{γ}
P13K
Akt
GSK3β
GATA-6
VCAM-1 Expression
vcam-1

Figure 4.2. Proposed pathway of LPA activating PI3K leading to chronic VCAM-1 expression.

VCAM-1 protein expression will be restored when mesothelial cells express an activated P13K following LPA1 knockdown.

4.3 Perspective on Constitutively Produced LPA Regulating Mesothelial VCAM-1 Expression.

In **Chapter 3**, we demonstrated that LPA acting through LPA1 promoted VCAM-1 accumulation in LP9 mesothelial cells, which constitutively produce LPA (Ren et al., 2006). However, inhibiting autocrine stimulation of VCAM-1 accumulation only occurred at later time points. Additionally, exogenous LPA treatment increased VCAM-1 expression above autorcrine stimulation after 24 hours of treatment. Furthermore, a delay in VCAM-1 synthesis was also observed. These data could suggest that LPA may regulate VCAM-1 expression indirectly through the production of a factor at later time points. In addition to LPA, mesothelial cells have been reported to secrete VEGF, which has been linked to LPA-induced VCAM-1 expression (Stadlmann et al., 2005).

4.3.1 LPA-induced VEGF Production Promotes Mesothelial VCAM-1 Expression

Vascular endothelial growth factor (VEGF) is a potent glycoprotein that stimulates angiogenesis and ascites accumulation in ovarian cancer (Ahmed and Stenvers, 2013; Byrne et al., 2003; Sherer et al., 2000). Mesothelial cells produce the VEGF family member VEGF-A (Gerber et al., 2006; Sako et al., 2006; Stadlmann et al., 2005). VEGF-A exists in several different isoforms due to alternative splicing of the gene, and $VEGF_{121}$ and $VEGF_{165}$ are the two predominant forms

found in mesothelial cells (Sako et al., 2003). LPA increases *VEGF-A* mRNA levels, while treatment with an LPA1,3 receptor antagonist, Ki16425, or pertussis toxin, an inhibitor of Gi proteins, significantly decreased LPA-induced VEGF-A secretion (Sako et al., 2006). Sako et. al showed LPA1 was the primary LPA receptor expressed in mesothelial cells (Sako et al., 2006). These findings suggest LPA stimulation of LPA1 leads to VEGF production in mesothelial cells and may contribute to increased VEGF levels found in the malignant ascites (Sherer et al., 2000).

In addition to promoting angiogenesis and vascular permeability, VEGF-A signaling through one of two receptor tyrosine kinases, vascular endothelial growth factor receptor (VEGFR) 1 and 2 to increase VCAM-1 gene expression (Ferrara and Davis-Smyth, 1997; Ferrara et al., 2003). Ferrara et al. showed that $VEGF_{165}$ regulated VCAM-1 gene expression through VEGFR2 (Fearnley et al., 2014). Additionally, Gerber and colleagues showed that VCAM-1 positive mesothelial cells produced 100-fold more VEGF-A as compared to other populations of cells in omentum samples, and that 85% of the VEGF found in the omentum samples comes from those mesothelial cells (Gerber et al., 2006). From these observations, it is plausible that LPA acting through LPA1 promotes VEGF expression leading to increased VCAM-1 accumulation in LP9 mesothelial cells (Figure 4.3).

To test this hypothesis, conditioned media from LP9 mesothelial cells should be analyzed for VEGF expression using a human VEGF-specific ELISA kit. This observation will confirm previous observations demonstrating that LP9/TERT-1, an immortalized LP9 mesothelial cell line, produced VEGF (Hillegass et al., 2010). Additionally, blocking or inhibiting LPA in LP9 mesothelial cells should reduce VEGF expression. Moreover, LP9 mesothelial cells could also be

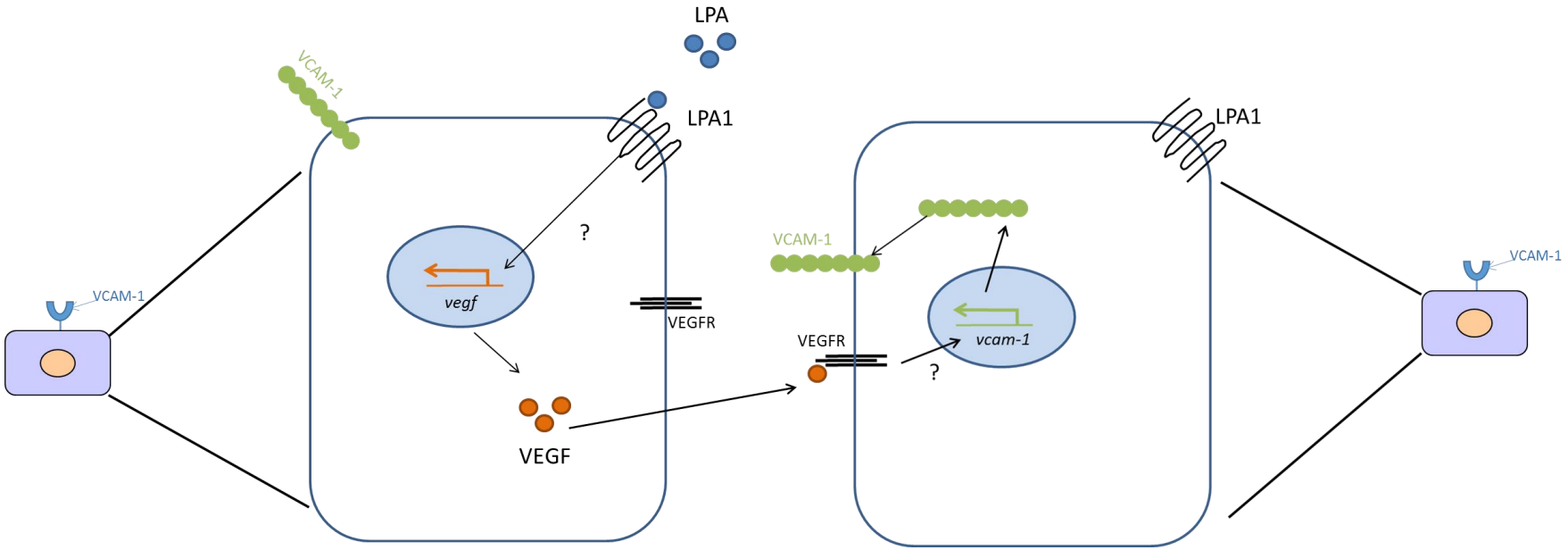
LPA
VCAM-1
LPA1
?
vegf
VEGFR
VCAM-1
VEGF
VCAM-1
LPA1
VCAM-1
VEGFR
vcam-1
?
VCAM-1

Figure 4.3. Model of LPA inducing VEGF production and secretion in mesothelial cells to promote mesothelial VCAM-1 expression. This model shows paracrine signaling between two mesothelial cells to promote VCAM-1 expression; however, autocrine production of VEGF could also lead to mesothelial VCAM-1 expression.

treated with VEGF to determine VCAM-1 mRNA and protein expression by qRT-PCR and immunoblot, respectively. We would expect an earlier increase in VCAM-1 expression than observed with LP9 cell autocrine production of LPA. With VEGF-A stimulating VEGFR2 signaling, the contribution of VEGFR to VCAM-1 expression should be examined in mesothelial cell knockdown studies. We expect to observe a decrease in VCAM-1 expression when VEGFR2 is knocked down. Moreover, in the context of LPA1 knockdown, LP9 cells should be treated with VEGF to observe a rescue in VCAM-1 expression. Additionally, conditioned media from mesothelial cells after LPA1 knockdown can be assessed using a multiplex cytokine array to determine other potential factors that may influence VCAM-1 expression. Upon determining the factor/s that are decreased after siRNA inhibition of *LPA1*, similar studies as above can be utilized to explore the role that factor plays in promoting VCAM-1 expression.

4.4 Perspective on VCAM-1 Degradation

In **Chapter 3**, data from pulse-chase experiments (± cycloheximide) with S^{35}-labeled amino acids after control or *LPA1* knockdown showed no difference in degradation of VCAM-1 (Figures 3.11); however, LP9 mesothelial cells displayed a decrease in VCAM-1 protein half-life after treatment with cycloheximide and LPA1 knockdown (Figure 3.10C). We propose the cells surface expression is being measured by cycloheximide treatment alone and S^{35}-labeling of VCAM-1 (± cycloheximide). This hypothesis is based on the flow cytometry data where we observe a 50% decrease in cell surface expression of VCAM-1 after LPA1 knockdown (Figure 3.3B). The cycloheximide treatment alone with LPA1 knockdown (Figure 3.10 B) also showed that 50% of

VCAM-1 remained after 4 hours of treatment. From these observations, I further hypothesize that once VCAM-1 reaches the cell surface, it is stabilized independently of LPA. In figure 3.12C, exogenous expression of GFP-VCAM-1 in LP9 cells rescued trans-mesothelial invasion after LPA1 knockdown suggesting that in the absence of LPA1 and utilizing a different promoter to expression GFP-VCAM-1, exogenous VCAM-1 was stabilized at the cell surface to interact with α4β1 integrin on the ovarian cancer cell to promote ovarian cancer cell invasion of the mesothelium.

To test this hypothesis, VCAM-1 localization would be observed after LPA1 knockdown with immunofluorescence (IF). LP9 cells should be treated with cycloheximide, collected as before, and examined by IF to observe the localization of VCAM-1. We would expect to observe VCAM-1 expression at the cell surface (± LPA1) and cycloheximide treatment. Additionally, permeabilizing the cells should also show cell surface expression after LPA1 knockdown and/or cycloheximide treatment. Moreover, flow cytometry should be repeated with permeabilized cells, and the expectation would be that siRNA inhibition of *LPA1* would result in a 50% reduction of VCAM-1 expression, similarly to the previous flow data (Figure 3.3B). To further test this hypothesis, VCAM-1 will be labeled with a non-radioactive alternative using the Click-iT HPG Alexa Fluor 488 protein synthesis assay kit. LP9 cells will be transfected with either control or *LPA1* siRNA for 20 hours and cultured in methionine-free media for 16 hours. Next, LP9 cells will be incubated for 4 hours in methionine-free media containing L-homopropargylglycine (HPG), an amino acid analog of methionine containing an Alexa Fluor 488 azide, and then chased with complete media. The fluorescently-tagged localization of newly synthesized VCAM-1 can

be detected by IF and confirmed by flow cytometry. We would expect to observe VCAM-1 expression only at the cell surface after LPA1 knockdown (± cycloheximide).

4.5 Perspective on Primary Human Mesothelial Cell Lines

In **Chapter 3**, we worked with mesothelial cells isolated from the ascites of ovarian cancer patients, LP9 and LP3 mesothelial cells (Connell and Rheinwald, 1983). Exposing human peritoneal mesothelial cells to factors in the malignant ascites differentially regulated genes related to cell cycle, cell signaling, cell movement, and protein synthesis (Matte et al., 2014a). One such factor explored was hepatocyte growth factor (HGF) (Matte et al., 2014b). In this study, HGF was found to be present in the malignant ascites at elevated concentrations as compared to benign fluids, and it promoted human peritoneal mesothelial cell migration (Matte et al., 2014b). Moreover, ascitic fluid from ovarian cancer patients was found to be hypoxic (Kim et al., 2006), and culturing mesothelial cells in hypoxic conditions altered the morphology of the cells from a cobblestone-like monolayer to a spindle-shaped fibroblast-like shape (Morishita et al., 2016). Additionally, hypoxia also induced the expression of hypoxia-inducible factor (HIF)-1α in mesothelial cells (Morishita et al., 2016). LP9 and LP3 mesothelial cells were isolated from the ascitic fluid of ovarian cancer patients (Wu et al., 1982), a hypoxic environment. From these observations, it is possible that LP9 and LP3 mesothelial cells have been "conditioned" by factors in the ascitic fluid to constitutively produce LPA (Ren et al., 2006) to promote the observed chronic expression of VCAM-1 (Slack-Davis et al., 2009).

LP9 and LP3 mesothelial cells were relevant to our studies because we were able to access the contributions of constitutively produce LPA to chronic VCAM-1 expression (Cannistra et al., 1994; Ren et al., 2006; Slack-Davis et al., 2009). Additionally, by utilizing two different mesothelial cells, it is possible that they represent different genetic backgrounds and give validity to our study. However, with these commercially available mesothelial cells that have been cultured and frozen since 1983 (Connell and Rheinwald, 1983), which may have resulted in modifications from their original phenotype (Kenny et al., 2007; Rampino et al., 2001). From this, isolated primary mesothelial cells from patients with ovarian cancer should be used at an early passage to minimize the concerns with the commercially available mesothelial cells to add further validity to our findings. Additionally, mesothelial cells that have not exposed to factors in the ascitic fluid would be ideal to test whether LPA can initiate and sustain the chronic VCAM-1 expression observed (Slack-Davis et al., 2009).

4.6 Perspective on the Tumor Influencing the Microenvironment to Initiate VCAM-1 Expression

Our lab demonstrated that both the tumor and factors in the microenvironment are important for initiating mesothelial VCAM-1 expression (Slack-Davis et al., 2009). Previously, it was demonstrated that a majority of peritoneal biopsies from ovarian cancer patients stained positive for VCAM-1 expression (13 of 14 ovarian cancer patients), whereas significantly fewer peritoneal biopsies from women with benign conditions stained positive for VCAM-1 (6 of 15) (Slack-Davis et al., 2009) (Figure 1.9). This observation suggests the presence of the tumor may be necessary

for chronic VCAM-1 expression. Moreover, in mice, VCAM-1 staining was observed on the mesothelium following 2 weeks of tumor growth as compared to non-tumor bearing mice (Slack-Davis et al., 2009). Furthermore, in **Chapter 2**, we reported significantly fewer wild type control mice staining positively for VCAM-1 expression two weeks after tumor initiation (2 of 7) as compared to LPP1 KO mice (5 of 8) (Nakayama et al., 2015) (Figure 2.3B). These observations suggest interactions with the tumor cells and the microenvironment are necessary to promote VCAM-1 expression.

A recent study also demonstrated that the presence of tumor cells was important to influence mesothelial cell gene expression (Kenny et al., 2014). The Kenny et al. study demonstrated that ovarian cancer cells co-cultured with mesothelial cells "conditioned" the mesothelial cells to induce fibronectin expression (Kenny et al., 2014). Additionally, conditioned media from ovarian cancer cells also stimulated fibronectin expression in mesothelial cells demonstrating that mesothelial cell "conditioning" is not limited to direct contact with the ovarian cancer cells but also factors secreted by the cancer cells will "condition" mesothelial cells (Kenny et al., 2014). This group further suggests that mesothelial cells become associated with cancer cells as "cancer-associated mesothelial cells" similarly to cancer-associated fibroblasts (Olumi et al., 1999) and cancer-associated adipocytes (Dirat et al., 2011; Nieman et al., 2013), and possibly this creates a tumor microenvironment that supports ovarian cancer growth and metastasis (Kenny et al., 2014).

These data support the notion that paracrine communication between tumor cells and mesothelial cells, as well as tumor secretion of factors into the tumor microenvironment "condition" mesothelial cells to upregulate VCAM-1. We have demonstrated that LPA can

promote VCAM-1 expression in “conditioned” mesothelial cells; however, we have not demonstrated whether LPA could initiate VCAM-1 expression in naïve cells. Furthermore, LPA may not be the only factor that contributes to VCAM-1 induction. Previous studies have shown that TNF-α (Wang et al., 2005), IL-1β (Watanabe et al., 2012)., and VEGF (Ahmed and Stenvers, 2013; Stadlmann et al., 2005) are secreted by the tumor cells and influence mesothelial cells, and this could influence VCAM-1 expression (Figure 4.4).

4.6.1 Ovarian Cancer Production of Factors to Induce Mesothelial VCAM-1 Expression

TNF-α , a well-known inducer of VCAM-1 expression, is elevated in malignant ascites (Moradi et al., 1993) and expressed by malignant ovarian cancer cells (Szlosarek et al., 2006). TNF-α is a positive regulator of ovarian cancer progression and associated with an unfavorable prognosis (Balkwill, 2009). TNF-α expression is elevated in women with ovarian cancer, and its expression correlates with increasing disease stage (Naylor et al., 1993). The ability of ovarian cancer cells to constitutively produce TNF-α was associated with increased tumor burden in a mouse model of peritoneal ovarian cancer metastasis, while inhibition of TNF-α expression resulted in decreased peritoneal dissemination and mesothelial invasion (Kulbe et al., 2007). Moreover, tumor-associated macrophages also contributed TNF-α to the malignant ascites and promoted ovarian cancer metastatic progression (Robinson-Smith et al., 2007). Stadlmann et. al demonstrated that treatment of TNF-α disrupted the integrity of human peritoneal mesothelial cell monolayer resulting in exposure of the mesothelial basement membrane (Stadlmann et al., 2003). Furthermore, TNF-α activates NF-κB through the canonical pathway leading to transcriptional

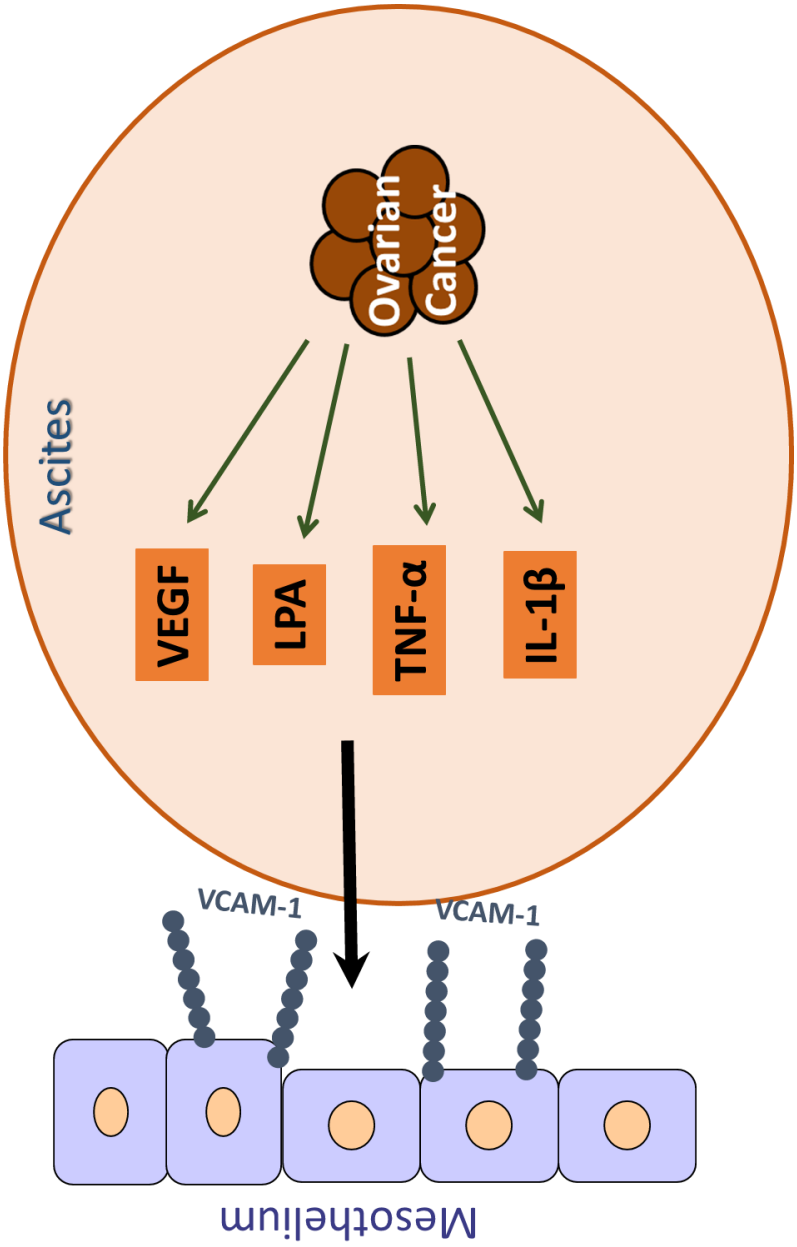
Ascites
Ovarian Cancer
VEGF
LPA
TNF-α
IL-1β
VCAM-1
VCAM-1
Mesothelium

Figure 4.4. Paracrine production of factors by ovarian cancers in the ascites could “condition” mesothelial cells to initiate mesothelial VCAM-1 expression.

upregulation of VCAM-1 (Collins et al., 1995). From these observations, TNF-α in the tumor microenvironment could induce chronic mesothelial VCAM-1 expression.

VCAM-1 expression is also induced by IL-1β (Collins et al., 1995). IL-1β was demonstrated to be elevated in the ascites of ovarian cancer patients as compared to benign fluid (Moradi et al., 1993). Additionally, upregulation of IL-1β in the ovarian cancer epithelium was observed (Schauer et al., 2013). Furthermore, elevated IL-1β expression correlated with reduced overall patient survival (Schauer et al., 2013). Additionally, ovarian cancer cells secrete IL-1β (Watanabe et al., 2012). Moreover, ovarian cancer cell secreted IL-1β influenced stromal cells and their gene expression (Schauer et al., 2013). Watanabe and group showed that ovarian cancer cell production of IL-1β induced the adhesion molecule β1 integrin on mesothelial cells and promoted peritoneal metastasis (Watanabe et al., 2012). From these observations, it is reasonable to speculate that ovarian cancer cell secreted IL-1β could influence mesothelial VCAM-1 expression.

In addition to mesothelial cells (previously described), ovarian cancer cells contribute VEGF to the tumor microenvironment to promote VCAM-1 expression (Lee et al., 2006; Park et al., 2007b). Established and primary ovarian cancer cell lines produced VEGF-A, and the primary cancer cells secreted higher levels of VEGF (mean = 5,046pg/ml) as compared to established cell lines (mean = 493 pg/ml) (Santin et al., 1999). Moreover, primary tumors from advanced stage ovarian cancer patients secreted more VEGF as compared to lower staged primary tumors from ovarian cancer patients (Santin et al., 1999). Additionally, LPA, at concentrations found in malignant ascites, induced VEGF production in ovarian cancer cells (Hu et al., 2001; Lee et al., 2006; Park et al., 2007b). Stadlmann and colleagues also demonstrated that IL-1β and TNF-α

significantly induced VEGF production (Stadlmann et al., 2005). These observations in conjunction with elevated VEGF concentrations in ascites (Ahmed and Stenvers, 2013) and its participation in the genesis of ascites accumulation (Byrne et al., 2003; Sherer et al., 2000), it is plausible that VEGF production by the tumor cells could initiate mesothelium VCAM-1 expression.

To explore the hypothesis that ovarian cancer cells are necessary to initiate mesothelial VCAM-1 expression, "non-conditioned," naïve primary mesothelial cells from patients with benign disease should be utilized. A co-culture of the naïve primary mesothelial cells and tumor cells labeled with GFP, as described by Kenny et. al, can be sorted by flow cytometry to assess VCAM-1 expression on the mesothelial cells (Kenny et al., 2014). We would expect to observe an increase in VCAM-1 expression after co-culturing "non-conditioned" mesothelial cells with labeled ovarian cancer cells. Moreover, conditioned media from the ovarian cancer cells or ascitic fluid from patients could be to treat the naïve primary mesothelial cells, which would be evaluated for VCAM-1 expression measured by western blot analysis. VCAM-1 expression is expected to increase with the conditioned media treatment. Furthermore, the expression of LPA, TNF-α, IL-1β, and VEGF should be assessed in the conditioned media, and expression of their receptors should be assessed in the naïve mesothelial cells. Knockdown of each receptor should be utilized in the naïve primary mesothelial cells. The expected outcome would be no change or a decrease in VCAM-1 expression with knockdown of each receptor and treatment with conditioned media from the ovarian cancer cells. From these studies, we will be able to demonstrate that both the cancer

cell and factors secreted in the tumor microenvironment by the cancer cell promote VCAM-1 expression.

4.7 Perspective on the Trans-Mesothelial Invasion Assay

Ovarian cancer cells metastasize by attaching to and invading through the mesothelium to access the underlying stroma and ECM (Iwanicki et al., 2011; Slack-Davis et al., 2009; Strobel and Cannistra, 1999). The trans-mesothelial invasion assay system used in **Chapter 3** aims to model aspects of peritoneal metastasis; however, this assay is also incomplete in truly replicating the human *in* vivo mesothelial invasion. The assay uses only two components, ovarian cancer cells and mesothelial cells, to model the interaction between the ovarian cancer cells and mesothelium; however, as described in **Chapter 1**, there are other components below the mesothelium that may participate in promoting mesothelial invasion. The mesothelial cell layer is attached to a basement membrane composed of ECM molecules including collagen types I and IV, laminin, vitronectin, and fibronectin, as well as stromal cells such as fibroblasts (Heyman et al., 2008; Lessan et al., 1999; Mueller and Fusenig, 2004; Strobel and Cannistra, 1999; Witz et al., 2001). The trans-mesothelial assay works by ovarian cancer cells attaching and invading a monolayer of mesothelial cells plated on a glass coverslip. The glass coverslip is not a physiologically relevant substrate because it lacks many of the components of the mesothelium such as other stromal cells. Therefore, it is conceivable that the ovarian cancer cells would respond differently on a more physiologically relevant substrate. To address this issue, we could utilize a three-dimensional *in vitro* model system to better assess the mechanism that governs mesothelial invasion. Kenny et

al. established a three-dimensional *in vitro* model system that included mesothelial cells, fibroblasts, and a defined ECM (Kenny et al., 2007). In this model, primary mesothelial cells and fibroblasts were isolated from patients who underwent surgery for benign conditions and human ascites from ovarian cancer patients (Kenny et al., 2007). In this model, early passaged fibroblasts were embedded in ECM, primarily collagen type I, and early passage mesothelial cells were added on top and cultured until a monolayer formed (Kenny et al., 2009; Kenny et al., 2007). Lastly, ovarian cancer cells were added on top of the monolayers and invasion was assessed (Kenny et al., 2007). From this model, it would be interesting to measure ovarian cancer cell invasion in the presence or absence of mesothelial VCAM-1.

4.8 Summary and Final Perspectives

The work in this thesis provides a further understanding of a role for LPA in regulating mesothelial VCAM-1 expression in the tumor microenvironment to promote ovarian cancer progression and peritoneal metastasis. Separately, LPA and VCAM-1 have already been associated with ovarian cancer progression and metastasis (Kim et al., 2006; Li et al., 2009; Sengupta et al., 2006; Slack-Davis et al., 2009), and cell adhesion is known to be regulated by LPA (Lee et al., 2004; Palmetshofer, 1999; Rizza, 1999). However, in ovarian cancer there have been no known studies linking these two molecules together to promote mesothelial invasion. Thus, the innovation of this thesis is in identifying a unique role for LPA in promoting chronic VCAM-1 expression on the mesothelium. In **Chapter 2**, we demonstrate that LPA metabolism in the microenvironment influences mesothelial invasion and VCAM-1 expression. These data are similar to findings

showing that both the tumor and stromal cell expression of PLA2β, a phospholipase that generates LPA, are important to promote tumorigenesis and metastasis in a syngeneic mouse model of ovarian cancer, similar to the *in vivo* model system we utilized (Li et al., 2010).

The studies in **Chapter 3** uncovered a novel role for LPA in the regulation of mesothelial VCAM-1 expression to promote ovarian cancer cell invasion of the mesothelium (Figure 4.5). The data from this thesis support *in vivo* findings demonstrating the role LPA plays in promoting ovarian cancer metastasis (Li et al., 2009; Li et al., 2010; Nakayama et al., 2015; Sengupta et al., 2006). Additionally, these data correspond to ovarian cancer patient data, which show elevated levels of LPA in malignant ascites and chronic VCAM-1 expression within the peritoneal lining of women with ovarian cancer (Slack-Davis et al., 2009; Xiao et al., 2001; Xu et al., 1995). We anticipate that these results will facilitate the development of more effective therapeutic regimens potentially through targeting the interplay between the tumor cells and non-transformed cells. Furthermore, this work has the potential to provide a model for other conditions associated with abundant LPA and chronic VCAM-1 expression, such as autoimmune diseases including multiple sclerosis and rheumatoid arthritis.

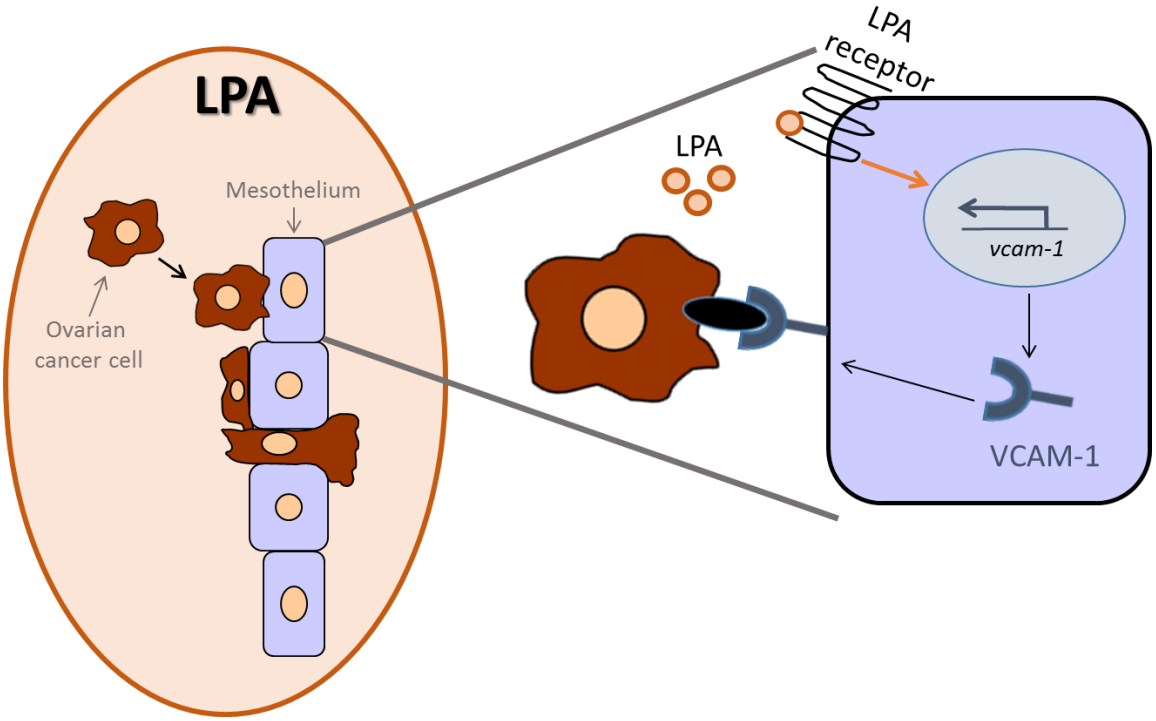
LPA
Mesothelium
Ovarian
cancer cell
LPA
receptor
LPA
vcam-1
VCAM-1

Figure 4.5. Summary model of overall findings. LPA influences the tumor microenvironment in part by regulating VCAM-1 protein expression on the mesothelium to promote mesothelial invasion.

Chapter 5. Materials and Methods

5.1 Cell Culture

Primary human mesothelial cell lines, LP9 and LP3 (Coriell Repository), were grown in 1:1 Medium 199:MCDB131 with 15% FBS, 10 ng/ml epidermal growth factor, and 0.4 ug/ml hydrocortisone. The mesothelial cell lines were passaged four times before new cells were thawed from frozen stocks. Experiments were done within those passages. SKOV3ip1 cells were grown in RPMI-1640 supplemented with 10% FBS (Slack-Davis et al., 2009). ID8 cells were generously provided by Dr. K. Roby (University of Kansas) (Roby et al., 2000) and cultured in DMEM supplemented with 4% fetal bovine serum, 100 units/mL penicillin, 100 μg/mL streptomycin, 5 μg/mL insulin, 5 μg/mL transferrin, and 5 ng/mL sodium selenite. They were passaged twice through C57Bl/6 mice to increase tumor take and decrease growth kinetics. The resultant cell line, ID8ip2, was transduced with lentivirus expressing luciferase (GeneCopoeia, Rockville, MD), and stably expressing populations (ID8ip2Luc) were obtained following puromycin (2 μg/mL) selection for 2 weeks.

5.2 Reagents

VPC51299 (kindly provided by Dr. Kevin Lynch, University of Virginia) were suspended in 0.5% fatty acid-free bovine serum albumin in phosphate-buffered saline and used at 10 μM concentration. (Figure 3. (East et al., 2011; Swaney et al., 2010). LPA (18:1, Sigma-Aldrich) was suspended in 0.5% fatty acid-free bovine serum albumin in phosphate-buffered saline and used 10 μM concentration. 0.5% fatty acid-free bovine serum albumin was used as a control.

5.3 Cell Transfections

SiRNA oligonucleotides were obtained from Dharmacon for human LPA1 (SMARTpool and individual oligos) and siGLO RISC-Free Control. GFP-tagged VCAM-1 plasmid was generously provided by Dr. Francisco Sánchez-Madrid (Universidad Autónoma de Madrid). LP9 or LP3 cells were plated for 24 hours prior to transfection protocol. The cells were harvested by trypsinization and counted at a concentration of 10^6 cells per sample. The trypsinized cels were pelleted by centrifugation, and supernatant removed. The cells were resuspended at a concentration of in 100µL of room temperature supplemented basic endothelial nucleofector solution (Lonza) per sample. 30 nM of siRNA or siCtrl was added to cell suspension and gently mixed. For experimentations with the GFP-tagged VCAM-1 plasmids, the plasmid was also added to either the siRNA or control cell suspension at the indicated concentration. The solution was transferred to the nuclofection kit cuvette making sure not to introduce bubbles and the cuvette was capped. Program T-23 was selected on the nucleofector and the cuvette was inserted. The selected program was applied to sample. After nucleofection of the sample, 500 uL of 37˚C warmed culture media was added to the cuvette and the sample was gently transferred to the appropriate culture dish with correct volume of culture media for that dish. The nucleofected cells were incubated for 24 to 48 hours before experimentation took place.

5.4 RIPA Cell Lysis

Following treatment, the media from the cells were aspirated; the cells were washed twice with ice cold PBS; and placed on ice. 100 µL of cold supplemented RIPA buffer (50 mM Hepes, 0.15 M NaCl, 2 mM EDTA, 0.1% Nonidet P40, and 0.05% sodium deoxycholate, pH 7.2

supplemented with protease inhibitors [Roche protease cocktail], 1 mM Na_3VO_4, 40 mM NaF, and 10 mM $Na_4P_2O_7$) was added to the cells. The cells were scraped into the RIPA buffer and transferred to 1.5 ml Eppendorf tube. The cell lysates were incubated on ice for 15 minutes before centrifuging at 13,000 RPM for 10 minutes at 4˚C. A BCA assay was complete for protein concentration prior to SDS-PAGE/Western blot analysis.

5.5 Western Blot Analysis

Cell lysates prepared in supplemented RIPA buffer were resolved on 8% SDS-PAGE gels, transferred to nitrocellulose, blocked in 5% nonfat milk/TBST, and blotted with the indicated antibodies overnight a 4ºC in 5% BSA/TBST. Antibodies included human-specific anti-VCAM-1 (H-276; Santa Cruz Biotechnology) (1:2000), anti-phospho-ERK (E7028; Sigma) (1:1000), anti-ERK (B3B9; gift from Dr. Michael Weber, University of Virginia) (1:10,000), and anti-actin (A1978; Sigma) (1:5000). Following the primary antibody incubation, three 10-minute washes in PBS/0.05% Tween 20 was completed. The membrane was then incubated with HRP-conjugated secondary antibodies, goat anti-mouse IgG or goat anti-rabbit IgG, at a dilution between 1:1,000 to 1:5,000 in PBS/0.05% Tween 20 for 1 hour. The membrane was washed three times for 10 minutes each in PBS containing 0.05% Tween 20 and protein bands visualization by ECL (Amersham Biosciences). Films were scanned and signal intensity determined using ImageJ.

5.6 Quantitative RT-PCR

After treatment, cells were washed with PBS and aspirated. RNA was extracted from LP9 or LP3 cells using Aurum total RNA mini kit (Bio-Rad). RNA concentrations were measured in

µg/mL using a NanoDrop (Thermo Scientific). iScript cDNA synthesis kit (Bio-Rad) was used to produce cDNA. Based on concentrations, 1 µg of RNA was calculated and RNase free H_20 was added to obtain a total volume of 15µL. A 20 µL reaction containing 4 µL of 5X iScript reaction mix, 1 µL of iScript reverse transcriptase, and the 15 µL of RNA template was added to iCycler. The reaction protocol is as follows: 5 minutes at 25˚C, 30 minutes at 42˚C, 5 minutes at 85˚C, and hold at 4˚C. After cDNA production, qRT-PCR master mix was made. The master mix contained Absolute Blue Syber Green ROX mix (Thermo Scientific) (10 µL), forward primer (0.4 µL), reverse primer (0.4 µL), and RNase free H_2O (7.2 µL). 2 µL of template cDNA was added to the master mix to have a total volume of 20 µL. The 20 µL reaction was added to a microplate and tightly sealed. The microplate was briefly centrifuged and Real-Time PCR was performed using the Step One Plus Real-Time PCR system (Applied Biosystems). The primers sequences can be found in **Table 5.1**. Data were analyzed using the delta-delta C_T method. The relative change in gene expression was normalized to GUSB and expressed relative to scrambled control.

5.7 Trans-mesothelial Invasion Assay

The trans-mesothelial migration assay was performed as described previously (Slack-Davis et al., 2009).

5.7.1 LPA Receptor Antagonist Treatment

LP9 cells were plated on glass coverslips to form monolayers. The monolayers were labeled with CellTracker Orange (Invitrogen) and SKOV3ip1 cells labeled with CellTracker Green (Invitrogen) 24 hours before treatment. The 10^5 labeled SKOV3ip1 cells were seeded on the labeled

Table 5.1 Primers used for qRT-PCR.

Gene	Primer Set	Sequence
LPA-1	A	Forward: GCTGCCATCTCTACTTCCATC Reverse: AAGCGGCGGTTGACATAGATT
LPA-1	B	Forward: CTTTGCTGGGTTGGCCTACTT Reverse: GAGTATTGGGTCCTGTGTTGAAC
LPA-1	C	Forward: CAACACAGGACCCAATACTCG Reverse: GAGCCATGTGCTAACAGTCAG
LPA-2	A	Forward: ACAGCCCGACTTTCACTTGAG Reverse: GCCCACAATGAGCATGACCA
LPA-2	B	Forward: TGTCGAGCCTGCTTGTCTTC Reverse: TGAGCGTGGTCTCTCGGTAG
LPA-2	C	Forward: CCTGGTCAAGACTGTTGTCATC Reverse: GACTCACAGCCTAAACCATCC
LPA-3	A	Forward: ACACTGATACTGTCGATGACTGG Reverse: GCAGAAAAACGTCCCAACACAC
LPA-3	B	Forward: TTAGCTGCTGCCGATTTCTTC Reverse: CTGGGCCTGTGTTAAACATCA
LPA-3	C	Forward: AACCGCTGGTTTCTCCGTC Reverse: AAGCAGTCAAGCTACTGTCCA
VCAM-1	A	Forward: CTTAAAATGCCTGGGAAGATGGT Reverse: GTCAATGAGACGGAGTCACCAAT
VCAM-1	B	Forward: CGAATGAGGGGACCACATCTA Reverse: TGTTCGTTCCCAAAACTAACAGG
VCAM-1	C	Forward: GGGAAGCCGATCACAGTCAAG Reverse: CTCCAGCCTGTCAAATGGGTA
VCAM-1	D	Forward: ATACCATCCGAAAGGCCCAGTTGA Reverse: AGAGCACGAGAAGCTCAGGAGAAA
VCAM-1	E	Forward: AAGGGAGCACTGGGTTGACTTTCA Reverse: TGGGAAAGTTGCACAGGAGTCTGA
Glucuronidase, beta	GUSB	Forward: CCGACTTCTCTGACAACCGAC Reverse: AGCCGACAAAATGCCGCAGACG

mesothelial monolayers and incubated for six hours in RPMI-1640 supplemented with 10% FBS (±) VPC51299 at indicated concentration. The coverslips were fixed and mounted. Confocal microscopy was used to obtain 1-μm Z-stacks on a LSM-700 confocal located in the microscope core. Image analysis was performed using Photoshop. SKOV3ip1 cells in an image from the top third of the Z-stack were pseudo-colored blue and merged with an image from the bottom third of the Z-stack. Percent trans-mesothelial invasion of SKOV3ip1 reflects the ratio of green to total cells in the merged image (Figure 5.1).

5.7.2 siRNA Inhibition

Following the cell transfection protocol, the 2 x 10^5nucleofected LP9 cells were plated on glass coverslips for 48 hours and monolayers were formed at that cell number. The monolayers were labeled with CellTracker Orange (Invitrogen) and SKOV3ip1 cells labeled with CellTracker Green (Invitrogen) 24 hours before treatment. The 10^5 labeled SKOV3ip1 cells were seeded on the labeled mesothelial monolayers and incubated for six hours in RPMI-1640 supplemented with 10% FBS. The coverslips were fixed and mounted. Confocal microscopy was used to obtain 1-μm Z-stacks on a LSM-700 confocal located in the microscope core. Image analysis was performed as previously described.

5.8 Metabolic Labeling

All experiments were performed following UVA radiation safety protocols.

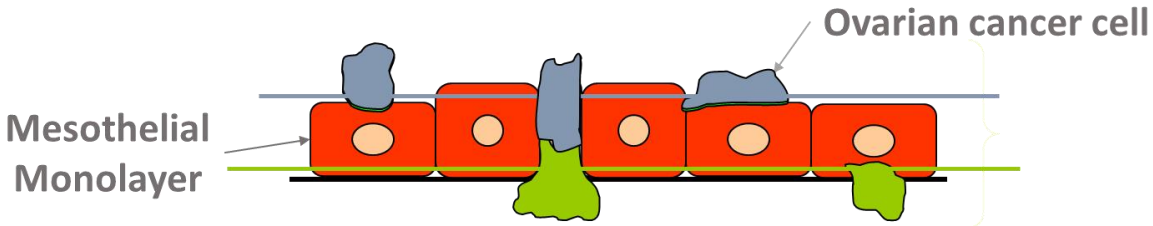
Ovarian cancer cell
Mesothelial
Monolayer

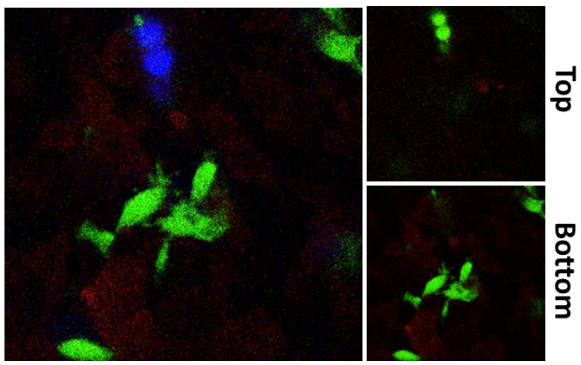
Top
Bottom

Figure 5.1. Schematic representation of ovarian cancer cell invasion of the mesothelial cell monolayer. Adapted from (Slack-Davis et al., 2009).

5.8.1 Pulse-labeling

LP9 cells were transfected with either control or *LPA1* smart pool siRNA for 20 hours, after which they were washed twice with PBS and incubated 16 hours in cysteine/methionine-free pulse-labeling medium (RPM1-1640, R7513; Sigma) containing 10% dialyzed FBS (Gibco) to deplete intracellular pool of methionine and cysteine. The cells were pulsed with pulse-labeling media (RPM1-1640, R7513; Sigma) containing [35-S]-Methionine/Cysteine (0.2 mCi/ml) and incubated for the indicated periods of time (Figure 5.2A). The [35-S]-Methionine/Cysteine pulse-labeling media was carefully aspirated and the cells were washed three times with PBS making sure to aspirate all PBS after the third wash. Samples were frozen at -80˚C until all samples were collected. The cells were lysed following the RIPA cell lysis protocol; however, protein concentration was not assessed. Cell lysates immunoprecipitated (later described) before they were resolved on 8% SDS-PAGE gels. Following SDS-PAGE, the gel was soaked for 1 hour in Gel soak solution (40% methanol, 10% Acetic Acid, and 5% Glycerol). The gel was then rinsed two times in H_2O for 5 minutes and dried between cellophane using a gel dryer (Bio-Rad). The gel was exposed to autoradiographic film for desired amount of time (16 hrs to 2 days) at -80˚C.

5.8.2 Pulse-Chase

For pulse-chase experiments, LP9 cells were transfected with either control or *LPA1* smart pool siRNA for 20 hours and cultured in cysteine/methionine-free media for 16 hours. LP9 cells were incubated for 4 hours in pulse-labeling media containing [35-S]-Methionine/Cysteine (0.2 mCi/ml); washed three times with PBS; and chased for 2, 4, 6, and 8 hours with complete medium

A

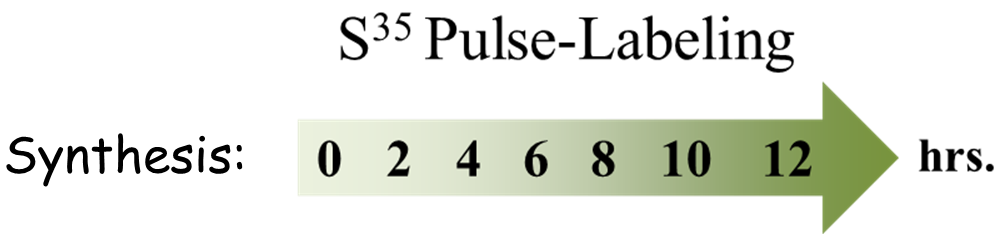
S35 Pulse-Labeling
Synthesis:
0 2 4 6 8 10 12
hrs.

B

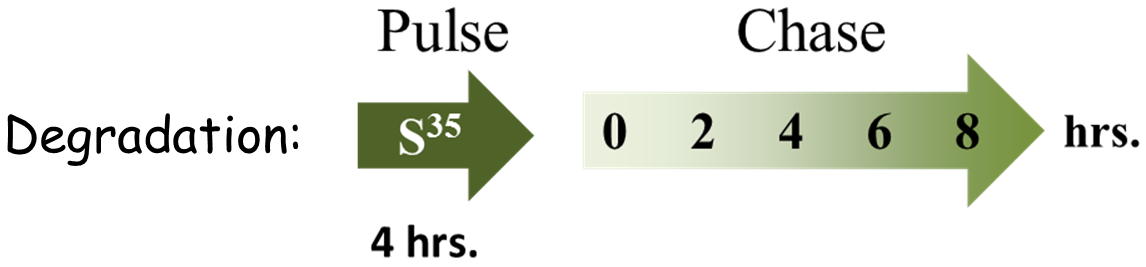
Pulse
Chase
Degradation:
S35
0 2 4 6 8
hrs.
4 hrs.

Figure 5.2. Schematic overview of metabolic labeling. **A.** Experimental set-up for determine VCAM-1 synthesis rate. **B.** Experimental design for determining VCAM-1 degradation rate.

for LP9 cells (Figure 5.2B). The complete media was carefully aspirated and the cells were washed three times with PBS making sure to aspirate all PBS after the third wash. Samples were frozen at -80˚C until all samples were collected. LP9 cells were lysed in supplemented RIPA buffer, immunoprecipitated (later described) for VCAM-1 (C-19, Santa Cruz), and resolved on an 8% SDS-PAGE gel, which was fixed in 40% Methanol, 10% Acetic Acid, 5% glycerol for 1 hour, dried between cellophane and exposed to autoradiographic film.

5.9 Immunoprecipitation

Cell lysates from metabolic labeling experiments were placed in a final volume of 500 µL of supplemented RIPA buffer. The primary antibody, VCAM-1 (C-19, Santa Cruz) or Rabbit Anti-mouse IgG (Jackson Labs), was added to the cell lysates at concentration of 1µg/mL and incubated by rotating overnight at 4˚C. After incubation, 100 µL of 50% Protein A slurry was added to cell lysate and antibody, and incubated for 2 hours at 4˚C. The cell lysates were centrifuged at max speeds for 30 seconds to pellet the Protein A sepharse. The pellet was washed with 500 µl of supplemented RIPA cell lysis and centrifuged for 30 seconds three times. The supernatant was aspirated between each wash and centrifuge and the washes were completed on ice. After the third wash and centrifuge, the pellet was resuspended in 12 µl of 4X sample buffer and 12 µl of 1X RIPA cell lysis buffer to a volume of 24 µl. The samples were boiled at 100˚C for 5 minutes and then centrifuged to pellet the Protein A sepharase. All the supernatant was loaded on the SDS-PAGE gel.

5.10 Flow Cytometry

LP9 cells (10^6 cells/ml) were transfected with siRNA against LPA1 and LPA2 and stained with PE-conjugated anti-human antibodies directed against VCAM-1 (CD106) or isotype antibodies as negative controls (all from Millipore). The stained samples were examined using a FACSCalibur cytometer (BD Biosciences) and data analyzed using FlowJo software version 9.4.10 for Macintosh (Tree Star). Geometric mean fluorescence intensity of anti-VCAM-1 stained samples was normalized to the isotype control and expressed relative to siCtrl.

5.11 Mouse Ovarian Cancer Peritoneal Metastasis

All animal experiments were performed following approval from the Institutional Animal Care and Use Committee at the University of Virginia. Six to 8 week-old female wild type (C57/BL6) or LPP1 hypomorphic (LPP1 KO) mice (n for each experiment indicated in figure legend) were injected intraperitoneally (IP) with 10^6 ID8ip2Luc cells in 200 μL PBS. Mice were observed 2-3 times per week by laboratory personnel and monitored for signs of distress (i.e., changes in appearance, respiration, activity, etc.) and weighed; mice showing signs of distress or losing greater than 15% body weight were euthanized and examined for tumor. Tumor burden was monitored weekly by measuring light emission following IP luciferin administration as an indication of luciferase activity using an IVIS imaging system (Molecular Imaging Core, University of Virginia). Total flux (photons/sec) was determined for the entire abdominal cavity. Upon experimental termination, mice were euthanized and tumor burden evaluated upon necropsy by counting the number of tumor nodules, and weighing the omentum (primary site of tumor implantation) and any additional tumor nodules. Formalin-fixed, paraffin-embedded tissues were

sectioned and H&E stained (University of Virginia Research Histology Core) to evaluate microscopic tumor burden and the extent of peritoneal invasion.

5.12 Statistical Analysis

All data were analyzed using GraphPad Prism 5.01 software. Trans-mesothelial invasion data were analyzed either using a one-way analysis of variance (ANOVA) followed by Newman-Keuls multiple comparison test or an unpaired T-test. Three way ANOVA was used to quantitative RT-PCR of *VCAM-1* to compare the effect of the knockdown of LPA1 at 4 times points, adjusting for experimental variation. Luminescence data were analyzed using 2-way analysis of variance (ANOVA) followed by Sidak's or Tukey's multiple comparisons test. The remaining data were analyzed by one-way ANOVA followed by Newman-Keuls multiple comparison test.

List of References

Adam, R.A., and Y.G. Adam. Malignant ascites: past, present, and future. *Journal of the American College of Surgeons*. 198:999-1011.

Ahmed, A.A., D. Etemadmoghadam, J. Temple, A.G. Lynch, M. Riad, R. Sharma, C. Stewart, S. Fereday, C. Caldas, A. deFazio, D. Bowtell, and J.D. Brenton. 2010. Driver mutations in TP53 are ubiquitous in high grade serous carcinoma of the ovary. *The Journal of Pathology*. 221:49-56.

Ahmed, N., and K.L. Stenvers. 2013. Getting to Know Ovarian Cancer Ascites: Opportunities for Targeted Therapy-Based Translational Research. *Frontiers in Oncology*. 3:256.

Amerongen, G.P.v.N., M.A. Vermeer, and V.W.M. van Hinsbergh. 2000. Role of RhoA and Rho Kinase in Lysophosphatidic Acid–Induced Endothelial Barrier Dysfunction. *Arteriosclerosis, Thrombosis, and Vascular Biology*. 20:e127-e133.

An, S., T. Bleu, O.G. Hallmark, and E.J. Goetzl. 1998. Characterization of a Novel Subtype of Human G Protein-coupled Receptor for Lysophosphatidic Acid. *Journal of Biological Chemistry*. 273:7906-7910.

Anliker, B., and J. Chun. 2004. Cell surface receptors in lysophospholipid signaling. *Seminars in Cell & Developmental Biology*. 15:457-465.

Balkwill, F. 2009. Tumour necrosis factor and cancer. *Nat Rev Cancer*. 9:361-371.

Barreiro, O., M. Yáñez-Mó, J.M. Serrador, M.C. Montoya, M. Vicente-Manzanares, R. Tejedor, H. Furthmayr, and F. Sánchez-Madrid. 2002. Dynamic interaction of VCAM-1 and ICAM-1 with moesin and ezrin in a novel endothelial docking structure for adherent leukocytes. *The Journal of Cell Biology*. 157:1233-1245.

Barthel, S.R., M.W. Johansson, D.M. McNamee, and D.F. Mosher. 2008. Roles of integrin activation in eosinophil function and the eosinophilic inflammation of asthma. *Journal of leukocyte biology*. 83:1-12.

Bell, D.A., T.A. Longacre, J. Prat, E.C. Kohn, R.A. Soslow, L.H. Ellenson, A. Malpica, M.H. Stoler, and R.J. Kurman. 2004. Serous borderline (low malignant potential, atypical proliferative) ovarian tumors: Workshop perspectives. *Human Pathology*. 35:934-948.

Bhasin, N., P. Carl, S. Harper, G. Feng, H. Lu, D.W. Speicher, and D.E. Discher. 2004. Chemistry on a Single Protein, Vascular Cell Adhesion Molecule-1, during Forced Unfolding. *Journal of Biological Chemistry*. 279:45865-45874.

Bian, D., C. Mahanivong, J. Yu, S.M. Frisch, Z.K. Pan, R.D. Ye, and S. Huang. 2005. The G12//13-RhoA signaling pathway contributes to efficient lysophosphatidic acid-stimulated cell migration. *Oncogene*. 25:2234-2244.

Bian, D., C. Mahanivong, J. Yu, S.M. Frisch, Z.K. Pan, R.D. Ye, and S. Huang. 2006. The G12//13-RhoA signaling pathway contributes to efficient lysophosphatidic acid-stimulated cell migration. *Oncogene*. 25:2234-2244.

Bian, D., S. Su, C. Mahanivong, R.K. Cheng, Q. Han, Z.K. Pan, P. Sun, and S. Huang. 2004. Lysophosphatidic Acid Stimulates Ovarian Cancer Cell Migration via a Ras-MEK Kinase 1 Pathway. *Cancer Research*. 64:4209-4217.

Bittinger, F., C.L. Klein, C. Skarke, C. Brochhausen, S. Walgenbach, O. Rohrig, H. Kohler, and C.J. Kirkpatrick. 1996. PECAM-1 expression in human mesothelial cells: an in vitro study. *Pathobiology : journal of immunopathology, molecular and cellular biology*. 64:320-327.

Bot, M., I. Bot, R. Lopez-Vales, C.H.A. van de Lest, J.S. Saulnier-Blache, J.B. Helms, S. David, T.J.C. van Berkel, and E.A.L. Biessen. 2010. Atherosclerotic Lesion Progression Changes Lysophosphatidic Acid Homeostasis to Favor its Accumulation. *The American Journal of Pathology*. 176:3073-3084.

Bourguignon, L.Y., E. Gilad, K. Rothman, and K. Peyrollier. 2005. Hyaluronan-CD44 interaction with IQGAP1 promotes Cdc42 and ERK signaling, leading to actin binding, Elk-1/estrogen receptor transcriptional activation, and ovarian cancer progression. *The Journal of biological chemistry*. 280:11961-11972.

Byrne, A.T., L. Ross, J. Holash, M. Nakanishi, L. Hu, J.I. Hofmann, G.D. Yancopoulos, and R.B. Jaffe. 2003. Vascular Endothelial Growth Factor-Trap Decreases Tumor Burden, Inhibits Ascites, and Causes Dramatic Vascular Remodeling in an Ovarian Cancer Model. *Clinical Cancer Research*. 9:5721-5728.

Cai, Q., Z. Zhao, C. Antalis, L. Yan, G. Del Priore, A.H. Hamed, F.B. Stehman, J.M. Schilder, and Y. Xu. 2012. Elevated and secreted phospholipase A(2) activities as new potential therapeutic targets in human epithelial ovarian cancer. *The FASEB Journal*. 26:3306-3320.

Cannistra, S.A., G.S. Kansas, J. Niloff, B. DeFranzo, Y. Kim, and C. Ottensmeier. 1993. Binding of ovarian cancer cells to peritoneal mesothelium in vitro is partly mediated by CD44H. *Cancer Res*. 53:3830-3838.

Cannistra, S.A., C. Ottensmeier, J. Niloff, B. Orta, and J. DiCarlo. 1995. Expression and function of beta 1 and alpha v beta 3 integrins in ovarian cancer. *Gynecol Oncol*. 58:216-225.

Cannistra, S.A., C. Ottensmeier, J. Tidy, and B. DeFranzo. 1994. Vascular cell adhesion molecule-1 expressed by peritoneal mesothelium partly mediates the binding of activated human T lymphocytes. *Exp Hematol*. 22:996-1002.

Carlos, T., and J. Harlan. 1994. Leukocyte-endothelial adhesion molecules. *Blood*. 84:2068-2101.

Carman, C.V., and T.A. Springer. 2004. A transmigratory cup in leukocyte diapedesis both through individual vascular endothelial cells and between them. *The Journal of Cell Biology*. 167:377-388.

Casey, R.C., K.M. Burleson, K.M. Skubitz, S.E. Pambuccian, T.R. Oegema Jr, L.E. Ruff, and A.P.N. Skubitz. 2001. β1-Integrins Regulate the Formation and Adhesion of Ovarian Carcinoma Multicellular Spheroids. *The American Journal of Pathology*. 159:2071-2080.

Choi, J.W., D.R. Herr, K. Noguchi, Y.C. Yung, C.-W. Lee, T. Mutoh, M.-E. Lin, S.T. Teo, K.E. Park, A.N. Mosley, and J. Chun. 2010. LPA Receptors: Subtypes and Biological Actions. *Annual Review of Pharmacology and Toxicology*. 50:157-186.

Chrzanowska-Wodnicka, M., and K. Burridge. 1994. Tyrosine phosphorylation is involved in reorganization of the actin cytoskeleton in response to serum or LPA stimulation. *Journal of Cell Science*. 107:3643-3654.

Chuang, P.I., B.A. Young, R.R. Thiagarajan, C. Cornejo, R.K. Winn, and J.M. Harlan. 1997. Cytoplasmic Domain of E-selectin Contains a Non-tyrosine Endocytosis Signal. *Journal of Biological Chemistry*. 272:24813-24818.

Collins, T., M. Read, A. Neish, M. Whitley, D. Thanos, and T. Maniatis. 1995. Transcriptional regulation of endothelial cell adhesion molecules: NF- kappa B and cytokine-inducible enhancers. *The FASEB Journal*. 9:899-909.

Connell, N.D., and J.G. Rheinwald. 1983. Regulation of the cytoskeleton in mesothelial cells: Reversible loss of keratin and increase in vimentin during rapid growth in culture. *Cell*. 34:245-253.

Contos, J.J.A., I. Ishii, and J. Chun. 2000. Lysophosphatidic Acid Receptors. *Molecular Pharmacology*. 58:1188-1196.

Croft, D., P. McIntyre, A. Wibulswas, and I. Kramer. 1999. Sustained Elevated Levels of VCAM-1 in Cultured Fibroblast-like Synoviocytes Can Be Achieved by TNF-[alpha] in Combination with Either IL-4 or IL-13 through Increased mRNA Stability. *The American Journal of Pathology*. 154:1149-1158.

Cybulsky, M.I., J.W. Fries, A.J. Williams, P. Sultan, R. Eddy, M. Byers, T. Shows, M.A. Gimbrone, Jr., and T. Collins. 1991. Gene structure, chromosomal location, and basis for alternative mRNA splicing of the human VCAM1 gene. *Proceedings of the National Academy of Sciences of the United States of America*. 88:7859-7863.

Davidson, B. 2004. Malignant effusions: From diagnosis to biology. *Diagnostic Cytopathology*. 31:246-254.

Davies, M.J., J.L. Gordon, A.J.H. Gearing, R. Pigott, N. Woolf, D. Katz, and A. Kyriakopoulos. 1993. The expression of the adhesion molecules ICAM-1, VCAM-1, PECAM, and E-selectin in human atherosclerosis. *The Journal of Pathology*. 171:223-229.

Dirat, B., L. Bochet, M. Dabek, D. Daviaud, S. Dauvillier, B. Majed, Y.Y. Wang, A. Meulle, B. Salles, S. Le Gonidec, I. Garrido, G. Escourrou, P. Valet, and C. Muller. 2011. Cancer-Associated Adipocytes Exhibit an Activated Phenotype and Contribute to Breast Cancer Invasion. *Cancer Research*. 71:2455-2465.

East, J.E., K.M. Carter, P.C. Kennedy, N.A. Schulte, M.L. Toews, K.R. Lynch, and T.L. Macdonald. 2011. Development of a phosphatase-resistant, L-tyrosine derived LPA1/LPA3 dual antagonist. *MedChemComm*. 2:325-330.

Eder, A.M., T. Sasagawa, M. Mao, J. Aoki, and G.B. Mills. 2000. Constitutive and Lysophosphatidic Acid (LPA)-induced LPA Production: Role of Phospholipase D and Phospholipase A. *Clinical Cancer Research*. 6:2482-2491.

Eichholtz, T., K. Jalink, I. Fahrenfort, and W.H. Moolenaar. 1993. The bioactive phospholipid lysophosphatidic acid is released from activated platelets. *Biochemical Journal*. 291:677-680.

Ezzati, M., A. Abdullah, A. Shariftabrizi, J. Hou, M. Kopf, J.K. Stedman, R. Samuelson, and S. Shahabi. 2014. Recent Advancements in Prognostic Factors of Epithelial Ovarian Carcinoma. *International Scholarly Research Notices*. 2014:953509.

Fagotti, A., V. Gallotta, F. Romano, F. Fanfani, C. Rossitto, A. Naldini, M. Vigliotta, and G. Scambia. 2010. Peritoneal carcinosis of ovarian origin. *World Journal of Gastrointestinal Oncology*. 2:102-108.

Fang, X., D. Gaudette, T. Furui, M. Mao, V. Estrella, A. Eder, T. Pustilnik, T. Sasagawa, R. Lapushin, S. Yu, R.B. Jaffe, J.R. Wiener, J.R. Erickson, and G.B. Mills. 2000a.

Lysophospholipid Growth Factors in the Initiation, Progression, Metastases, and Management of Ovarian Cancer. *Annals of the New York Academy of Sciences*. 905:188-208.

Fang, X., S. Yu, R. LaPushin, Y. Lu, T. Furui, L.Z. Penn, D. Stokoe, J.R. Erickson, R.C. Bast, and G.B. Mills. 2000b. Lysophosphatidic acid prevents apoptosis in fibroblasts via G(i)-protein-mediated activation of mitogen-activated protein kinase. *Biochemical Journal*. 352:135-143.

Fearnley, G.W., A.F. Odell, A.M. Latham, N.A. Mughal, A.F. Bruns, N.J. Burgoyne, S. Homer-Vanniasinkam, I.C. Zachary, M.C. Hollstein, S.B. Wheatcroft, and S. Ponnambalam. 2014. VEGF-A isoforms differentially regulate ATF-2–dependent VCAM-1 gene expression and endothelial–leukocyte interactions. *Molecular Biology of the Cell*. 25:2509-2521.

Feldman, G.B., R.C. Knapp, S.E. Order, and S. Hellman. 1972. The Role of Lymphatic Obstruction in the Formation of Ascites in a Murine Ovarian Carcinoma. *Cancer Research*. 32:1663-1666.

Ferrara, N., and T. Davis-Smyth. 1997. The Biology of Vascular Endothelial Growth Factor. *Endocrine Reviews*. 18:4-25.

Ferrara, N., H.-P. Gerber, and J. LeCouter. 2003. The biology of VEGF and its receptors. *Nat Med*. 9:669-676.

Fishman, D.A., Y. Liu, S.M. Ellerbroek, and M.S. Stack. 2001. Lysophosphatidic Acid Promotes Matrix Metalloproteinase (MMP) Activation and MMP-dependent Invasion in Ovarian Cancer Cells. *Cancer Research*. 61:3194-3199.

Gardner, M.J., J.B. Catterall, L.M.H. Jones, and G.A. Turner. 1996. Human ovarian tumour cells can bind hyaluronic acid via membrane CD44: a possible step in peritoneal metastasis. *Clinical and Experimental Metastasis*. 14:325-334.

Gardner, M.J., L.M.H. Jones, J.B. Catterall, and G.A. Turner. 1995. Expression of cell adhesion molecules on ovarian tumour cell lines and mesothelial cells, in relation to ovarian cancer metastasis. *Cancer Letters*. 91:229-234.

Garlanda, C., and A. Mantovani. 1999. Cytokines and Adhesion Molecules in Mesothelial Cell Pathophysiology. *Sepsis*. 3:271-283.

Gerber, S.A., V.Y. Rybalko, C.E. Bigelow, A.A. Lugade, T.H. Foster, J.G. Frelinger, and E.M. Lord. 2006. Preferential Attachment of Peritoneal Tumor Metastases to Omental Immune Aggregates and Possible Role of a Unique Vascular Microenvironment in Metastatic Survival and Growth. *The American Journal of Pathology*. 169:1739-1752.

Gerrard, J.M., S.E. Kindom, D.A. Peterson, J. Peller, K.E. Krantz, and J.G. White. 1979. Lysophosphatidic acids. Influence on platelet aggregation and intracellular calcium flux. *The American Journal of Pathology*. 96:423-438.

Goldsmith, Z.G., J.H. Ha, M. Jayaraman, and D.N. Dhanasekaran. 2011. Lysophosphatidic Acid Stimulates the Proliferation of Ovarian Cancer Cells via the gep Proto-Oncogene Gα(12). *Genes & cancer*. 2:563-575.

Guillermet-Guibert, J., K. Bjorklof, A. Salpekar, C. Gonella, F. Ramadani, A. Bilancio, S. Meek, A.J.H. Smith, K. Okkenhaug, and B. Vanhaesebroeck. 2008. The p110β isoform of phosphoinositide 3-kinase signals downstream of G protein-coupled receptors and is

functionally redundant with p110γ. *Proceedings of the National Academy of Sciences of the United States of America*. 105:8292-8297.

Hennessy, B.T., R.L. Coleman, and M. Markman. 2009. Ovarian cancer. *The Lancet*. 374:1371-1382.

Hession, C., P. Moy, R. Tizard, P. Chisholm, C. Williams, M. Wysk, L. Burkly, K. Miyake, P. Kincade, and R. Lobb. 1992. Cloning of murine and rat vascular cell adhesion molecule-1. *Biochem Biophys Res Commun*. 183:163-169.

Hession, C., R. Tizard, C. Vassallo, S.B. Schiffer, D. Goff, P. Moy, G. Chi-Rosso, S. Luhowskyj, R. Lobb, and L. Osborn. 1991. Cloning of an alternate form of vascular cell adhesion molecule-1 (VCAM1). *Journal of Biological Chemistry*. 266:6682-6685.

Heyman, L., S. Kellouche, J. Fernandes, S. Dutoit, L. Poulain, and F. Carreiras. 2008. Vitronectin and Its Receptors Partly Mediate Adhesion of Ovarian Cancer Cells to Peritoneal Mesothelium in vitro. *Tumor Biology*. 29:231-244.

Heyman, L., J. Leroy-Dudal, J. Fernandes, D. Seyer, S. Dutoit, and F. Carreiras. 2010. Mesothelial vitronectin stimulates migration of ovarian cancer cells. *Cell Biology International*. 34:493-502.

Hillegass, J.M., A. Shukla, M.B. MacPherson, J.P. Bond, C. Steele, and B.T. Mossman. 2010. Utilization of gene profiling and proteomics to determine mineral pathogenicity in a human mesothelial cell line (LP9/TERT-1). *Journal of toxicology and environmental health. Part A*. 73:423-436.

Holtsberg, F.W., M.R. Steiner, J.N. Keller, R.J. Mark, M.P. Mattson, and S.M. Steiner. 1998. Lysophosphatidic Acid Induces Necrosis and Apoptosis in Hippocampal Neurons. *Journal of Neurochemistry*. 70:66-76.

Hu, Y.L., M.K. Tee, E.J. Goetzl, N. Auersperg, G.B. Mills, N. Ferrara, and R.B. Jaffe. 2001. Lysophosphatidic acid induction of vascular endothelial growth factor expression in human ovarian cancer cells. *J Natl Cancer Inst*. 93:762-768.

Imamura, F., T. Horai, M. Mukai, K. Shinkai, M. Sawada, and H. Akedo. 1993. Induction of in Vitro Tumor Cell Invasion of Cellular Monolayers by Lysophosphatidic Acid or Phospholipase D. *Biochemical and Biophysical Research Communications*. 193:497-503.

Inoue, M., M.H. Rashid, R. Fujita, J.J.A. Contos, J. Chun, and H. Ueda. 2004. Initiation of neuropathic pain requires lysophosphatidic acid receptor signaling. *Nat Med*. 10:712-718.

Iwanicki, M.P., R.A. Davidowitz, M.R. Ng, A. Besser, T. Muranen, M. Merritt, G. Danuser, T. Ince, and J.S. Brugge. 2011. Ovarian Cancer Spheroids Use Myosin-Generated Force to Clear the Mesothelium. *Cancer Discovery*:144-157.

Jayson, G.C., E.C. Kohn, H.C. Kitchener, and J.A. Ledermann. 2014. Ovarian cancer. *The Lancet*. 384:1376-1388.

Jelovac, D., and D.K. Armstrong. 2011. Recent Progress in the Diagnosis and Treatment of Ovarian Cancer. *CA: A Cancer Journal for Clinicians*. 61:183-203.

Jeon, E.S., S.C. Heo, I.H. Lee, Y.J. Choi, J.H. Park, K.U. Choi, D.Y. Park, D.-S. Suh, M.-S. Yoon, and J.H. Kim. 2010. Ovarian cancer-derived lysophosphatidic acid stimulates secretion of VEGF and stromal cell-derived factor-1[alpha] from human mesenchymal stem cells. *Exp Mol Med*. 42:280-293.

Jones, L.M.H., M.J. Gardner, J.B. Catterall, and G.A. Turner. 1995. Hyaluronic acid secreted by mesothelial cells: a natural barrier to ovarian cancer cell adhesion. *Clinical and Experimental Metastasis*. 13:373-380.

Jonjić, N., G. Peri, S. Bernasconi, F.L. Sciacca, F. Colotta, P. Pelicci, L. Lanfrancone, and A. Mantovani. 1992. Expression of adhesion molecules and chemotactic cytokines in cultured human mesothelial cells. *The Journal of Experimental Medicine*. 176:1165-1174.

Jourquin, J., N. Yang, Y. Kam, C. Guess, and V. Quaranta. 2006. Dispersal of epithelial cancer cell colonies by lysophosphatidic acid (LPA). *Journal of Cellular Physiology*. 206:337-346.

Kai, M., F. Sakane, Y.J. Jia, S. Imai, S. Yasuda, and H. Kanoh. 2006. Lipid phosphate phosphatases 1 and 3 are localized in distinct lipid rafts. *Journal of biochemistry*. 140:677-686.

Kenny, H.A., C.Y. Chiang, E.A. White, E.M. Schryver, M. Habis, I.L. Romero, A. Ladanyi, C.V. Penicka, J. George, K. Matlin, A. Montag, K. Wroblewski, S.D. Yamada, A.P. Mazar, D. Bowtell, and E. Lengyel. 2014. Mesothelial cells promote early ovarian cancer metastasis through fibronectin secretion. *J Clin Invest*:4614-4628.

Kenny, H.A., S. Dogan, M. Zillhardt, A. Mitra, S.D. Yamada, T. Krausz, and E. Lengyel. 2009. Organotypic Models of Metastasis: A 3 Dimensional Culture Mimicking the Human Peritoneum and Omentum for the Study of the Early Steps of Ovarian Cancer Metastasis. *Cancer treatment and research*. 149:335-351.

Kenny, H.A., S. Kaur, L.M. Coussens, and E. Lengyel. 2008. The initial steps of ovarian cancer cell metastasis are mediated by MMP-2 cleavage of vitronectin and fibronectin. *The Journal of Clinical Investigation*. 118:1367-1379.

Kenny, H.A., T. Krausz, S.D. Yamada, and E. Lengyel. 2007. Use of a novel 3D culture model to elucidate the role of mesothelial cells, fibroblasts and extra-cellular matrices on adhesion and invasion of ovarian cancer cells to the omentum. *International Journal of Cancer*. 121:1463-1472.

Kim, K.-S., S. Sengupta, M. Berk, Y.-G. Kwak, P.F. Escobar, J. Belinson, S.C. Mok, and Y. Xu. 2006. Hypoxia Enhances Lysophosphatidic Acid Responsiveness in Ovarian Cancer Cells and Lysophosphatidic Acid Induces Ovarian Tumor Metastasis In vivo. *Cancer Research*. 66:7983-7990.

Kim, S., B. Kim, and Y.S. Song. 2016. Ascites modulates cancer cell behavior, contributing to tumor heterogeneity in ovarian cancer. *Cancer Science*. 107:1173-1178.

Kipps, E., D.S.P. Tan, and S.B. Kaye. 2013. Meeting the challenge of ascites in ovarian cancer: new avenues for therapy and research. *Nat Rev Cancer*. 13:273-282.

Koshiyama, M., N. Matsumura, and I. Konishi. 2014. Recent Concepts of Ovarian Carcinogenesis: Type I and Type II. *BioMed Research International*. 2014:11.

Kulbe, H., R. Thompson, J.L. Wilson, S. Robinson, T. Hagemann, R. Fatah, D. Gould, A. Ayhan, and F. Balkwill. 2007. The Inflammatory Cytokine Tumor Necrosis Factor-α Generates an Autocrine Tumor-Promoting Network in Epithelial Ovarian Cancer Cells. *Cancer Research*. 67:585-592.

Kurman, R.J., and I.-M. Shih. 2008. Pathogenesis of Ovarian Cancer. Lessons from Morphology and Molecular Biology and their Clinical Implications. *International journal of gynecological pathology : official journal of the International Society of Gynecological Pathologists*. 27:151-160.

Kurosu, H., T. Maehama, T. Okada, T. Yamamoto, S.-i. Hoshino, Y. Fukui, M. Ui, O. Hazeki, and T. Katada. 1997. Heterodimeric Phosphoinositide 3-Kinase Consisting of p85 and p110β Is Synergistically Activated by the βγ Subunits of G Proteins and Phosphotyrosyl Peptide. *Journal of Biological Chemistry*. 272:24252-24256.

Landen, C.N., Jr., M.J. Birrer, and A.K. Sood. 2008. Early events in the pathogenesis of epithelial ovarian cancer. *J Clin Oncol*. 26:995-1005.

Larbi, K.Y., A.R. Allen, F.W.K. Tam, D.O. Haskard, R.R. Lobb, P.M.R. Silva, and S. Nourshargh. 2000. VCAM-1 has a tissue-specific role in mediating interleukin-4–induced eosinophil accumulation in rat models: evidence for a dissociation between endothelial-cell VCAM-1 expression and a functional role in eosinophil migration. *Blood*. 96:3601-3609.

Lee, H., E.J. Goetzl, and S. An. 2000. Lysophosphatidic acid and sphingosine 1-phosphate stimulate endothelial cell wound healing. *American Journal of Physiology - Cell Physiology*. 278:C612-C618.

Lee, H., C.I. Lin, J.-J. Liao, Y.-W. Lee, H.Y. Yang, C.-Y. Lee, H.-Y. Hsu, and H.L. Wu. 2004. Lysophospholipids increase ICAM-1 expression in HUVEC through a G_i- and NF-κB-dependent mechanism. *American Journal of Physiology - Cell Physiology*. 287:C1657-C1666.

Lee, J., S.Y. Park, E.K. Lee, C.G. Park, H.C. Chung, S.Y. Rha, Y.K. Kim, G.-U. Bae, B.K. Kim, J.-W. Han, and H.Y. Lee. 2006. Activation of Hypoxia-Inducible Factor-1α Is Necessary for Lysophosphatidic Acid–Induced Vascular Endothelial Growth Factor Expression. *Clinical Cancer Research*. 12:6351-6358.

Lee, S.-C., Y. Fujiwara, J. Liu, J. Yue, Y. Shimizu, D.D. Norman, Y. Wang, R. Tsukahara, E. Szabo, R. Patil, S. Banerjee, D.D. Miller, L. Balazs, M.C. Ghosh, C.M. Waters, T. Oravecz, and G.J. Tigyi. 2015. Autotaxin, LPA Receptors (1 and 5) Exert Disparate Functions in Tumor Cells Versus the Host Tissue Microenvironment in Melanoma Invasion and Metastasis. *Molecular cancer research : MCR*. 13:174-185.

Lee, T.C., Y. Zhang, C. Aston, R. Hintz, J. Jagirdar, M.A. Perle, M. Burt, and W.N. Rom. 1993. Normal human mesothelial cells and mesothelioma cell lines express insulin-like growth factor I and associated molecules. *Cancer Res*. 53:2858-2864.

Lee, Y., A. Miron, R. Drapkin, M.R. Nucci, F. Medeiros, A. Saleemuddin, J. Garber, C. Birch, H. Mou, R.W. Gordon, D.W. Cramer, F.D. McKeon, and C.P. Crum. 2007. A candidate precursor to serous carcinoma that originates in the distal fallopian tube. *The Journal of Pathology*. 211:26-35.

Lengyel, E. 2010. Ovarian Cancer Development and Metastasis. *The American Journal of Pathology*. 177:1053-1064.

Lertkiatmongkol, P., D. Liao, H. Mei, Y. Hu, and P.J. Newman. 2016. Endothelial functions of platelet/endothelial cell adhesion molecule-1 (CD31). *Current opinion in hematology*. 23:253-259.

Lessan, K., D.J. Aguiar, T. Oegema, L. Siebenson, and A.P. Skubitz. 1999. CD44 and beta1 integrin mediate ovarian carcinoma cell adhesion to peritoneal mesothelial cells. *Am J Pathol*. 154:1525-1537.

Leung, D.W. 2001. The structure and functions of human lysophosphatidic acid acyltransferases. *Front Biosci*. 6:D944-953.

Levanon, K., C. Crum, and R. Drapkin. 2008. New Insights Into the Pathogenesis of Serous Ovarian Cancer and Its Clinical Impact. *Journal of Clinical Oncology*. 26:5284-5293.

Ley, K., and Y. Huo. 2001. VCAM-1 is critical in atherosclerosis. *Journal of Clinical Investigation*. 107:1209-1210.

Li, H., D. Wang, H. Zhang, K. Kirmani, Z. Zhao, R. Steinmetz, and Y. Xu. 2009. Lysophosphatidic acid stimulates cell migration, invasion, and colony formation as well as tumorigenesis/metastasis of mouse ovarian cancer in immunocompetent mice. *Molecular Cancer Therapeutics*. 8:1692-1701.

Li, H., X. Ye, C. Mahanivong, D. Bian, J. Chun, and S. Huang. 2005. Signaling Mechanisms Responsible for Lysophosphatidic Acid-induced Urokinase Plasminogen Activator Expression in Ovarian Cancer Cells. *Journal of Biological Chemistry*. 280:10564-10571.

Li, H., Z. Zhao, G. Wei, L. Yan, D. Wang, H. Zhang, G.E. Sandusky, J. Turk, and Y. Xu. 2010. Group VIA phospholipase A2 in both host and tumor cells is involved in ovarian cancer development. *The FASEB Journal*. 24:4103-4116.

Li, P., I. Sanz, R.J. O'Keefe, and E.M. Schwarz. 2000. NF-κB Regulates VCAM-1 Expression on Fibroblast-Like Synoviocytes. *The Journal of Immunology*. 164:5990-5997.

Li, Y., M.I. Gonzalez, J.L. Meinkoth, J. Field, M.G. Kazanietz, and G.I. Tennekoon. 2003. Lysophosphatidic Acid Promotes Survival and Differentiation of Rat Schwann Cells. *Journal of Biological Chemistry*. 278:9585-9591.

Luo, Z., Q. Wang, W.B. Lau, B. Lau, L. Xu, L. Zhao, H. Yang, M. Feng, Y. Xuan, Y. Yang, L. Lei, C. Wang, T. Yi, X. Zhao, Y. Wei, and S. Zhou. 2016. Tumor microenvironment: The culprit for ovarian cancer metastasis? *Cancer Letters*. 377:174-182.

Maier, U., A. Babich, and B. Nürnberg. 1999. Roles of Non-catalytic Subunits in Gβγ-induced Activation of Class I Phosphoinositide 3-Kinase Isoforms β and γ. *Journal of Biological Chemistry*. 274:29311-29317.

Maruta, T., T. Yanagita, K. Matsuo, Y. Uezono, S. Satoh, T. Nemoto, N. Yoshikawa, H. Kobayashi, M. Takasaki, and A. Wada. 2008. Lysophosphatidic acid-LPA1 receptor–Rho–Rho kinase-induced up-regulation of Nav1.7 sodium channel mRNA and protein in adrenal chromaffin cells: enhancement of 22Na+ influx, 45Ca2+ influx and catecholamine secretion. *Journal of Neurochemistry*. 105:401-412.

Matte, I., D. Lane, D. Bachvarov, C. Rancourt, and A. Piché. 2014a. Role of malignant ascites on human mesothelial cells and their gene expression profiles. *BMC Cancer*. 14:288-288.

Matte, I., D. Lane, C. Laplante, P. Garde-Granger, C. Rancourt, and A. Piché. 2014b. Ovarian cancer ascites enhance the migration of patient-derived peritoneal mesothelial cells via cMet pathway through HGF-dependent and –independent mechanisms. *International Journal of Cancer*:n/a-n/a.

Matte, I., D. Lane, C. Laplante, C. Rancourt, and A. Piché. 2012. Profiling of cytokines in human epithelial ovarian cancer ascites. *American Journal of Cancer Research*. 2:566-580.

Meerschaert, J., and M. Furie. 1994. Monocytes use either CD11/CD18 or VLA-4 to migrate across human endothelium in vitro. *The Journal of Immunology*. 152:1915-1926.

Meerschaert, J., and M. Furie. 1995. The adhesion molecules used by monocytes for migration across endothelium include CD11a/CD18, CD11b/CD18, and VLA-4 on monocytes and ICAM-1, VCAM-1, and other ligands on endothelium. *The Journal of Immunology*. 154:4099-4112.

Meunier, L., M.-L. Puiffe, C. Le Page, A. Filali-Mouhim, M. Chevrette, P.N. Tonin, D.M. Provencher, and A.-M. Mes-Masson. 2010. Effect of Ovarian Cancer Ascites on Cell Migration and Gene Expression in an Epithelial Ovarian Cancer In Vitro Model. *Translational Oncology*. 3:230-238.

Meyer zu Heringdorf, D., and K.H. Jakobs. 2007. Lysophospholipid receptors: Signalling, pharmacology and regulation by lysophospholipid metabolism. *Biochimica et Biophysica Acta (BBA) - Biomembranes*. 1768:923-940.

Mills, G.B., and W.H. Moolenaar. 2003. The emerging role of lysophosphatidic acid in cancer. *Nat Rev Cancer*. 3:582-591.

Moradi, M.M., L.F. Carson, B. Weinberg, A.F. Haney, L.B. Twiggs, and S. Ramakrishnan. 1993. Serum and ascitic fluid levels of interleukin-1, interleukin-6, and tumor necrosis factor-alpha in patients with ovarian epithelial cancer. *Cancer*. 72:2433-2440.

Morishita, Y., S. Ookawara, I. Hirahara, S. Muto, and D. Nagata. 2016. HIF-1α mediates Hypoxia-induced epithelial–mesenchymal transition in peritoneal mesothelial cells. *Renal Failure*. 38:282-289.

Mueller, M.M., and N.E. Fusenig. 2004. Friends or foes [mdash] bipolar effects of the tumour stroma in cancer. *Nat Rev Cancer*. 4:839-849.

Muller, W.A., S.A. Weigl, X. Deng, and D.M. Phillips. 1993. PECAM-1 is required for transendothelial migration of leukocytes. *J Exp Med*. 178:449-460.

Murga, C., S. Fukuhara, and J.S. Gutkind. 2000. A Novel Role for Phosphatidylinositol 3-Kinase β in Signaling from G Protein-coupled Receptors to Akt. *Journal of Biological Chemistry*. 275:12069-12073.

Mutsaers, S.E. 2004. The mesothelial cell. *Int J Biochem Cell Biol*. 36:9-16.

Mutsaers, S.E., and S. Wilkosz. 2007. Structure and function of mesothelial cells. *Cancer treatment and research*. 134:1-19.

Nakayama, J., T.A. Raines, K.R. Lynch, and J.K. Slack-Davis. 2015. Decreased Peritoneal Ovarian Cancer Growth in Mice Lacking Expression of Lipid Phosphate Phosphohydrolase 1. *PLoS ONE*. 10:e0120071.

Naylor, M.S., G.W. Stamp, W.D. Foulkes, D. Eccles, and F.R. Balkwill. 1993. Tumor necrosis factor and its receptors in human ovarian cancer. Potential role in disease progression. *The Journal of Clinical Investigation*. 91:2194-2206.

Niedbala, M.J., K. Crickard, and R.J. Bernacki. 1985. Interactions of human ovarian tumor cells with human mesothelial cells grown on extracellular matrix. An in vitro model system for studying tumor cell adhesion and invasion. *Experimental cell research*. 160:499-513.

Nieman, K.M., I.L. Romero, B. Van Houten, and E. Lengyel. 2013. Adipose tissue and adipocytes supports tumorigenesis and metastasis(). *Biochimica et biophysica acta*. 1831:1533-1541.

Nikitopoulou, I., N. Oikonomou, E. Karouzakis, I. Sevastou, N. Nikolaidou-Katsaridou, Z. Zhao, V. Mersinias, M. Armaka, Y. Xu, M. Masu, G.B. Mills, S. Gay, G. Kollias, and V. Aidinis. 2012. Autotaxin expression from synovial fibroblasts is essential for the pathogenesis of modeled arthritis. *The Journal of Experimental Medicine*.

O'Brien, K.D., M.D. Allen, T.O. McDonald, A. Chait, J.M. Harlan, D. Fishbein, J. McCarty, M. Ferguson, K. Hudkins, C.D. Benjamin, and et al. 1993. Vascular cell adhesion molecule-1 is expressed in human coronary atherosclerotic plaques. Implications for the mode of progression of advanced coronary atherosclerosis. *J Clin Invest*. 92:945-951.

Offner, F.A., H. Feichtinger, S. Stadlmann, P. Obrist, C. Marth, P. Klingler, B. Grage, M. Schmahl, and C. Knabbe. 1996. Transforming growth factor-beta synthesis by human peritoneal mesothelial cells. Induction by interleukin-1. *The American Journal of Pathology*. 148:1679-1688.

Olumi, A.F., G.D. Grossfeld, S.W. Hayward, P.R. Carroll, T.D. Tlsty, and G.R. Cunha. 1999. Carcinoma-associated Fibroblasts Direct Tumor Progression of Initiated Human Prostatic Epithelium. *Cancer Research*. 59:5002-5011.

Osborn, L., C. Hession, R. Tizard, C. Vassallo, S. Luhowskyj, G. Chi-Rosso, and R. Lobb. 1989. Direct expression cloning of vascular cell adhesion molecule 1, a cytokine-induced endothelial protein that binds to lymphocytes. *Cell*. 59:1203-1211.

Ozols, R.F. 2005. Treatment goals in ovarian cancer. *International journal of gynecological cancer : official journal of the International Gynecological Cancer Society*. 15:3-11.

Pagès, C., M.-F. Simon, P. Valet, and J.S. Saulnier-Blache. 2001. Lysophosphatidic acid synthesis and release. *Prostaglandins & Other Lipid Mediators*. 64:1-10.

Palmetshofer, A.A. 1999. Lysophosphatidic acid activates nuclear factor kappa B and induces proinflammatory gene expression in endothelial cells. *Thrombosis and haemostasis*. 82:1532-1537.

Park, K.S., M.-K. Kim, H.Y. Lee, S.D. Kim, S.Y. Lee, J.M. Kim, S.H. Ryu, and Y.-S. Bae. 2007a. S1P stimulates chemotactic migration and invasion in OVCAR3 ovarian cancer cells. *Biochemical and Biophysical Research Communications*. 356:239-244.

Park, S.Y., K.J. Jeong, J. Lee, D.S. Yoon, W.S. Choi, Y.K. Kim, J.W. Han, Y.M. Kim, B.K. Kim, and H.Y. Lee. 2007b. Hypoxia enhances LPA-induced HIF-1α and VEGF expression: Their inhibition by resveratrol. *Cancer Letters*. 258:63-69.

Pigott, R., L.P. Dillon, I.H. Hemingway, and A.J. Gearing. 1992. Soluble forms of E-selectin, ICAM-1 and VCAM-1 are present in the supernatants of cytokine activated cultured endothelial cells. *Biochem Biophys Res Commun*. 187:584-589.

Prat, J. 2015. Staging Classification for Cancer of the Ovary, Fallopian Tube, and Peritoneum: Abridged Republication of Guidelines From the International Federation of Gynecology and Obstetrics (FIGO). *Obstetrics & Gynecology*. 126:171-174.

Ptaszynska, M.M., M.L. Pendrak, R.W. Bandle, M.L. Stracke, and D.D. Roberts. 2008. Positive Feedback between Vascular Endothelial Growth Factor-A and Autotaxin in Ovarian Cancer Cells. *Molecular Cancer Research*. 6:352-363.

Puiffe, M.-L., C. Le Page, A. Filali-Mouhim, M. Zietarska, V. Ouellet, P.N. Tonin, M. Chevrette, D.M. Provencher, and A.-M. Mes-Masson. 2007. Characterization of Ovarian Cancer Ascites on Cell Invasion, Proliferation, Spheroid Formation, Gene Expression in an In Vitro Model of Epithelial Ovarian Cancer. *Neoplasia (New York, N.Y.)*. 9:820-IN828.

Puls, L.E., T. Duniho, J.E. Hunter Iv, R. Kryscio, D. Blackhurst, and H. Gallion. The Prognostic Implication of Ascites in Advanced-Stage Ovarian Cancer. *Gynecologic Oncology*. 61:109-112.

Rampino, T., G. Cancarini, M. Gregorini, P. Guallini, M. Maggio, A. Ranghino, G. Soccio, and A. Dal Canton. 2001. Hepatocyte growth factor/scatter factor released during peritonitis is active on mesothelial cells. *Am J Pathol*. 159:1275-1285.

Ren, J., Y.-j. Xiao, L.S. Singh, X. Zhao, Z. Zhao, L. Feng, T.M. Rose, G.D. Prestwich, and Y. Xu. 2006. Lysophosphatidic Acid Is Constitutively Produced by Human Peritoneal Mesothelial Cells and Enhances Adhesion, Migration, and Invasion of Ovarian Cancer Cells. *Cancer Research*. 66:3006-3014.

Rieppi, M., V. Vergani, C. Gatto, G. Zanetta, P. Allavena, G. Taraboletti, and R. Giavazzi. 1999. Mesothelial cells induce the motility of human ovarian carcinoma cells. *International Journal of Cancer*. 80:303-307.

Rizza, C.C. 1999. Lysophosphatidic acid as a regulator of endothelial/leukocyte interaction. *Laboratory investigation*. 79:1227-1235.

Robinson-Smith, T.M., I. Isaacsohn, C.A. Mercer, M. Zhou, N. Van Rooijen, N. Husseinzadeh, M.M. McFarland-Mancini, and A.F. Drew. 2007. Macrophages Mediate Inflammation-Enhanced Metastasis of Ovarian Tumors in Mice. *Cancer Research*. 67:5708-5716.

Roby, K.F., C.C. Taylor, J.P. Sweetwood, Y. Cheng, J.L. Pace, O. Tawfik, D.L. Persons, P.G. Smith, and P.F. Terranova. 2000. Development of a syngeneic mouse model for events related to ovarian cancer. *Carcinogenesis*. 21:585-591.

Rother, E., R. Brandl, D.L. Baker, P. Goyal, H. Gebhard, G. Tigyi, and W. Siess. 2003. Subtype-Selective Antagonists of Lysophosphatidic Acid Receptors Inhibit Platelet Activation Triggered by the Lipid Core of Atherosclerotic Plaques. *Circulation*. 108:741-747.

Said, N.A., I. Najwer, M.J. Socha, D.J. Fulton, S.C. Mok, and K. Motamed. 2007. SPARC Inhibits LPA-Mediated Mesothelial-Ovarian Cancer Cell Crosstalk. *Neoplasia (New York, N.Y.)*. 9:23-35.

Sako, A., J. Kitayama, D. Shida, R. Suzuki, T. Sakai, H. Ohta, and H. Nagawa. 2006. Lysophosphatidic Acid (LPA)-Induced Vascular Endothelial Growth Factor (VEGF) by Mesothelial Cells and Quantification of Host-Derived VEGF in Malignant Ascites. *Journal of Surgical Research*. 130:94-101.

Sako, A., J. Kitayama, H. Yamaguchi, S. Kaisaki, H. Suzuki, K. Fukatsu, S. Fujii, and H. Nagawa. 2003. Vascular endothelial growth factor synthesis by human omental mesothelial cells is augmented by fibroblast growth factor-2: possible role of mesothelial cell on the development of peritoneal metastasis. *The Journal of surgical research*. 115:113-120.

Sankaranarayanan, R., and J. Ferlay. 2006. Worldwide burden of gynaecological cancer: The size of the problem. *Best Practice & Research Clinical Obstetrics & Gynaecology*. 20:207-225.

Santin, A.D., P.L. Hermonat, A. Ravaggi, M.J. Cannon, S. Pecorelli, and G.P. Parham. 1999. Secretion of vascular endothelial growth factor in ovarian cancer. *European journal of gynaecological oncology*. 20:177-181.

Sashio, T., K. Hiroaki, N. Takeda, T. Asano, S. Tsuji, M. Kondo, Y. Hasegawa, and K. Shimokata. 2012. Possible Involvement of Sphingosine-1-Phosphate/Gi/RhoA Pathways in Adherence of Eosinophils to Pulmonary Endothelium. *Allergology International*. 61:283-293.

Scalici, J.M., S. Arapovic, E.J. Saks, K.A. Atkins, G. Petroni, L.R. Duska, and J.K. Slack-Davis. 2016. Mesothelium expression of vascular cell adhesion molecule-1 (VCAM-1) is associated with an unfavorable prognosis in epithelial ovarian cancer (EOC). *Cancer*:n/a-n/a.

Scalici, J.M., S. Thomas, C. Harrer, T.A. Raines, J. Curran, K.A. Atkins, M.R. Conaway, L. Duska, K.A. Kelly, and J.K. Slack-Davis. 2013. Imaging VCAM-1 as an Indicator of Treatment Efficacy in Metastatic Ovarian Cancer. *Journal of Nuclear Medicine*:1883-1889.

Schauer, I.G., J. Zhang, Z. Xing, X. Guo, I. Mercado-Uribe, A.K. Sood, P. Huang, and J. Liu. 2013. Interleukin-1β Promotes Ovarian Tumorigenesis through a p53/NF-κB-Mediated Inflammatory Response in Stromal Fibroblasts. *Neoplasia (New York, N.Y.)*. 15:409-420.

Schorge, J.O., C. McCann, and M.G. Del Carmen. 2010. Surgical Debulking of Ovarian Cancer: What Difference Does It Make? *Reviews in Obstetrics and Gynecology*. 3:111-117.

Sciorra, V.A., and A.J. Morris. 2002. Roles for lipid phosphate phosphatases in regulation of cellular signaling. *Biochimica et Biophysica Acta (BBA) - Molecular and Cell Biology of Lipids*. 1582:45-51.

Sehouli, J., F. Senyuva, C. Fotopoulou, U. Neumann, C. Denkert, L. Werner, and O.-Ö. Gülten. 2009. Intra-abdominal tumor dissemination pattern and surgical outcome in 214 patients with primary ovarian cancer. *Journal of Surgical Oncology*. 99:424-427.

Sengupta, S., K.S. Kim, M.P. Berk, R. Oates, P. Escobar, J. Belinson, W. Li, D.J. Lindner, B. Williams, and Y. Xu. 2006. Lysophosphatidic acid downregulates tissue inhibitor of metalloproteinases, which are negatively involved in lysophosphatidic acid-induced cell invasion. *Oncogene*. 26:2894-2901.

Shaw, P.A., M. Rouzbahman, E.S. Pizer, M. Pintilie, and H. Begley. 2009. Candidate serous cancer precursors in fallopian tube epithelium of BRCA1/2 mutation carriers. *Mod Pathol*. 22:1133-1138.

Sherer, D.M., R. Eliakim, and O. Abulafia. 2000. The Role of Angiogenesis in the Accumulation of Peritoneal Fluid in Benign Conditions and the Development of Malignant Ascites in the Female. *Gynecologic and Obstetric Investigation*. 50:217-224.

Shimada, H., and L.E. Rajagopalan. 2010. Rho Kinase-2 Activation in Human Endothelial Cells Drives Lysophosphatidic Acid-mediated Expression of Cell Adhesion Molecules via NF-κB p65. *Journal of Biological Chemistry*. 285:12536-12542.

Siegel, R.L., K.D. Miller, and A. Jemal. 2015. Cancer statistics, 2015. *CA: A Cancer Journal for Clinicians*. 65:5-29.

Slack-Davis, J.K., K.A. Atkins, C. Harrer, E.D. Hershey, and M. Conaway. 2009. Vascular Cell Adhesion Molecule-1 Is a Regulator of Ovarian Cancer Peritoneal Metastasis. *Cancer Research*. 69:1469-1476.

Smicun, Y., O. Gil, K. Devine, and D.A. Fishman. 2007. S1P and LPA have an attachment-dependent regulatory effect on invasion of epithelial ovarian cancer cells. *Gynecologic Oncology*. 107:298-309.

So, J., J. Navari, F.-Q. Wang, and D.A. Fishman. 2004. Lysophosphatidic acid enhances epithelial ovarian carcinoma invasion through the increased expression of interleukin-8. *Gynecologic Oncology*. 95:314-322.

Stadlmann, S., A. Amberger, J. Pollheimer, G. Gastl, F.A. Offner, R. Margreiter, and A.G. Zeimet. 2005. Ovarian carcinoma cells and IL-1β-activated human peritoneal mesothelial cells are possible sources of vascular endothelial growth factor in inflammatory and malignant peritoneal effusions. *Gynecologic Oncology*. 97:784-789.

Stadlmann, S., R. Raffeiner, A. Amberger, R. Margreiter, A.G. Zeimet, B. Abendstein, P.L. Moser, G. Mikuz, B. Klosterhalfen, and F.A. Offner. 2003. Disruption of the integrity of human peritoneal mesothelium by interleukin-1beta and tumor necrosis factor-alpha. *Virchows Archiv : an international journal of pathology*. 443:678-685.

Steiner, M.R., F.W. Holtsberg, J.N. Keller, M.P. Mattson, and S.M. Steiner. 2000. Lysophosphatidic Acid Induction of Neuronal Apoptosis and Necrosis. *Annals of the New York Academy of Sciences*. 905:132-141.

Strobel, T., and S.A. Cannistra. 1999. β1-Integrins Partly Mediate Binding of Ovarian Cancer Cells to Peritoneal Mesothelium in Vitro. *Gynecologic Oncology*. 73:362-367.

Sun, W., and J. Yang. 2010. Molecular basis of lysophosphatidic acid-induced NF-[kappa]B activation. *Cellular Signalling*. 22:1799-1803.

Sutphen, R., Y. Xu, G.D. Wilbanks, J. Fiorica, E.C. Grendys, J.P. LaPolla, H. Arango, M.S. Hoffman, M. Martino, K. Wakeley, D. Griffin, R.W. Blanco, A.B. Cantor, Y.-j. Xiao, and J.P. Krischer. 2004. Lysophospholipids Are Potential Biomarkers of Ovarian Cancer. *Cancer Epidemiology Biomarkers & Prevention*. 13:1185-1191.

Swaney, J.S., C. Chapman, L.D. Correa, K.J. Stebbins, R.A. Bundey, P.C. Prodanovich, P. Fagan, C.S. Baccei, A.M. Santini, J.H. Hutchinson, T.J. Seiders, T.A. Parr, P. Prasit, J.F. Evans, and D.S. Lorrain. 2010. A novel, orally active LPA(1) receptor antagonist inhibits lung fibrosis in the mouse bleomycin model. *British Journal of Pharmacology*. 160:1699-1713.

Swerlick, R., K. Lee, L. Li, N. Sepp, S. Caughman, and T. Lawley. 1992. Regulation of vascular cell adhesion molecule 1 on human dermal microvascular endothelial cells. *The Journal of Immunology*. 149:698-705.

Szlosarek, P.W., M.J. Grimshaw, H. Kulbe, J.L. Wilson, G.D. Wilbanks, F. Burke, and F.R. Balkwill. 2006. Expression and regulation of tumor necrosis factor α in normal and malignant ovarian epithelium. *Molecular Cancer Therapeutics*. 5:382-390.

Tanyi, J.L., Y. Hasegawa, R. Lapushin, A.J. Morris, J.K. Wolf, A. Berchuck, K. Lu, D.I. Smith, K. Kalli, L.C. Hartmann, K. McCune, D. Fishman, R. Broaddus, K.W. Cheng, E.N. Atkinson, J.M. Yamal, R.C. Bast, E.A. Felix, R.A. Newman, and G.B. Mills. 2003a. Role of Decreased Levels of Lipid Phosphate Phosphatase-1 in Accumulation of Lysophosphatidic Acid in Ovarian Cancer. *Clinical Cancer Research*. 9:3534-3545.

Tanyi, J.L., A.J. Morris, J.K. Wolf, X. Fang, Y. Hasegawa, R. Lapushin, N. Auersperg, Y.J. Sigal, R.A. Newman, E.A. Felix, E.N. Atkinson, and G.B. Mills. 2003b. The Human Lipid

Phosphate Phosphatase-3 Decreases the Growth, Survival, and Tumorigenesis of Ovarian Cancer Cells. *Cancer Research*. 63:1073-1082.

Tokumura, A., T. Kume, K. Fukuzawa, M. Tahara, K. Tasaka, J. Aoki, H. Arai, K. Yasuda, and H. Kanzaki. 2007. Peritoneal fluids from patients with certain gynecologic tumor contain elevated levels of bioactive lysophospholipase D activity. *Life Sciences*. 80:1641-1649.

Tomsig, J.L., A.H. Snyder, E.V. Berdyshev, A. Skobeleva, C. Mataya, V. Natarajan, D.N. Brindley, and K.R. Lynch. 2009. Lipid phosphate phosphohydrolase type 1 (LPP1) degrades extracellular lysophosphatidic acid in vivo. *The Biochemical journal*. 419:611-618.

Tsoyi, K., H.J. Jang, I.T. Nizamutdinova, K. Park, Y.M. Kim, H.J. Kim, H.G. Seo, J.H. Lee, and K.C. Chang. 2010. PTEN differentially regulates expressions of ICAM-1 and VCAM-1 through PI3K/Akt/GSK-3β/GATA-6 signaling pathways in TNF-α-activated human endothelial cells. *Atherosclerosis*. 213:115-121.

Tsoyi, K., W.S. Kim, Y.M. Kim, H.J. Kim, H.G. Seo, J.H. Lee, H.S. Yun-Choi, and K.C. Chang. 2009. Upregulation of PTEN by CKD712, a synthetic tetrahydroisoquinoline alkaloid, selectively inhibits lipopolysaccharide-induced VCAM-1 but not ICAM-1 expression in human endothelial cells. *Atherosclerosis*. 207:412-419.

Umetani, M., C. Mataki, N. Minegishi, M. Yamamoto, T. Hamakubo, and T. Kodama. 2001. Function of GATA Transcription Factors in Induction of Endothelial Vascular Cell Adhesion Molecule-1 by Tumor Necrosis Factor-α. *Arteriosclerosis, Thrombosis, and Vascular Biology*. 21:917-922.

Valet, P., C. Pagès, O. Jeanneton, D. Daviaud, P. Barbe, M. Record, J.S. Saulnier-Blache, and M. Lafontan. 1998. Alpha2-adrenergic receptor-mediated release of lysophosphatidic acid by adipocytes. A paracrine signal for preadipocyte growth. *Journal of Clinical Investigation*. 101:1431-1438.

van Corven, E.J., A. Groenink, K. Jalink, T. Eichholtz, and W.H. Moolenaar. 1989. Lysophosphatidate-induced cell proliferation: Identification and dissection of signaling pathways mediated by G proteins. *Cell*. 59:45-54.

Wang, D., Z. Zhao, A. Caperell-Grant, G. Yang, S.C. Mok, J. Liu, R.M. Bigsby, and Y. Xu. 2008. S1P differentially regulates migration of human ovarian cancer and human ovarian surface epithelial cells. *Molecular cancer therapeutics*. 7:1993-2002.

Wang, E., Y. Ngalame, M.C. Panelli, H. Nguyen-Jackson, M. Deavers, P. Mueller, W. Hu, C.A. Savary, R. Kobayashi, R.S. Freedman, and F.M. Marincola. 2005. Peritoneal and Subperitoneal Stroma May Facilitate Regional Spread of Ovarian Cancer. *Clinical Cancer Research*. 11:113-122.

Warn, R., P. Harvey, A. Warn, A. Foley-Comer, P. Heldin, M. Versnel, N. Arakaki, Y. Daikuhara, G.J. Laurent, S.E. Herrick, and S.E. Mutsaers. 2001. HGF/SF induces mesothelial cell migration and proliferation by autocrine and paracrine pathways. *Experimental cell research*. 267:258-266.

Watanabe, T., T. Hashimoto, T. Sugino, S. Soeda, H. Nishiyama, Y. Morimura, H. Yamada, S. Goodison, and K. Fujimori. 2012. Production of IL1-beta by ovarian cancer cells induces

mesothelial cell beta1-integrin expression facilitating peritoneal dissemination. *Journal of Ovarian Research*. 5:7.

Weiner, J.A., and J. Chun. 1999. Schwann cell survival mediated by the signaling phospholipid lysophosphatidic acid. *Proceedings of the National Academy of Sciences of the United States of America*. 96:5233-5238.

Westermann, A.M., E. Havik, F.R. Postma, J.H. Beijnen, O. Dalesio, W.H. Moolenaar, and S. Rodenhuis. 1998. Malignant effusions contain lysophosphatidic acid (LPA)-like activity. *Annals of Oncology*. 9:437-442.

Witz, C.A., I.A. Montoya-Rodriguez, S. Cho, V.E. Centonze, L.F. Bonewald, and R.S. Schenken. 2001. Composition of the Extracellular Matrix of the Peritoneum. *Journal of the Society for Gynecologic Investigation*. 8:299-304.

Wu, Y.-J., L.M. Parker, N.E. Binder, M.A. Beckett, J.H. Sinard, C.T. Griffiths, and J.G. Rheinwald. 1982. The mesothelial keratins: A new family of cytoskeletal proteins identified in cultured mesothelial cells and nonkeratinizing epithelia. *Cell*. 31:693-703.

Xiao, Y.-j., B. Schwartz, M. Washington, A. Kennedy, K. Webster, J. Belinson, and Y. Xu. 2001. Electrospray Ionization Mass Spectrometry Analysis of Lysophospholipids in Human Ascitic Fluids: Comparison of the Lysophospholipid Contents in Malignant vs Nonmalignant Ascitic Fluids. *Analytical Biochemistry*. 290:302-313.

Xiao, Y., Y. Chen, A.W. Kennedy, J. Belinson, and Y. Xu. 2000. Evaluation of plasma lysophospholipids for diagnostic significance using electrospray ionization mass spectrometry (ESI-MS) analyses. *Ann N Y Acad Sci*. 905:242-259.

Xu, Y., D.C. Gaudette, J.D. Boynton, A. Frankel, X.J. Fang, A. Sharma, J. Hurteau, G. Casey, A. Goodbody, and A. Mellors. 1995. Characterization of an ovarian cancer activating factor in ascites from ovarian cancer patients. *Clinical Cancer Research*. 1:1223-1232.

Ye, X. 2008. Lysophospholipid signaling in the function and pathology of the reproductive system. *Human Reproduction Update*. 14:519-536.

Ye, X., I. Ishii, M.A. Kingsbury, and J. Chun. 2002. Lysophosphatidic acid as a novel cell survival/apoptotic factor. *Biochimica et Biophysica Acta (BBA) - Molecular and Cell Biology of Lipids*. 1585:108-113.

Yu, S., M.M. Murph, Y. Lu, S. Liu, H.S. Hall, J. Liu, C. Stephens, X. Fang, and G.B. Mills. 2008. Lysophosphatidic Acid Receptors Determine Tumorigenicity and Aggressiveness of Ovarian Cancer Cells. *Journal of the National Cancer Institute*. 100:1630-1642.